In presenting the dissertation as a partial fulfillment of the requirements for an advanced degree from the Georgia Institute of Technology, I agree that the Library of the Institute shall make it available for inspection and circulation in accordance with its regulations governing materials of this type. I agree that permission to copy from, or to publish from, this dissertation may be granted by the professor under whose direction it was written, or, in his absence, by the Dean of the Graduate Division when such copying or publication is solely for scholarly purposes and does not involve potential financial gain. It is understood that any copying from, or publication of, this dissertation which involves potential financial gain will not be allowed without written permission.

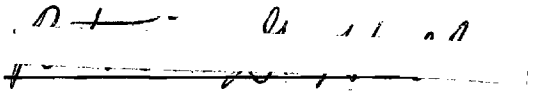

3/17/65
b

CDD POLES IN PION-KAON DISPERSION RELATIONS

A THESIS

Presented to

The Faculty of the Division of Graduate

Studies and Research

by

Patricia Groves Hull

In Partial Fulfillment

of the Requirements for the Degree

Doctor of Philosophy

in the School of Physics

Georgia Institute of Technology

April, 1969

CDD POLES IN PION-KAON DISPERSION RELATIONS

Approved:

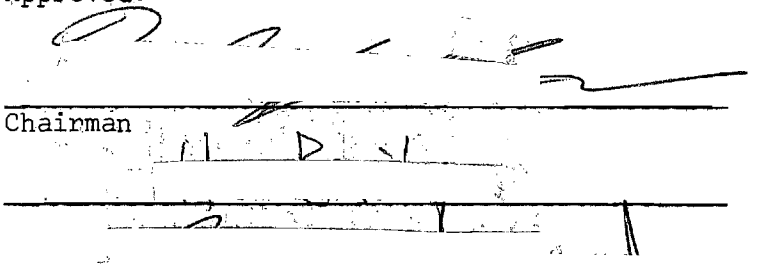

Chairman

Date approved by Chairman: May 28, 1970

ACKNOWLEDGMENTS

I would like to thank my thesis advisor, Dr. Ian R. Gatland for suggesting the thesis problem and for stimulating discussions which provided invaluable aid in its solution. I would also like to thank the National Science Foundation for financial assistance during the research for this thesis.

TABLE OF CONTENTS

LIST OF TABLES

LIST OF ILLUSTRATIONS

SUMMARY

The objective of this thesis is to determine whether or not a CDD pole can be inserted into an existing single resonance solution for the pion-kaon scattering amplitude without destroying postulated properties of analyticity, unitarity or crossing symmetry. For the case of the pion-pion interaction, a program including inelastic scattering was run by Bransden and Moffat and solutions with a CDD pole appeared with the pole always occurring close to the original P-wave resonance position. The effect of the pole was to split the resonance into two parts, one on each side of the CDD pole. This split resonance solution implies that the theory allows for the existence of two particles with identical quantum numbers but slightly different masses. It is of considerable interest to verify the theoretical possibility for such a solution for interactions involving particles of unequal masses, particularly for pion-nucleon scattering, since it might help solve some of the difficulties that have been encountered in the mass formulas derived from SU(3) symmetry. The nucleon's spin angular momentum complicates the mathematics of the analysis and since the kaon has the same I-spin as the nucleon, the pion-kaon interaction is analogous in all respects except spin angular momentum. It is for this reason that the pion-kaon interaction is chosen for consideration here.

A convenient set of variables for the problem is chosen and the Mandelstam Representation is employed to express the pion-kaon amplitude

in terms of these variables. From this expression, the cut plane in which the amplitude is analytic is determined. Cauchy's Integral Theorem is applied to an appropriate contour in this plane and a dispersion relation connecting the real part of the partial wave amplitude to its discontinuities across the cuts is obtained. The Mandelstam Representation is employed once again, this time to obtain equations which relate the discontinuities of the partial-wave amplitudes across the unphysical cuts to the discontinuities across the physical cut. These equations are usually called "crossing equations." Thus, if the discontinuity across the physical cut is known, the crossing equations and the dispersion relation determine the real part of the amplitude everywhere. Unfortunately, this quantity is not generally known. However, the unitarity condition leads to a simple analytic expression for the imaginary part of the inverse amplitude in the physical region leaving only the real part of the inverse amplitude unknown there. In a general method of solution such as the N/D or 1/A method, an iteration scheme is set up to generate the real part of the inverse amplitude but obtaining a solution to the pion-kaon scattering problem is not of interest here. What is important is the effect of a CDD pole on an existing single resonance solution. Therefore, a form of the real part of the inverse amplitude is assumed which produces the experimental K^* resonance solution. The subtraction constants are determined by requiring that the experimentally observed resonance position and width be unchanged by a calculation of the amplitude using the crossing equations and dispersion relation. A CDD pole is then inserted into the inverse amplitude

function and the real part of the amplitude is calculated. The consistency of the scheme depends upon the CDD pole leaving the P-wave subtraction constants unchanged. The effects on the subtraction constants for a wide range of CDD pole strengths and positions are shown to be quite small. It is concluded that a split resonance solution can be produced from a single resonance solution without violating analyticity, unitarity or crossing symmetry for interactions involving particles with unequal masses.

CHAPTER I

INTRODUCTION

Section 1. The One-dimensional Dispersion Relation

Dispersion relations were first introduced in 1926-27 in the historic papers of Kronig[1] and Kramers.[2] Both Kronig and Kramers were concerned with the classical dispersion of light and the relation between the real (dispersive) and the imaginary (absorptive) parts of the complex index of refraction. Kramers, whose paper was the more detailed of the two, showed that a specific relation between the real and imaginary parts, referred to as a dispersion relation, was based on the fundamental requirement of causality. He first showed that the dispersion relation followed from the requirement that the index of refraction, viewed as a function of complex frequency, be an analytic function in the upper half plane and approach unity at infinity. It was necessary to extend the definition of the index of refraction $n(\omega)$ to include negative frequencies; thus $n(-\omega)$ was defined to be $n^*(\omega)$. This relationship between $n(-\omega)$ and $n(\omega)$ has come to be known as "crossing symmetry." Kramers then showed that in a medium described by such an index of refraction, signals could not propagate faster than the velocity of light.

Interest in the subject waned during the next 20 years; then in 1946, Kronig[3] suggested that the causality requirement might be imposed on the S-matrix for elementary particle processes to limit its form. Subsequently a number of investigations were made in the form of the

S-matrix in relativistic and non-relativistic theory. Some of these investigations were based on the idea of causality and others were based on the properties of the S-matrix stemming from customary assumptions of local, Hermitian interactions, unitarity and completeness.

A new era in dispersion relations was begun in 1954 with a paper by Gell-Mann, Goldberger and Thirring[4] in which a quantum mechanical proof of the dispersion relation for the forward scattering of light was based on the microscopic causality condition that the commutator (anti-commutator) of two bosons (fermions) at different points in space-time must vanish for space-like separations of the two points. This proof was based on the use of perturbation theory for the E-M interaction, but Goldberger[5] soon remedied that deficiency.

The next logical step was the extension of dispersion relations to the forward scattering of particles with mass. Goldberger[6] investigated the problem theoretically and he and others applied the resulting dispersion relations specifically to the problem of forward scattering of pions by nucleons. The first real comparison of this theory with experiment was made by Anderson, Davidon and Kruse.[7] This comparison was sufficiently favorable to continue the interest in dispersion relations for particles with mass.

In order to obtain a more effective dynamical theory of scattering processes, a generalization of the dispersion relations from forward to non-forward scattering was necessary. This was done in a heuristic way by Gell-Mann and Polkinghorne, and independently by Goldberger, Nambu and Oehme (unpublished). The dispersion relations they obtained

were in the energy variable of the problem with the Lorentz invariant momentum transfer held constant. These dispersion relations were applied to pion-nucleon scattering by Chew, Goldberger, Low and Nambu.[8]

As these dispersion relations were being applied to specific scattering problems, rigorous proofs were given to place the relations on a firm theoretical foundation. A proof for forward scattering was given by Symanzik[9] and general proofs were given by several authors, one of the first and most complex proofs being given by Bogoliubov.[10] These proofs showed that the fixed momentum transfer dispersion relations were valid provided that the momentum transfer was less than some maximum and that certain inequalities in the masses of the particles were satisfied.

From 1954 to 1958 dispersion relations were applied to a number of problems such as pion-pion, pion-deuteron, nucleon and Kaon-nucleon scattering, electro-magnetic form factors of nucleons and decay processes involving strong interactions as well as weak interactions.

Section 2. The Mandelstam Representation

Although applications of the type of dispersion relations discussed so far are still being made, the emphasis has shifted to the double dispersion relations given by the Mandelstam representation. Mandelstam[11] first conjectured the double dispersion relation in 1958 in connection with pion-nucleon scattering. The double dispersion relation is a prescription for extending collision amplitudes into the complex plane, and it attributes certain analytic properties to the amplitude as a function not only of the complex energy variable, but

also of the complex momentum transfer. Thus the Mandelstam representation provides a much more powerful tool than the ordinary dispersion relations. Unfortunately, the double dispersion relations are non-linear integral equations which are, in some cases, singular. The strength of the representation rests on two general features: (a) The location of singularities is determined by the total "masses" of actual physical systems; the higher the mass the farther from the origin is the associated singularity. Now, among the strongly interacting particles there are none of zero mass; thus, the total "mass" of strongly interacting physical systems systematically tends to increase with the number of particles, and the singularities near the origin tend to be determined by one- and two-particle configurations. If there are aspects of the physical problem that are controlled mainly by "near-by" singularities, then one can make a meaningful comparison of theory with experiment without a complete understanding of "faraway" singularities in which multiparticle configurations play a role. (b) The "strength" of singularities is related to physical cross sections and restricted by unitarity, so that in a limited region of the complex plane the behavior of an S-matrix element tends to be controlled by the closest singularities. More precisely, an analytic function is determined through the Cauchy relations by a kind of Coulomb's law for a potential due to point charges (poles) and line charges (branch cuts). The line-charge "density" is the discontinuity across the cut, which is proportional to physical cross sections and therefore limited in magnitude. There is assurance therefore that the "Coulomb's law" reciprocal dependence on

distance, which favors near-by singularities, will not be overwhelmed by an increasing strength of singularity with distance. From a practical standpoint, this feature of the S-matrix approach is of tremendous importance to a theory of strong interactions, permitting an orderly and systematic series of approximations whose validity is subject to realistic appraisal without any assumptions as to the magnitude of coupling constants.

The range of the force in the conventional point of view corresponds to the reciprocal distance from the origin in the complex momentum plane of the associated singularity. This relationship is, of course, traceable to the uncertainty principle. The unphysical singularities of an elastic-scattering amplitude correspond to the systems that can be "exchanged" between the particles undergoing scattering. Only by exchanges can a force be transmitted, and it is well known that according to the uncertainty principle the range of the force is proportional to $1/E$, if E is the total energy necessary to create the exchanged system. The "near-by" singularities, associated with one- and two-particle configurations, are the "long-range forces." The forces that cannot be calculated reliably (but only put limits on) are those of short range which involve three-particle and higher multiplicity exchange. Until general S-matrix elements, involving more than two particles can be calculated, exchange at this stage must be treated phenomenologically.

There seems to be no way to avoid a discussion of low-angular momentum partial waves. The fundamental dynamical problem becomes the

determination of the partial-wave amplitude given the discontinuity across its unphysical cuts. Two approaches to the problem have been presented: The first by Chew and Low,[12] which was subsequently modified by Chew and Mandelstam,[13] and the second by Moffat.[14] The first approach, now referred to as the N/D method, is based on the assumption that the partial wave amplitudes, $A_\ell^I(s)$, can be written as the ratio of two functions--a denominator function, D_ℓ, which contains only the right-hand or "physical" cut and a numerator function, N_ℓ, which contains only the left-hand or "unphysical" cut. This assumption is certainly valid in the case of pion-pion scattering since Omnes[15] has written an explicit form of D_ℓ in terms of the phase shift which clearly has only the right-hand cut and in addition, it has the phase $\exp(-i\delta_\ell)$ along this cut. Since $A_\ell = N_\ell/D_\ell$, and A_ℓ has the phase $\exp(i\delta_\ell)$ along the positive real axis, the numerator function is real along this axis and the right-hand cut is absent for N_ℓ. Now, the defining properties of N_ℓ and D_ℓ, together with the unitarity condition and the Cauchy integral theorem are used to obtain two coupled linear equations that can be converted into a single equation for one unknown function. If the assumption that N_ℓ vanish at ∞ is made, the equation for D_ℓ is a linear equation of the non-singular Fredholm type and can be solved by any number of standard methods. The second approach might be called the inverse amplitude or the 1/A method. In this approach, the partial-wave amplitudes are determined in terms of the unitarity condition and the known branch cuts and poles of the inverse amplitudes. By application of crossing symmetry,[13] a numerical iteration scheme is set up to obtain P-wave dominant

solutions. Both the N/D and the 1/A approaches led to solutions which contained an ambiguity first emphasized by Castillejo, Dalitz and Dyson.[16] It appeared that poles along the real axis (CDD poles) could be added to the denominator function without destroying postulated properties of analyticity, unitarity or crossing symmetry. This ambiguity was fortunate in a way, since it allowed for the inclusion of stable or unstable "elementary" particles into the scheme by adding appropriate CDD poles. Each such CDD pole produces a zero in $D_\ell(s)$ close to the pole if the residue of the pole is small; and if the position of the CDD pole occurs on the negative real axis where $D_\ell(s)$ is real, the associated zero is also likely to be on the negative real axis. In such a case there would be a pole in the partial-wave amplitude $A_\ell(s)$ that could be interpreted as a stable particle. The position and residue of the CDD pole correspond to the mass and coupling constant of the new particle. If a CDD pole is introduced on the positive real axis, the associated zero usually occurs away from the real axis due to the complexity of $D_\ell(s)$. If the sign of the residue is correctly chosen, the zero of $D_\ell(s)$ can be made to appear on the "unphysical sheet" of the Riemann surface, and therefore it does not violate the postulated properties of analyticity. The corresponding pole on the unphysical sheet for $A_\ell(s)$ represents the unstable particle, which again is characterized by two parameters. Since the real part of the denominator vanishes somewhere near the pole, the phase shift goes through 90 degrees and a resonance appears. The phase shift behavior is shown graphically in Figure 1. This phase shift behavior should not be confused with the

phase shift behavior due to a "dynamical" resonance. A dynamical resonance is due to the intermediate states of another channel, i.e., the forces involved in the interaction.

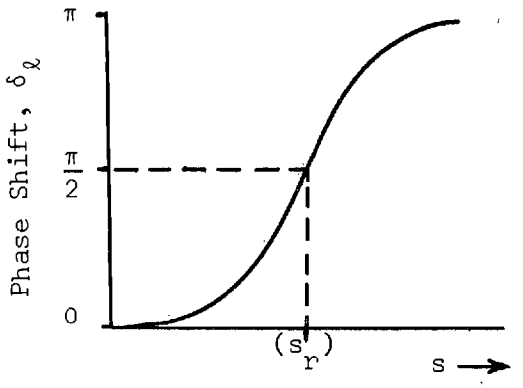

Figure 1. The Partial-Wave Phase Shift After the Introduction of a CDD Pole. The Resonance Position Corresponds to the Mass Squared of the New "Unstable" Particle.

At the present time, the Mendelstam representation is being applied to a number of scattering problems involving strong interactions, and in particular, the pion-pion interaction. Pion-pion scattering is experimentally elusive, but it appears that it must be understood before further substantial progress is possible in the theory.

Section 3. The CDD Pole in Pion-Pion Scattering Amplitudes

The dispersion relation analysis referred to as the N/D method in the previous section is arbitrary to the extent of these CDD poles in the denominator function or the inverse amplitude, and these poles cannot be found by numerical iteration on a computer since they introduce infinities in the physical region which correspond to zeros in the

amplitudes. However, in the presence of any inelastic scattering the elastic scattering has a lower bound which is non-zero. The CDD poles may still exist, but are moved off the real axis into the negative half energy-plane. Such poles can be treated by computer. For the case of purely elastic pion-pion scattering solutions exhibiting a P-wave resonance were found by Bransden and Moffat.[17] A program including inelastic scattering was then run by Bransden, Gatland and Moffat[18] and solutions with CDD poles appeared but with one peculiar property. The CDD pole always occurred close to the original P-wave resonance position. The result of this pole was to split the resonance into two parts, one on each side of the CDD pole, but still close together. It appeared that in any P-wave resonance type of solution a CDD pole could be placed close to the resonance position without disturbing the consistency requirements of the analysis, in particular, the crossing equations. The position and strength of the pole was not completely arbitrary, however, but was restricted somewhat by the crossing equations.[19]

Section 4. The Importance of the CDD Pole

The split resonance solution produced from contributions of inelastic intermediate states implies that two particles with identical quantum numbers but slightly different masses can exist. This hypothesis has not yet been tested for scattering amplitudes of particles with unequal masses. It would be of considerable interest to verify the theoretical possibility of such resonances for this case for two reasons. First, the structure of many resonances observed experimentally is nebulous and it is possible that a split resonance is being observed in some

of these data. Second, the existence of two particles with the same quantum numbers and different masses might help to solve some of the difficulties that have been encountered in the mass formulas derived from SU(3) symmetry.

An analysis of the pion-nucleon interaction including a CDD pole would be desirable since this interaction is experimentally observable. The intrinsic angular momentum of the nucleon, however, complicates the mathematics of the analysis. The Kaon has the same I-spin as the nucleon so that the pion-kaon interaction is analogous to the pion-nucleon interaction in all respects except spin angular momentum. Unfortunately this interaction is observable only indirectly due to the short lifetime of the Kaon (10^{-8} sec).

Section 5. The K^* Meson

A meson resonance, the K^*, first reported by Alston *et al.*,[20] appears as a peak in the πK mass distribution in reactions like

$$K^- + p \rightarrow \begin{cases} p + \bar{K}^o + \pi \\ p + K^- + \pi^o \end{cases} \qquad (1.1a)$$

and

$$K^+ + p \rightarrow p + K^o + \pi^+. \qquad (1.1b)$$

This resonance has a mass of about 885 MeV, and a width, Γ = 50 MeV. The data is shown in Figure 2. The I-spin is determined to be 1/2 from the observation of the branching ratio

$$R = \frac{\Gamma(K^{*-} \rightarrow \bar{K}^{o} + \pi^{-})}{\Gamma(K^{*} \rightarrow K^{-} + \pi^{o})} = 1.4 \pm 0.4 \qquad (1.2)$$

which is predicted to be two if I = 1/2 and 1/2 if I = 3/2. This assignment is confirmed by the absence of a peak in the $\pi^{-}K^{o}$ spectrum in the reaction

$$\pi^{-} + p \rightarrow \Sigma^{+} + \pi^{-} + K^{o}. \qquad (1.3)$$

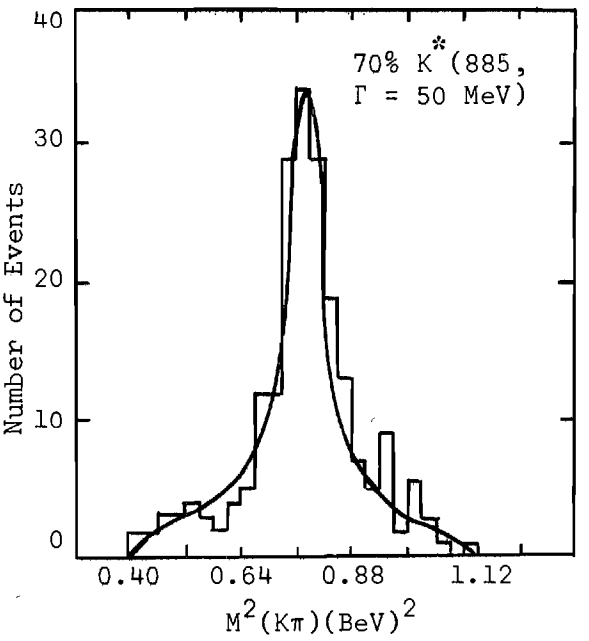

Figure 2. $M^2(K\pi)$ for 209 $\Sigma^0 K^+ \pi^-$ Events at Incident Pion Momenta of 2.17 and 2.25 BeV/c. The Curve Represents a Breit-Wigner Resonance Form for the K^* with Mass 885 MeV and Full Width at Half-Maximum Γ = 50 MeV, Weighted with Nonresonant Phase Space (70% K^*, 30% Phase Space). This Curve Was Taken from Article by Gerald A. Smith, *et al.*, Reference 21.

Gerald A. Smith *et al.*[21] present convincing evidence that the K^* has spin one and odd spatial parity based on a spin-alignment effect in the reaction $\pi^- p \to \Sigma^o K^*$. In an attempt to observe the K^* spin-alignment effects, three angles are constructed, α, β, and γ, all of which are measured in the K^* rest system: α is the angle of decay with respect to a unit vector $\hat{n}$ normal to the production plane for the two-body final state; β is the angle of decay with respect to a unit vector $\hat{I}$ along the direction of the incident pion in the K^* rest frame; and γ is the angle of decay with respect to the direction $\hat{I} \times \hat{n}$. The experimental distributions in three angles are given in Figure 3. The curves are a result of a maximum-likelihood fit to a polynomial in the cosine of the angle up to second order. The data in $\cos\alpha$ and $\cos\gamma$ are fit satisfactorily with only terms in even powers of $\cos\alpha$ and $\cos\gamma$, whereas the distribution in $\cos\beta$ is essentially isotropic. If the spin of the K^* is assumed to be 1^-, a single K and K^* exchange model, as shown in Figure 4, provides a satisfactory fit to these data providing a mixture of the K and K^* exchange is allowed.

There is now evidence for nine vector mesons and it is pertinent to ask how these fit into the unitary symmetry scheme. The ρ-meson with $Y = 0$ and $T = 1$ and the K^*-meson with $Y = \pm 1$ and $T = 1/2$ seem like good candidates for an octet assignment with either the ω or the ϕ, both of which have $Y = 0$ and $T = 0$, with the remaining meson perhaps belonging to the singlet representation.

An application of the Gell-Mann-Okubo mass formula predicts that the mass of the $Y = T = 0$ member of the octet should be given by

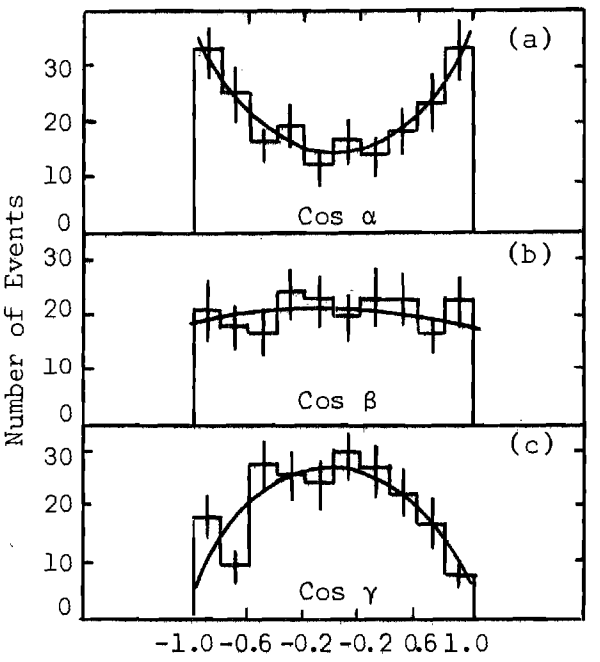

Figure 3. (a) K^* Decay Relative to the Normal, $\hat{n}$, to the $\Sigma^0 K^*$ Production Plane. The Curve is an Independent Maximum-Likelihood Fit of the Form $1 + (1.59 \pm 0.55)\cos^2\alpha$ with a χ^2 Value of 2.4 for Eight Degrees of Freedom. (b) K^* Decay Relative to $\hat{I}$, the Direction of the Incident Pion in the K^* Rest Frame. The Curve is an Independent Maximum-Likelihood Fit of the Form $1 - (0.11 \pm 0.21)\cos^2\beta$ with a χ^2 Value of 2.7 for Eight Degrees of Freedom. (c) K^* Decay Relative to $\hat{I} \times \hat{n}$. The Curve is of the Form $1 - (0.74 \pm 0.11)\cos^2\gamma$ with a χ^2 Value of 12.9 for Eight Degrees of Freedom. This Curve Was Taken from Article by Gerald A. Smith, *et al.*, Reference 21.

$$m^2 = \frac{4m^2(K^*) - m^2(\rho)}{3} = (930\ \text{MeV})^2, \qquad (1.4)$$

(if, as customary for bosons, m^2 is used in the formula). The mass of the ω is about 782 MeV and the mass of the ϕ is 1020 MeV, so neither particle has a mass which is close to the predicted value. Sakurai[22] has suggested a way to save the mass formula by pointing out that since SU(3) is a badly violated symmetry, there will be transitions between the unitary singlet eigenstate and the i-spin singlet member of the octet. The transitions will be "medium strong" because they violate SU(3) but not i-spin conservation. The singlet member of the octet and the unitary singlet are then written as a mixture of the ω and the ϕ.

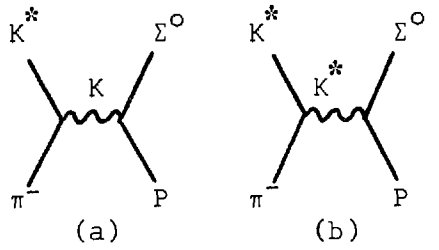

Figure 4. Possible Diagrams Contributing to ΣK^* Production

Another approach to the problem of saving the mass formula might be to observe that the ρ and/or the K^* resonances might actually be split by the presence of a CDD pole near the dynamical resonance position. The mechanism by which the pole is introduced is not well understood, but it is presumably "medium strong" in nature. The "mass" of the ρ and the K^*

which should be used in the mass formula is the mass associated with the primitive resonance position. It is also possible within the framework of this theory to note that the ω and the ϕ might be the two parts of a single resonance split by a medium strong interaction (CDD pole). The primitive resonance position would then be about 900 MeV, which offers a much better fit in the mass formula. It has already been shown that the ρ could be split by the introduction of a CDD pole.[18] To determine whether or not the K^* could be split is one of the objectives of this thesis.

CHAPTER II

A FORMAL SOLUTION FOR PION-KAON SCATTERING

Section 1. The Invariant Amplitude

For a given scattering process a collision operator S can be defined such that

$$P_{fi} = |\langle f|S|i\rangle|^2, \tag{2.1}$$

where P_{fi} is the probability of a transition from a given initial state $|i\rangle$ to a final state $|f\rangle$. In order to insure the conservation of angular momentum, S is assumed to be a rotationally invariant operator. Furthermore, the fact that there must be a unit probability for the system to end in *some* state, together with the physical assumption that the states $S|i\rangle$ are complete implies that the S-matrix, $\langle f|S|i\rangle$, must be unitary.

For reasons of convenience, in his 1945 paper, Möller[18] introduced a matrix S-1 and then in addition factored out an energy-momentum delta function, leaving a Lorentz-invariant function of n-1 momentum variables, where n is the number of particles involved (incoming and outgoing). For the case n = 4, this reduced matrix is referred to as the "invariant amplitude." There is no standard normalization of this invariant amplitude; therefore it will be chosen as close as possible to the "physical amplitude" $f(\theta)$, which is defined except for a phase, by the barycentric

system differential cross-section formula

$$\frac{d\sigma}{d\Omega} = \frac{q_f}{q_i} |f(\theta)|^2. \tag{2.2}$$

Here q_f and q_i are the final and initial magnitudes of the momenta and θ is the scattering angle. Of course q_f and q_i are equal for elastic scattering. The phase will be conventional, i.e. $f(\theta)$ becomes real as the interaction becomes weak, positive for attraction and negative for repulsion in the elastic case. In particular, for elastic scattering of particles with zero spin,

$$f(\theta) = \frac{1}{q} \sum_{\ell=0}^{\infty} (2\ell+1) e^{i\delta_\ell} \sin\delta_\ell P_\ell(\cos\theta), \tag{2.3}$$

where δ_ℓ is the phase shift in the state of orbital angular momentum ℓ. Möller[23] showed that the factor connecting the physical amplitude for zero spin to the invariant amplitude is simply W, the total energy in the barycentric system. Thus the invariant amplitude A is normalized by the formula

$$A = \frac{W}{2} f. \tag{2.4}$$

This particular choice of normalization corresponds to the choice made by Chew and Low[12] for pion-pion scattering. This normalization is not universal. In particular, Lee[24] and later Lee and Cho[25] chooses A = Wf in their papers on pion-Kaon scattering. For particles with zero spin,

the invariant amplitude A can depend only on the invariants that can be formed from the three independent four-momenta remaining after energy-momentum conservation is applied.

Section 2. Kinematics

A scattering problem involving pions and Kaons in which there are two incoming particles and two outgoing particles is of concern here. The symbols (p_1,α) and $(-p_3,\beta)$ represent the pion momenta and isospin indices of the incoming and outgoing pions, respectively, and p_2, $-p_4$ represent the incoming and outgoing Kaon momenta. Three reactions, usually called "Channels," are possible. They are

$$\text{I.}\quad \pi(p_1,\alpha) + K(p_2) \rightarrow \pi(-p_3,\beta) + K(-p_4), \tag{2.5a}$$

$$\text{II.}\quad \pi(p_3,\beta) + K(p_2) \rightarrow \pi(-p_1,\alpha) + K(-p_4), \tag{2.5b}$$

$$\text{III.}\quad \pi(p_1,\alpha) + \pi(p_3,\beta) \rightarrow \bar{K}(-p_2) + K(-p_4). \tag{2.5c}$$

The convenient invariant variables for the double dispersion representation are the squares of the total center-of-mass energies for the three reactions. Thus, the following variables are defined

$$s = (p_1+p_2)^2 = (p_3+p_4)^2, \tag{2.6a}$$

$$u = (p_3+p_2)^2 = (p_1+p_4)^2, \tag{2.6b}$$

$$t = (p_1+p_3)^2 = (p_2+p_4)^2. \tag{2.6c}$$

These variables s, u, and t are not independent, but are related by

$$s + u + t = 2(M^2+\mu^2), \tag{2.7}$$

where M is the Kaon mass and μ is the pion mass.

It will prove useful at times to express s, u and t in terms of the center-of-mass variables, the magnitude of the three-momenta and the scattering angle. For example, for reaction I, where k is the CM three-momentum and θ is the scattering angle

$$s = M^2 + \mu^2 + 2k^2 + 2\sqrt{(k^2+M^2)(k^2+\mu^2)}, \tag{2.8a}$$

$$t = -2k^2(1-\cos\theta), \tag{2.8b}$$

$$u = 2M^2 + 2\mu^2 - s - t. \tag{2.8c}$$

For reaction III, where p and q are the CM three-momenta for the Kaon and pion, respectively and φ is the scattering angle

$$s = -p^2 - q^2 + 2pq\cos\phi, \tag{2.9a}$$

$$u = -p^2 - q^2 - 2pq\cos\phi, \tag{2.9b}$$

$$t = 4(p^2+M^2) = 4(q^2+\mu^2). \qquad (2.9c)$$

Section 3. Charge States

The degrees of freedom of charge and spin have been ignored in Eqs. (2.4) and (2.5). However, internal degrees of freedom may always be absorbed into invariant matrices whose coefficients are invariant functions of the s, u, and t variables only. The number of such functions depends on the complexity of the internal degrees of freedom, and generally the vector addition rule can be used in counting. For example, the pion has zero spin and isotopic spin 1, while the kaon has zero spin and isotopic spin 1/2. For the K-K system, the total spin is zero and the different possible total I-spin values are 0 and 1, so two independent invariant K-K amplitudes are required. The possible I-spin values for the π-K system are 1/2 and 3/2 and the total spin is zero, so again two independent invariant π-K amplitudes are required. If either one or both of the incoming particles has a non-zero spin the counting would of course be more complicated and the total number of invariant amplitudes would be increased. For example, in the π-N system where the nucleon has a spin of 1/2, there are four invariant amplitudes.

The construction of invariant spin matrices is not necessary for the π-K system since both particles have zero spin. The only problem is the construction of charge matrices. The choice of charge matrices is irrelevant to analyticity properties of the amplitudes, although certain choices may be more convenient than others for calculation.

A possible π-K reaction including the three channels for the reaction is shown in Figure 5.

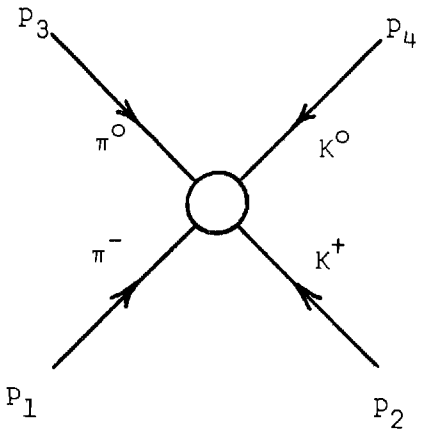

Figure 5. The Three Possible Channels for the πK Reaction:

I. $\pi^- + K^+ \rightarrow \pi^o + K^o$,

II. $\pi^o + K^+ \rightarrow \pi^+ + K^o$,

III. $\pi^- + \pi^o \rightarrow K^- + K^o$.

Now, rather than specifying the charge, the pion lines are labeled by the conventional isotopic vector index that takes on values 1, 2, 3. The index α is associated with a pion of momentum p_1 and an index β is associated with a pion of momentum p_3. Kaon charge degrees of freedom may be suppressed into initial and final isospiners, and the problem is then to form two charge-independent combinations of kaon isotopic-spin operators, τ_k. A possible choice is $\frac{1}{2}[\tau_\beta\tau_\alpha+\tau_\alpha\tau_\beta] = \delta_{\beta\alpha}$ and $\frac{1}{2}[\tau_\beta,\tau_\alpha]$, the one symmetric and the other antisymmetric under pion exchange. In terms of this choice of matrices, the complete amplitude for a π-K diagram of the type shown in Figure 1 has the form

$$A_{\beta\alpha} = A^{(+)}\delta_{\beta\alpha} + A^{(-)}\,[\tau_\beta,\tau_\alpha]. \tag{2.10}$$

For reaction I there are two independent isospin states, I = 1/2 and I = 3/2. The relations between the eigenamplitudes of total isospin, $A^{1/2}$ and $A^{3/2}$, and the amplitudes, $A^{(\pm)}$, are calculated in Appendix A. The results are

$$A^{1/2} = A^{(+)} + 2A^{(-)}, \tag{2.11a}$$

$$A^{3/2} = A^{(+)} - A^{(-)}. \tag{2.11b}$$

For reaction II, which is related to reaction I by an interchange of two pions, the obvious result is

$$\bar{A}^{1/2} = A^{(+)} - 2A^{(-)}, \tag{2.12a}$$

$$\bar{A}^{3/2} = A^{(+)} + A^{(-)}. \tag{2.12b}$$

And finally for reaction III

$$B^{(0)} = \sqrt{6}\,A^{(+)}, \tag{2.13a}$$

$$B^{(1)} = 2\,A^{(-)}, \tag{2.13b}$$

where $B^{(0)}$ and $B^{(1)}$ are the eigenamplitudes for the isospin states I = 0, and I = 1, respectively.

Section 4. Analyticity of the Amplitudes

It is now convenient to state the substitution law, which in the present framework takes a very simple form. It is postulated that a single analytic function of two variables, A(x,y), describes all three channels of the pion-kaon interaction. The variables x and y represent any two of the three variables, s, u, and t defined by Eq. (2.9). (Recall that only two of these three variables are independent.) The channel is selected by merely assigning the values of the variables. For example, if the variables s and t are chosen, A(s,t), is the amplitude for Channel I when s is the square of the CM total energy and t is the momentum transfer, and it is the amplitude for Channel III when s becomes the momentum transfer and t becomes the square of the CM total energy. For Channel II, this identification of these two variables is not quite so simple since u is the square of the CM total energy and t is the momentum transfer. However, s can be written in terms of u and t, and again the amplitude can be written as a function of the CM total energy and momentum transfer for this channel. Since the ranges for the three channels are non-overlapping, one must have a procedure of continuation to give this postulate any physical content. Such a procedure is provided by the Mandelstam representation, which postulates a singularity structure permitting analytic continuation between the three physical regions.

The Mandelstam representation is used for the two invariant amplitudes $A^{(+)}$ and $A^{(-)}$. This representation expresses $A^{(+)}$ and $A^{(-)}$ as analytic functions of the complex variables s, u, and t except for poles

on the real axis and cuts along certain hyperplanes. The poles come from bound states of the system, and the cuts come from the threshold energies for the allowed virtual transitions. Although s, u and t are not independent, it is useful to keep all three variables in order to write the amplitudes in a form which is symmetric in the three variables.

For the pion-kaon scattering problem discussed here, poles which are produced by bound states will not be included. If bound states do exist their effects can be taken into account at another point in the calculations. It is interesting to note, however, that MacDowell[26] has determined the cut plane for pion-nucleon scattering which includes such poles. The cuts in the s, u or t-planes are found directly from the Mandelstam representation, i.e.

$$A^{\pm} = \frac{1}{\pi^2} \int_{(M+\mu)^2}^{\infty} ds' \int_{(M+\mu)^2}^{\infty} du' \frac{A^{\pm}_{12}(s',u')}{(s'-s)(u'-u)} + \frac{1}{\pi^2} \int_{(M+\mu)^2}^{\infty} ds' \int_{4\mu^2}^{\infty} dt' \frac{A^{\pm}_{13}(s',t')}{(s'-s)(t'-t)}$$

$$+ \frac{1}{\pi^2} \int_{(M+\mu)^2}^{\infty} du' \int_{4\mu^2}^{\infty} dt' \frac{A^{\pm}_{23}(u',t')}{(u'-u)(t'-t)} . \qquad (2.14)$$

The spectral functions A_{ij} are non-zero only when an argument is equal to the square of the mass of an actual physical system that has the quantum numbers of the corresponding channel. It turns out that constraints exist on the possible masses that can occur in intermediate configurations for one channel, given the mass of the intermediate configuration of another channel. For example, the spectral function A_{13} will be non-zero to the right of curve C shown in Figure 6.

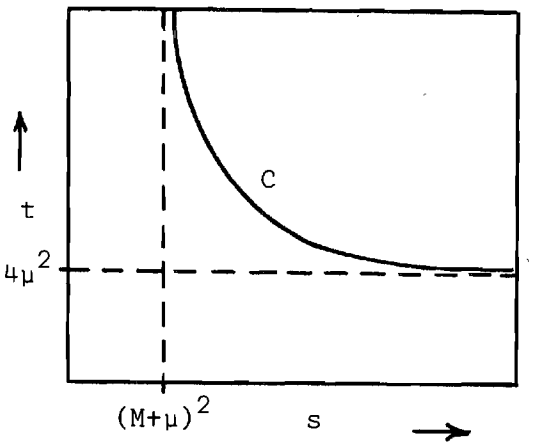

Figure 6. Region in Which the Spectral Function A_{13} is Non-Zero

The equation of C is calculated from pion-nucleon scattering by Mandelstam[11] on the basis of Feynman diagrams and by consistency requirements based on unitarity. The equation for the curve is given by

$$t^{\frac{1}{2}} = 2(M^2-x)^{\frac{1}{2}}[1 + (M^2-x)/4k^2]^{\frac{1}{2}}, \tag{2.15a}$$

where

$$k^2 = [s - (M+\mu)^2][s - (M-\mu)^2]/4s, \tag{2.15b}$$

and

$$x = (M^2-\mu^2)^2/s. \tag{2.15c}$$

This curve approaches asymptotically the lines $s = (M+\mu)^2$ and $t = 4\mu^2$. The spectral functions A_{12} and A_{23} will be non-zero in regions determined by similar curves.

Section 5. Singularities in the S-Plane

The singularities which arise in the s-plane for reaction I are due only to zero denominators in the integrals of the Mandelstam representation. These singularities lie on the lines of the complex s-plane defined by the equations

$$\begin{aligned} &\text{a.} \quad s' - s = 0, \\ &\text{b.} \quad u' - u = 0, \\ &\text{c.} \quad t' - t = 0, \end{aligned} \tag{2.16}$$

where s', u' and t' are parameters assuming the values within the limits of integration in Eq. (2.14). As s' takes on values along the real axis from $(M+\mu)^2$ to ∞ , the s-plane develops a cut from $(M+\mu)^2$ to ∞ along the real axis. This cut is usually called the 'physical' or 'unitary' cut for Channel I.

The cuts arising in the s-plane from the equations u' - u = 0 and t' - t = 0 are determined by writing u and t in terms of s and the scattering angle for reaction I, θ, and then allowing u' and t' to vary over their appropriate physical ranges while $\cos\theta$ varies from -1 to 1. The cuts in the s-plane due to these two equations, (2.16a) and (2.16b), are best handled separately, and are referred to as the cuts arising from the intermediate states of Channel II and Channel III, respectively.

The Cut Due to the Intermediate States of Channel II

In order to determine the values of s for which the equation u' - u = 0, recall the Equations (2.8a), (2.8b), and (2.8c) which related u and t to the CM-momentum, k, and the scattering angle, θ, i.e.

$$t = -2k^2(1-\cos\theta), \tag{2.17a}$$

$$u = 2M^2 + 2\mu^2 - s - t, \tag{2.17b}$$

and

$$k^2 = \frac{(s - (M+\mu)^2)(s - (M-\mu)^2)}{4s} \tag{2.17c}$$

Then u is written

$$u = 2M^2 + 2\mu^2 - s + \frac{(s - (M+\mu)^2)(s - (M-\mu)^2)}{2s}(1-\cos\theta). \tag{2.18}$$

The equation u' - u is then a quadratic in s which may be written

$$(1+z)s^2 + 2[u' - (1+z)(M^2+\mu^2)]s - (1-z)(M^2-\mu^2)^2 = 0, \tag{2.19}$$

where

$$z = \cos\theta. \tag{2.20}$$

The two solutions for s are easily found from the quadratic formula. They are

$$s = \frac{-[u' - (1+z)(M^2+\mu^2)] \pm \sqrt{[(u' -(1+z)(M^2+\mu^2)]^2 + (1+z)(1-z)(M^2-\mu^2)^2}}{(1+z)} \tag{2.21}$$

The root when the positive sign is chosen in front of the radical is called s_1 and the root when the negative sign is chosen in front of the

radical is called s_2. Then

$$\lim_{z\to+1} s_1 = \frac{-[u'-2(M^2+\mu^2)] + \sqrt{[u'-2(M^2+\mu^2)]^2 + 0}}{2} = 0. \qquad (2.22)$$

The limit of s_1 as z approaches -1 is the indeterminate form of 0/0. L'Hospital's rule may be applied in this case and when the numerator and the denominator are differentiated with respect to z+1 the following result is obtained

$$\lim_{z\to-1} s_1 = \frac{(M^2-\mu^2)^2}{u'} . \qquad (2.23)$$

For s_2 we have

$$\lim_{z\to+1} s_2 = 2(M^2+\mu^2) - u', \qquad (2.24)$$

and

$$\lim_{z\to-1} s_2 = -\infty. \qquad (2.25)$$

The variable u' is now allowed to run from $(M+\mu)^2$ to ∞ to determine the cuts arising from this channel. From Eq. (2.22) we have the point s = 0, and from Eq. (2.23) we have

$$\lim_{u'\to\infty} \frac{(M^2-\mu^2)^2}{u'} = 0, \qquad (2.26)$$

$$\lim_{u' \to (M+\mu)^2} \frac{(M^2-\mu^2)^2}{u'} = (M-\mu)^2. \tag{2.27}$$

From Eq. (2.24) we have

$$\lim_{u' \to \infty} [2(M^2+\mu^2) - u'] = -\infty, \tag{2.28}$$

$$\lim_{u' \to (M+\mu)^2} [2(M^2+\mu^2) - u'] = (M-\mu)^2. \tag{2.29}$$

From Equations (2.22) and (2.23) note that the root s_1 assumes values between 0 and $(M^2-\mu^2)^2/u'$ as z varies from 1 to -1. The upper limit then varies from $(M-\mu)^2$ to 0 as u' runs from $(M+\mu)^2$ to ∞, as shown by Equations (2.26) and (2.27). Thus, the s-plane must contain a cut from 0 to $(M-\mu)^2$. The root, s_2, assumes values from $-\infty$ to $2M^2 + 2\mu^2 - u'$ as z varies from -1 to 1 as shown by Equations (2.24) and (2.25). As u' runs from $(M+\mu)^2$ to ∞, the upper limit varies from $(M-\mu)^2$ to $-\infty$, as shown in Equations (2.28) and (2.29). Therefore, an additional cut which runs from $-\infty$ to $(M-\mu)^2$ is necessary in the s-plane.

The Cut Due to the Intermediate States of Channel III

This cut arises when t' - t = 0. The expression may be written as

$$t' - 2k^2(1-z) = 0, \tag{2,30}$$

where again we let $z = \cos\theta$. This expression is solved for k^2 to give

$$k^2 = \frac{-t'}{2(1-z)} . \tag{2.31}$$

The right-hand side of this equation varies from $-\infty$ to $-\mu^2$ as t' varies from $4\mu^2$ to ∞ and z varies from -1 to +1. Now k^2 is expressed as a function of s and s is observed as k^2 varies from $-\infty$ to $-\mu^2$. Recall that

$$s_{\pm} = M^2 + \mu^2 + 2k^2 \pm 2\sqrt{(M^2+k^2)(\mu^2+k^2)}. \tag{2.32}$$

Then

$$\lim_{k^2\to-\infty} s_+ = -\infty, \tag{2.33}$$

$$\lim_{k^2\to-M^2} s_+ = -(M^2-\mu^2), \tag{2.34}$$

The limit of s_- as k^2 approaches $-\infty$ is of the form 0/0. L'Hospital's rule is applied here to give the result

$$\lim_{k^2\to-\infty} s_- = 0, \tag{2.35}$$

and, finally

$$\lim_{k^2\to-M} s_- = -(M^2-\mu^2). \tag{2.36}$$

Thus for k^2 from $-\infty$ to $-M^2$, both solutions for s are real and describe two branch lines on the real axis from $-\infty$ to $-(M^2-\mu^2)$, and from $-(M^2-\mu^2)$ to 0. Now, as k^2 varies from $-M^2$ to $-\mu^2$, s becomes complex, with the two roots

$$s_{\pm} = M^2 + \mu^2 + 2k^2 \pm 2i\sqrt{-(M^2+k^2)(\mu^2+k^2)}. \qquad (2.37)$$

Note that in the region of complex s,

$$|s| = (M^2-\mu^2) = \text{constant}. \qquad (2.38)$$

Thus, there is a cut in the s-plane around the circumference of a circle of radius $(M^2-\mu^2)$ and center at the origin. Also note that

$$\lim_{k^2\to-\mu^2} s_- = +(M^2-\mu^2). \qquad (2.39)$$

The cut s-plane is shown in Figure 7.

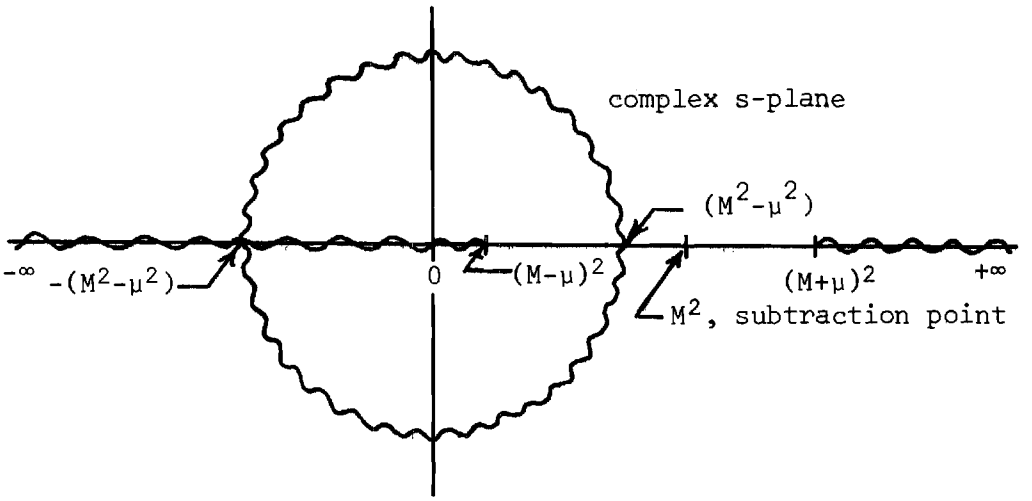

Figure 7. The Cut s-Plane (~ Denotes Cut)

Section 6. Singularities in the t-Plane

The cuts in the t-plane for reaction III are found in a manner similar to that employed in the previous calculations. The equations which give s, u and t in terms of the CM momenta p^2 and q^2 of the kaon and the pion, respectively, and ϕ, the CM scattering angle, are

$$s = -p^2 + 2pq\cos\phi - q^2 \tag{2.40a}$$

$$t = 4(p^2+M^2) = 4(q^2+\mu^2), \tag{2.40b}$$

$$u = -s - t + 2M^2 + 2\mu^2. \tag{2.40c}$$

The physical cut comes from the expression

$$t' - t = 0. \tag{2.41}$$

This cut runs from $4\mu^2$ to ∞ as t' varies from $4\mu^2$ to ∞.

The left-hand or "unphysical" cuts are given by

$$u' - u = 0, \tag{2.42a}$$

$$s' - s = 0. \tag{2.42b}$$

By writing u and s in terms of t and ϕ in the above equations and then letting $\cos\phi$ vary from -1 to +1 and u' and s' vary from $(M+\mu)^2$ to ∞,

cuts develop from $-\infty$ to 0. The cut t-plane is shown in Figure 9, shown on page 39.

It will be convenient to think of the cut s-plane as containing three sets of singularities: (1) the "physical" cut from $(M+\mu)^2$ to ∞ along the positive real axis, (2) the "circular" cut due to the intermediate states of Channel III, and (3) the "left" cut from $-\infty$ to $(M-\mu)^2$ along the real axis due to the intermediate states of Channel II and Channel III.

From perturbation theory it appears that a subtraction constant is needed for the amplitude $A^{(+)}(s,t)$. The subtraction point is in principle arbitrary, but for convenience the following conditions are imposed on the subtraction point: First, it must be symmetric in s and u, and secondly it should not overlap with the singularities of the partial wave amplitudes. A convenient point, satisfying the above criteria, is

$$s_o = u_o = M^2, \quad t_o = 2\mu^2,$$
$$s_o + u_o + t_o = 2M^2 + 2\mu^2. \tag{2.43}$$

Other subtraction points satisfying the same criteria may be chosen in subsequent calculations, but the point defined above will be used unless otherwise noted.

Section 7. Partial Wave Amplitudes

A partial-wave amplitude for Channel I is defined by

$$A_\ell^I(s) = \frac{1}{2}\int_{-1}^{1} d\cos\theta\ P_\ell(\cos\theta)\ A^I(s,t(\cos\theta)), \qquad (2.44)$$

where I can be either 1/2 or 3/2. In a certain region--including the physical interval s greater than $(M+\mu)^2$ and $\cos\theta$ between 1 and -1--the full amplitude can be represented by the series

$$A^I(s,t(\cos\theta)) = \sum_{\ell=0}^{\infty} (2\ell+1)\ A_\ell^I(s)\ P_\ell(\cos\theta), \qquad (2.45)$$

but even outside this region $A_\ell^I(s)$ may be defined by Equation (2.44). In fact, $A_\ell^I(s)$ shall be extended to the entire complex s-plane, where three sets of singularities were found in $A^I(s,u,t)$ corresponding to the three channels of the problem. Then $A_\ell^I(s)$ is analytic in the cut s-plane shown in Figure 7 on page 31.

From Equations (2.3) and (2.4) the following expression is written for $A_\ell^I(s)$,

$$A_\ell^I(s) = \frac{\sqrt{s}}{2k} \exp(i\delta_\ell^I)\ \sin\delta_\ell^I, \qquad (2.46a)$$

where k is the CM-momentum for Channel I and is related to the square of the CM-total energy, s, by

$$k^2 = [s - (M+\mu)^2][s - (M-\mu)^2]/4s. \qquad (2.46b)$$

For Channel III, it is more convenient to write the partial wave amplitudes in terms of $A^{\pm}(s,t)$ rather than the eigenamplitudes, $B^{(0,1)}(s,t)$ by

$$B_{\ell}^{\pm}(t) = \frac{1}{2}\frac{1}{(pq)^{\ell}}\int_{-1}^{1} d(\cos\phi)P_{\ell}(\cos\phi)\ A^{\pm}(s(\cos\phi),t), \qquad (2.47)$$

where q and p are the incoming pion momentum and outgoing kaon momentum, respectively, and ϕ is the CM-scattering angle for reaction III. The $B_{\ell}^{\pm}(t)$ are related to the $B_{\ell}^{(0,1)}(t)$ through Equations (2.13a) and (2.13b) and have particularly simple analytic properties which will be discussed in the next section. The corresponding functions for the case of pion-nucleon scattering have been discussed in detail by Frazer and Fulco.[29] The momenta p and q are related to t by the equations

$$t = 4(p^2+M^2) = 4(q^2+\mu^2). \qquad (2.48)$$

Section 8. Dispersion Relations

A subtracted form of the dispersion relation for the partial-wave amplitudes will be written. It is unlikely that a subtraction is needed for the P-wave, but a subtraction is most surely needed for the S-wave, so it will be included in the general form. To obtain the dispersion relation, Cauchy's integral theorem is applied for the contour Γ shown in Figure 8.

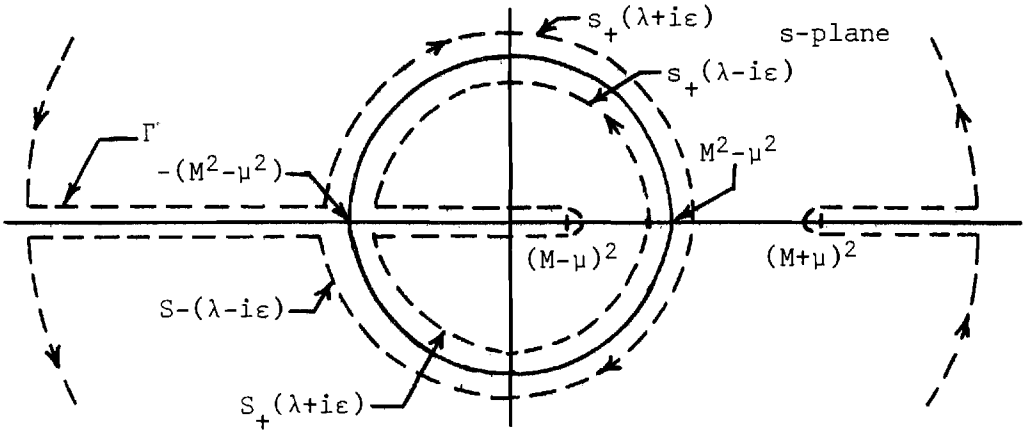

Figure 8. Contour of Integration for Cauchy's Integral Theorem

Then

$$A_\ell^I(s) = \alpha_\ell^I + \frac{s - M^2}{2\pi i} \int_\Gamma \frac{ds'\ A_\ell^I(s')}{(s'-s)(s'-M^2)}\ , \qquad (2.49)$$

where the subtraction point is taken to be M^2.

The integration around the outer circle is taken in the limit as the radius of the circle approaches infinity. In this limit, it is assumed that the integrand vanishes; therefore there is no contribution from that segment of the contour. If the remaining part of the contour is divided into sections, $A_\ell^I(s)$ becomes

$$A_\ell^I(s) = \alpha_\ell^I + \frac{s - M^2}{2\pi i} \int_{-\infty}^{(M-\mu)^2} \frac{ds'\ A_\ell^I(s'+i\varepsilon)}{(s'-s)(s'-M^2)} + \frac{s - M^2}{2\pi i} \int_{(M-\mu)^2}^{-\infty} \frac{ds'\ A_\ell^I(s'-i\varepsilon)}{(s'-s)(s'-M^2)}$$

$$+ \frac{s - M^2}{2\pi i} \int_{(M+\mu)^2}^{\infty} \frac{ds'\ A_\ell^I(s'+i\varepsilon)}{(s'-s)(s'-M^2)} + \frac{s - M^2}{2\pi i} \int_{\infty}^{(M+\mu)^2} \frac{ds'\ A_\ell^I(s'-i\varepsilon)}{(s'-s)(s'-M^2)}$$

$$+\frac{s-M^2}{2\pi i}\int_{-(M^2-\mu^2)\text{ around upper half-circle}}^{M^2-\mu^2}\frac{ds'\ A_\ell^I(s'\text{ above cut})}{(s'-s)(s'-M^2)}+\frac{s-M^2}{2\pi i}\int_{(M^2-\mu^2)\text{ around upper half-circle}}^{-(M^2-\mu^2)}\frac{ds'\ A_\ell^I(s'\text{ below cut})}{(s'-s)(s'-M^2)}$$

+ terms similar to the two above for lower half-circle. (2.50)

Now a dummy variable of integration is defined by

$$s_\pm = 2\lambda + M^2 + \mu^2 \pm 2i\sqrt{(M^2+\lambda)(-\mu^2-\lambda)}, \tag{2.51}$$

which takes s_+ around the upper half-circle and s_- around the lower half circle as it takes on values from $-M^2$ to $-\mu^2$. Thus a change of variables from s' to λ for the four terms involving the circular cut allows an integration over a real variable. For the upper half-circle

$$ds' = ds_+ = \frac{2s_+ d\lambda}{(s_+-M^2-\mu^2-2\lambda)}, \tag{2.52}$$

and for the lower half-circle

$$ds' = ds_- = \frac{2s_- d\lambda}{(s_--M^2-\mu^2-2\lambda)}. \tag{2.53}$$

Now, if the limit as ε approaches zero is taken, the first two terms can be combined under one integral ($-\infty$ to $(M-\mu)^2$), the third and fourth terms can be combined under an integral from $(M+\mu)^2$ to ∞, the fifth and

sixth terms can be combined under an integral that goes from $-(M^2-\mu^2)$ to $(M^2-\mu^2)$ around the upper half-circle, and the seventh and eighth terms can be combined under an integral around the lower half-circle. In addition, note that $A_\ell^I(s)$ is a real analytic function since it is real on the real axis, thus the discontinuity across the cuts along the real axis is just 2i times the imaginary part of $A_\ell^I(s)$. Then

$$\lim_{\epsilon\to 0} \frac{1}{2i} [A_\ell^I(s+i\epsilon) - A^I(s-i\epsilon)] = \text{Im } A^I(s), \tag{2.54a}$$

$$\lim_{\epsilon\to 0} \frac{1}{2i} [A_\ell^I(s_\pm(\lambda+i\epsilon)) - A_\ell^I(s_\pm(\lambda-i\epsilon))] = M_\ell^I(s_\pm), \tag{2.54b}$$

where the second equation is just the defining equation for $M_\ell^I(s_\pm)$. The dispersion relation is now written

$$A_\ell^I(s) = \alpha_\ell^I + \frac{s-M^2}{\pi}\int_{(M+\mu)^2}^{\infty} \frac{ds'\ \text{Im } A_\ell^I(s')}{(s'-s)(s'-M^2)} + \frac{s-M^2}{\pi}\int_{-\infty}^{(M-\mu)^2} \frac{ds'\,\text{Im } A_\ell^I(s')}{(s'-s)(s'-M^2)}$$

$$+ F_\ell^I(s) + F_\ell^{I*}(s^*), \tag{2.55}$$

where

$$F_\ell^I(s) = \frac{s-M^2}{\pi}\int_{-M^2}^{-\mu^2} \frac{d\lambda\ 2s_+(\lambda)\ M^I(s_+)}{(s_+-M^2-\mu^2-2\lambda)(s_+-s)(s_+-M^2)}. \tag{2.56}$$

For real s, Equation (2.55) can be rewritten by combining the last two functions, $F_\ell^I(s)$ and $F_\ell^{I*}(s^*)$.

$$F_\ell^I(s) + F_\ell^{I*}(s^*) = \frac{s - M^2}{\pi} \int_{-M^2}^{-\mu^2} \frac{d\lambda\ 2s_+ M_\ell^I(s_+)g^* + 2s_+^* M_\ell^I(s_+^*)g}{|g|^2} . \qquad (2.57)$$

where $g = (s_+ - M^2 - \mu^2 - 2\lambda)(s_+ - s)(s_+ - s_o)$. The integrand is now in the form of an identity for complex variables, i.e.

$$\frac{gf^* + g^*f}{|f|^2} = 2\ \mathrm{Re}(g/f), \qquad (2.58)$$

thus,

$$F_\ell^I(s) + F_\ell^{I*}(s^*) = \frac{2(s-s_o)}{\pi}\ \mathrm{Re} \int_{-M^2}^{-\mu^2} \frac{d\lambda\ 2s_+ M_\ell^I(s_+)}{(s_+ - M^2 - \mu^2 - 2\lambda)(s_+ - s_o)(s_+ - s)} . \qquad (2.59)$$

Section 9. Dispersion Relations for t-Plane

The t-plane is less complicated than the s-plane. The cut plane together with a contour Γ are shown in Figure 9.

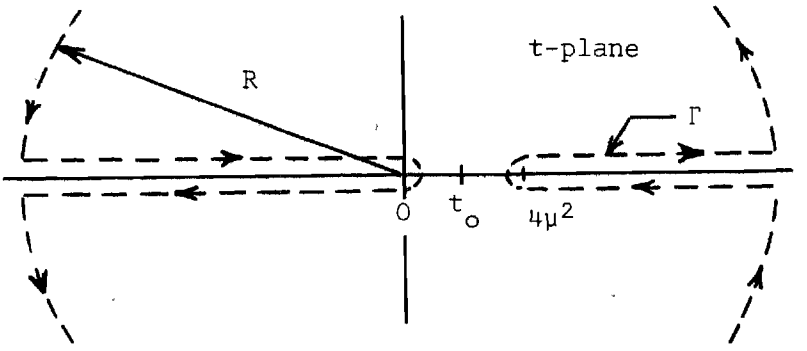

Figure 9. The Cut t-Plane and Contour of Integration

The Cauchy integral is applied to the contour Γ. The integral around the circle vanishes in the limit as R approaches infinity provided the amplitudes decrease rapidly enough. Note that the Pauli principle admits only symmetric states for this process. For I = 0, (1), the two pions in the initial channel must be an even (odd) angular momentum state. The dispersion relations for Channel III (t-plane) derived from integrations around the contour are

$$B_\ell^\pm(t) = \beta_\ell^\pm + \frac{(t-t_o)}{\pi}\int_{-\infty}^{o} \frac{dt' \ \mathrm{Im}\ B_\ell^\pm(t')}{(t'-t)(t'-t_o)} + \frac{(t-t_o)}{\pi}\int_{4\mu^2}^{\infty} \frac{dt' \ \mathrm{Im}\ B_\ell^\pm(t')}{(t'-t)(t'-t_o)} . \quad (2.60)$$

CHAPTER III

THE CROSSING EQUATIONS

Section 1. Crossing Symmetry

A principle related to the substitution law, which applies when there are two or more identical particles among the four involved in a particular diagram, is the "crossing symmetry." Exchanging two identical particles at most changes the sign of the amplitude, and such an interchange means switching two of the variables s, u, and t, and leaving the third alone. For example, suppose particles 1 and 3 are identical. Then, depending on whether these are bosons or fermions, the amplitude is either symmetric or antisymmetric under the exchange of p_1 and p_3, that is, interchanging s and u, leaving t alone. If particles 1 and 3 are both incoming or both outgoing--the symmetry in question is just the Pauli principle. If one is incoming and the other outgoing, however, the symmetry cannot be so identified. In this case, if one starts with physical values of s, u, and t, the exchange in question necessarily leads to non-physical values because of the non-overlapping nature of the energy and momentum transfer ranges. Thus crossing symmetry has a general meaning only when continuation of the amplitude into unphysical regions is possible. Such a continuation is of course allowed by the Mandelstam representation.

This proposed "crossing symmetry" can be used in order to determine the partial-wave amplitudes in any scattering problem involving two

or more identical particles, such as the pion-kaon interaction. Through crossing symmetry it is possible to relate the discontinuities across the unphysical cuts of the partial-wave amplitudes to the discontinuities across its physical cuts. Such a relation is called a "crossing equation." Once the discontinuities across all the cuts are known, the dispersion relations then determine the partial-wave amplitudes to within a subtraction constant.

In the following sections the crossing equations for the s-plane (the physical region for Channel I) and the t-plane (the physical region for Channel III) of the pion-kaon interaction are derived from the Mandelstam representation. But first, it will be useful to exhibit the connection between the Mandelstam representation, Equation (2.14), and one-dimensional dispersion relations. First observe that in the physical region of Channel I, say, the only denominators that vanish in Equation (2.14) are those containing the factor s'-s. Remembering the identity

$$\frac{1}{s' - s} = P \frac{1}{s' - s} + i\pi\delta(s'-s), \tag{3.1}$$

the imaginary part of A in this region is easily calculated to be

$$A_1^{\pm}(s,u,t) = \frac{1}{\pi} \int_{(M+\mu)^2}^{\infty} du' \frac{A_{12}^{\pm}(s,u')}{u' - u} + \frac{1}{\pi} \int_{4\mu^2}^{\infty} dt' \frac{A_{13}^{\pm}(s,t')}{t' - t} . \tag{3.2}$$

Outside this region $A_1(s,u,t)$ is *defined* by the above equation and referred to as the absorptive part for Channel I even though it will

itself become complex when one of the remaining denominators in Equation (2.14) vanishes. Note that for fixed s, A_1 is an analytic function of t (or u) with u (or t) determined by the relation $s + u + t = 2M^2 + 2\mu^2$.

In a similar way the functions $A_2^{\pm}(s,u,t)$ and $A_3^{\pm}(s,u,t)$ are defined to be the absorptive parts for Channels II and III, respectively, and are written

$$A_2^{\pm}(s,u,t) = \frac{1}{\pi}\int_{(M+\mu)^2}^{\infty} ds' \frac{A_{12}^{\pm}(s',u)}{s' - s} + \frac{1}{\pi}\int_{4\mu^2}^{\infty} dt' \frac{A_{23}^{\pm}(u,t')}{t' - t}, \quad (3.3)$$

$$A_3^{\pm}(s,u,t) = \frac{1}{\pi}\int_{(M+\mu)^2}^{\infty} ds' \frac{A_{13}^{\pm}(s',t)}{s' - s} + \frac{1}{\pi}\int_{(M+\mu)^2}^{\infty} du' \frac{A_{23}^{\pm}(u',t)}{u' - u}. \quad (3.4)$$

It is then simply a matter of algebra to verify that the Mandelstam representation can be written in three possible ways in terms of $A_1^{\pm}$, $A_2^{\pm}$, and $A_3^{\pm}$:

$$A^{\pm}(s,u,t) = \frac{1}{\pi}\int_{(M+\mu)^2}^{\infty} du' \frac{A_2^{\pm}(s,u',2M^2+2\mu^2-s-u')}{(u'-u)}$$

$$+ \frac{1}{\pi}\int_{4\mu^2}^{\infty} dt' \frac{A_3(s,2M^2+2\mu^2-s-t',t')}{(t'-t)}, \quad (3.5)$$

$$= \frac{1}{\pi}\int_{(M+\mu)^2}^{\infty} ds' \frac{A_1(s',u,2M^2+2\mu^2-s'-u)}{(s'-s)}$$

$$+ \frac{1}{\pi} \int_{4\mu^2}^{\infty} dt' \frac{A_3^{\pm}(2M^2+2\mu^2-u-t',u,t')}{(t'-t)} , \tag{3.6}$$

$$= \frac{1}{\pi} \int_{(M+\mu)^2}^{\infty} ds' \frac{A_1(s',2M^2+2\mu^2-s'-t,t)}{(s'-s)}$$

$$+ \frac{1}{\pi} \int_{(M+\mu)^2}^{\infty} du' \frac{A_2(2M^2+2\mu^2-u'-t,u',t)}{(u'-u)} , \tag{3.7}$$

The first form is usually called the one-dimensional dispersion relation for fixed s, the second for fixed u, and the third for fixed t.

Section 2. The Crossing Equations for S-Plane

In this section, an equation relating the absorptive part of the amplitudes, $A_\ell^I(s)$, on the unphysical cut to the absorptive parts of $A_\ell^I(s)$ and $B_\ell^{\pm}(t)$ on their physical cuts is derived. The total amplitude as given by Equation (2.65) is in a convenient form for calculating the absorptive part of the partial-wave amplitudes in the unphysical region of Channel I. Recall the defining equation for the partial-wave amplitudes

$$A_\ell^I(s) = \frac{1}{2} \int_{-1}^{1} d(\cos\theta)\, P_\ell(\cos\theta)\, A^I(s,u,t), \tag{3.8}$$

and the equations relating the total amplitudes for fixed I-spin for Channel I, $A^I(s,u,t)$, and the amplitudes $A^{\pm}(s,u,t)$

$$A^I(s,u,t) = A^+(s,u,t) + \xi^I A^-(s,u,t), \tag{3.9}$$

where

$$\xi^I = \begin{pmatrix} 2 \\ -1 \end{pmatrix}. \tag{3.10}$$

The partial-wave amplitudes are now written in terms of $A_2^{\pm}$ and $A_3^{\pm}$:

$$A_\ell^I(s) = \frac{1}{2}\int_{-1}^{1} d(\cos\theta) P_\ell(\cos\theta) \left\{ \frac{1}{\pi}\int_{(M+\mu)^2}^{\infty} du' \frac{A_2^+(s,u',t(s,u'))}{(u'-u)} \right.$$

$$+ \frac{1}{\pi}\int_{4\mu^2}^{\infty} dt' \frac{A_3^+(s,u(s,t'),t')}{(t'-t)} + \xi^I \left[\frac{1}{\pi}\int_{(M+\mu)^2}^{\infty} du' \frac{A_2^-(s,u',t(s,u'))}{(u'-u)} \right.$$

$$\left. \left. + \frac{1}{\pi}\int_{4\mu^2}^{\infty} dt' \frac{A_3^-(s,u(s,t'),t')}{(t'-t)} \right] \right\}. \tag{3.11}$$

If the value of s is fixed at a negative value in its momentum-transfer range, then the two absorptive parts of the amplitude, $A_2^{\pm}$ and $A_3^{\pm}$, that occur in Equation (3.11) both correspond to scattering in a more or less physical region of their corresponding channels. In order to carry out the indicated integration over $\cos\theta$, the variables u and t may be written in terms of s and $\cos\theta$ with the aid of Equation (2.8) or, more conveniently, the variable of integration may be changed from $\cos\theta$ to u in the terms involving $A_2^{\pm}$ and to t in terms involving $A_3^{\pm}$ by using the same set of equations,

$$t = -2k^2(1-\cos\theta), \tag{3.12}$$

$$u = 2M^2 + 2\mu^2 - s + 2k^2(1-\cos\theta), \tag{3.13}$$

where,

$$k^2 = [s - (M+\mu)^2][s - (M-\mu)^2]/4s. \tag{3.14}$$

The absorptive part of the partial-wave amplitude is obtained from Equation (3.11) for values of s in the unphysical region of Channel I with the aid of the identity

$$\frac{1}{z' - z - i} = P\,\frac{1}{(z'-z)} + i\pi\delta(z'-z). \tag{3.15}$$

For real $A_2^{\pm}$ and $A_3^{\pm}$, i.e., $s \notin [(M+\mu)^2,\infty]$, $A_\ell^I(s)$ has an imaginary part only when one or both of the denominators, (u'-u) and (t'-t) vanish. In order to discuss values of s for which this occurs, it is convenient to divide the unphysical region of s into three segments: (1) values of s from $-\infty$ to 0 on the real axis, (2) values of s from 0 to $(M-\mu)^2$ on the real axis, and (3) values of s on the circle, $|s| = (M^2-\mu^2)$. In the first segment, both u and t assume physical values as $\cos\theta$ varies from -1 to 1, thus the denominators (u'-u) and (t'-t) in Equation (3.11) both vanish somewhere in the integrations over $\cos\theta$ and u' (or t'). In the second segment, only the denominator (u'-u) vanishes, and in the third segment, only the denominator (t'-t) vanishes during the integrations. Furthermore, in the physical region of u and t, the functions $A_2^{\pm}$ and $A_3^{\pm}$ are just the imaginary parts of the amplitudes for Channel II and Channel III, respectively. Then

$$\text{Im } A_{\ell}^{I}(s) = \frac{1}{2}\int_{-1}^{1} d(\cos\theta)P_{\ell}(\cos\theta)\Big\{[A_2^{+}(s,u,t) + \xi^{I}A_2^{-}(s,u,t)]$$

$$+ [A_3^{+}(s,u,t) + \xi^{I}A_3^{-}(s,u,t)]\Big\}, \qquad (3.16)$$

for values of s from $-\infty$ to 0 along the real axis. For values of s from 0 to $(M-\mu)^2$ along the real axis, the absorptive part of the partial-wave amplitude contains only the terms involving $A_2^{\pm}$ terms, in Equation (3.16), and for values of s on the circle $|s| = M^2 - \mu^2$, the absorptive part of the partial-wave amplitude contains only the terms involving $A_3^{\pm}$. In the physical region of Channel III, the functions $A_3^{\pm}$ are given by

$$A_3^{\pm}(s,u,t) = \text{Im } B^{\pm}(s,u,t), \qquad (3.17)$$

and in the physical region of Channel II, the functions $A_2^{\pm}$ are given by

$$A_2^{\pm}(s,u,t) = A_1^{\pm}(u,s,t) = \pm\text{Im } A^{\pm}(u,s,t), \qquad (3.18)$$

where the symmetry properties of the $A^{\pm}$ are used in order to relate the absorptive part of the amplitude for Channel II, (A_2), to the absorptive part of the amplitude for Channel I, (A_1). Equations (2.11a) and (2.11b) are solved for A^{+} and A^{-} to give

$$A^{+} = (1/3)A^{1/2} + (2/3)A^{3/2}, \qquad (3.20a)$$

$$A^{-} = (1/3)A^{1/2} - (1/3)A^{3/2}. \qquad (3.20b)$$

With the aid of Equation (3.18), it is possible to carry out the following derivation:

$$A_2^+ + \xi^I A_2^- = \text{Im } A^+(u,s,t) - \xi^I \text{Im } A^-(u,s,t)$$

$$= (1/3)\text{Im } A^{1/2} + (2/3)\text{Im } A^{3/2} - \xi^I[(1/3)\text{Im } A^{1/2} - (1/3)\text{Im}A^{3/2}]$$

$$= \frac{1}{3}(1-\xi^I)\text{Im } A^{1/2} + \frac{1}{3}(2+\xi^I)\text{Im } A^{3/2}. \qquad (3.21)$$

If a 2×2 matrix, α, is defined such that

$$\alpha_{I,1/2} = \frac{1}{3}(1-\xi^I), \qquad (3.22a)$$

$$\alpha_{I,3/2} = \frac{1}{3}(2+\xi^I), \qquad (3.22b)$$

it is now possible to write

$$A_2^+(s,u,t) + \xi^I A_2^-(s,u,t) = \sum_{I'=1/2,3/2} \alpha_{II'} \text{Im } A^{I'}(u,s,t). \qquad (3.19)$$

Note that α is a unimodular matrix. Recalling the definition of $\xi^I = \begin{pmatrix} 2 \\ -1 \end{pmatrix}$, the matrix components are written

$$\alpha_{II'} = \begin{pmatrix} -1/3 & 4/3 \\ 2/3 & 1/3 \end{pmatrix}. \qquad (3.23)$$

For the terms involving Im $A^I(u,s,t)$ in Equation (3.16), $\cos\theta$ is written as a function of u and s and the integration is carried over u instead of $\cos\theta$. In the terms involving Im $B^{\pm}(s,u,t)$, $\cos\theta$ is written as a function of t and s and the integration is carried over t instead of $\cos\theta$. Recall the equations relating the variables s, u, and t to the CM-momentum, k, and the scattering angle, θ.

$$t = -2k^2(s) \cdot (1-\cos\theta), \tag{3.24a}$$

$$u = 2M^2 + 2\mu^2 - s + 2k^2(s)(1-\cos\theta). \tag{3.24b}$$

For fixed s, the change of variable of integration from $\cos\theta$ to u or t can be made by noting that

$$d(\cos\theta) = \frac{dt}{2k^2(s)} = \frac{-du}{2k^2(s)}, \tag{3.25}$$

and

$$t_{(\cos\theta=+1)} = 0, \tag{3.26a}$$

$$t_{(\cos\theta=-1)} = -4k^2(s), \tag{3.26b}$$

$$u_{(\cos\theta=+1)} = 2M^2 + 2\mu^2 - s, \tag{3.26c}$$

$$u_{(\cos\theta=-1)} = 2M^2 + 2\mu^2 - s + 4k^2(s)$$

$$= 2M^2 + 2\mu^2 - s + \frac{(s - (M+\mu)^2)(s - (M-\mu)^2)}{s} ,$$

$$= \frac{(M+\mu)^2(M-\mu)^2}{s} . \qquad (3.26d)$$

For values of s in the unphysical region (on the circular or left cut), $k^2(s)$ varies from $-\infty$ to $-\mu^2$. Then, upon interchanging the limits of integration over t, the integral runs from t = 0 up to a number greater than or equal to $4\mu^2$. The functions Im $B^{\pm}(s,u,t)$ are zero in the region from t = 0 to $4\mu^2$, so nothing is lost if the lower limit is moved up to $4\mu^2$. In the integration over u, it is convenient to consider, first, values of s from 0 to $(M-\mu)^2$. In this region, the upper limit assumes values from $(M+\mu)^2$ to $2M^2 + 2\mu^2$, and the lower limit assumes values from $(M+\mu)^2$ to ∞. The functions Im $A^I(u,s,t)$ are non-zero for these values of s, since u is in the physical region. Next, consider values of s from $-\infty$ to 0. The upper limit now assumes values from $2M^2 + 2\mu^2$ to ∞ and the lower limit assumes values from $-\infty$ to 0. The spectral functions $A^{\pm}_{12}$ and $A^{\pm}_{23}$ vanish when u is in the unphysical region, thus $A^{\pm}_2$ vanishes. If the lower limit is set at the physical threshold for u, $(M+\mu)^2$, again nothing will be lost since this allows the integration over all non-zero values of $A^{\pm}_2$. Finally, the absorptive part of the amplitude for values of s in the unphysical region along the real axis can be written

$$\text{Im } A^I_\ell(s) = \theta(-s)\, M^I_\ell(s) + N^I_\ell(s), \qquad (3.27)$$

where the functions $M^I_\ell(s)$ and $N^I_\ell(s)$ are given by

$$M_\ell^I(s) = \frac{-1}{4k^2(s)} \int_{4\mu^2}^{-4k^2(s)} dt\, P_\ell\left(1 + \frac{t}{2k^2(s)}\right)[\mathrm{Im}\, B^+(s,u,t) + \xi^I \mathrm{Im}\, B^-(s,u,t)], \tag{3.28}$$

$$N_\ell^I(s) = \frac{-1}{4k^2(s)} \int_{c(s)}^{2M^2+2\mu^2} du\, P_\ell\left(1 + \frac{2M^2+2\mu^2-u-s}{2k^2(s)}\right) \sum_{I'} \alpha_{II'} \mathrm{Im}\, A^{I'}(u,s,t). \tag{3.29}$$

The function c(s) equals $(M+\mu)^2(M-\mu)^2/s$ for s between zero and $(M-\mu)^2$ and $(M+\mu)^2$ for s less than zero, and $k^2(s)$ is given by Equation (3.14) Similar functions were obtained by Oehme[27] in a discussion of πN scattering. The absorptive part of $A_\ell^I(s)$ is given by $M_\ell^I(s)$ on the circle. The function $N_\ell^I(s)$ is usually called the absorptive part of the partial wave amplitude due to the intermediate states of Channel II, and $M_\ell^I(s)$ is called the absorptive part of the partial-wave amplitude due to the intermediate states of Channel III. Equation (3.27) is referred to as the crossing equation for Channel I.

For low energies, only the S and P-waves are significant and the absorptive parts of the amplitudes Im $A^I(u,s,t)$ and Im $B^\pm(s,u,t)$ can be expanded in terms of their partial waves. If partial waves above the P-wave are neglected, these functions can be written

$$\mathrm{Im}\, B^+(s,u,t) = \frac{1}{\sqrt{6}} \mathrm{Im}\, B^\circ(s,u,t) = \frac{1}{\sqrt{6}} \mathrm{Im}\, B_\circ(t), \tag{3.30}$$

$$\mathrm{Im}\, B^-(s,u,t) = \frac{1}{2} \mathrm{Im}\, B^1(s,u,t) = \frac{3}{2} \frac{(s-M^2-\mu^2+\frac{t}{2})}{\sqrt{(t-4\mu^2)(4M^2-t)}} \mathrm{Im}\, B_1(t), \tag{3.31}$$

$$\text{Im } A^{I}(u,s,t) = \text{Im } A^{I}_{o}(u) + 3\left[1 + \frac{2M^2+2\mu^2-u-s}{2p^2(u)}\right]\text{Im } A^{I}_{o}(u), \qquad (3.32)$$

where

$$p^2(u) = (u - (M+\mu)^2)(u - (M-\mu)^2)/4u. \qquad (3.33)$$

Section 3. The Crossing Equations for t-Plane

In this section, an equation relating the absorptive part of the partial-wave amplitude on the unphysical cut for Channel III to the absorptive part of the amplitude on the physical cut for Channel I is derived. This equation is called the crossing equation for Channel III. If the value of t is fixed at a negative value in its momentum-transfer range in Equation (3.7), then the two absorptive parts, A_1 and A_2 correspond to scattering in a physical region of Channel I and Channel II, respectively. Thus the one-dimensional dispersion relation for fixed t can be written

$$A^{\pm}(s,u,t) = \frac{1}{\pi}\int_{(M+\mu)^2}^{\infty} dx\left[\frac{\text{Im } A^{\pm}(s,u(x,t),t)}{x - s} \pm \frac{\text{Im } A^{\pm}(x,s(x,t),t)}{x - u}\right], \qquad (3.34)$$

where the symmetry properties of the amplitude have allowed the substitution of the absorptive part of the amplitude for Channel I in place of the absorptive part of the amplitude for Channel II. The imaginary part of $A^{\pm}(s,u,t)$ can be found with the aid of the identity given by Equation (3.15).

$$\text{Im } A^{\pm}(s,u,t) = \text{Im } A^{\pm}(s,u,t) \pm \text{Im } A^{\pm}(u,s,t). \tag{3.35}$$

The above result combined with Equations (2.11a) and (2.11b) gives

$$\text{Im } A^{\pm}(s,u,t) = \frac{2}{3}\left[\text{Im } A^{1/2}(s,u,t) + \begin{pmatrix} 2 \\ -1 \end{pmatrix} \text{Im } A^{3/2}(s,u,t)\right]. \tag{3.36}$$

The imaginary part of the ℓth partial wave for Channel III is defined by

$$\text{Im } B_{\ell}^{\pm}(t) = \frac{1}{2(pq)^{\ell}} \int_{-1}^{1} d(\cos\phi) P_{\ell}(\cos\phi) \text{ Im } A^{\pm}(s,u,t), \tag{3.37}$$

where p and q are the kaon and pion momenta and ϕ is the scattering angle in the CM system. Equations (2.9a) and (2.9c) are used to write $\cos\phi$ in terms of s and t and the integration is carried over s instead of $\cos\phi$ to give

$$\text{Im } B_{\ell}^{\pm}(t) = \frac{1}{4(pq)^{\ell+1}} \int_{(M+\mu)^2}^{-t/2+M^2+\mu^2+2\sqrt{(M^2-t/4)(\mu^2-t/4)}} ds\, P_{\ell}\left(\frac{t/2+s-M^2-\mu^2}{2pq}\right) \frac{2}{3} [\text{Im } A^{1/2}(s,u,t)$$

$$+ \begin{pmatrix} 2 \\ -1 \end{pmatrix} \text{Im } A^{3/2}(s,u,t)]. \tag{3.38}$$

The amplitudes Im $A^{I}(s,u,t)$ can be expanded in terms of the partial waves of Channel I, and if D-waves and higher are negligible

$$\text{Im } A^I(s,u,t) = \text{Im } A_o^I(s) + 3\left[1 + \frac{t}{2k^2(s)}\right]\text{Im } A_1^I(s). \qquad (3.39)$$

It should be pointed out that the results obtained in this section are not used in the actual analysis presented in this thesis. However, in a more general approach to the problem of pion-kaon scattering, the crossing equations for the t-plane would certainly be of interest. These equations are not difficult to calculate once the one dimensional dispersion relations have been written down; thus they are calculated here for the sake of completeness and for future reference.

CHAPTER IV

UNITARITY

Section 1. The Unitarity Condition

An expression for the unitarity condition below the threshold for inelastic scattering for Channel I is

$$\text{Im } A_\ell^I(s) = \frac{2k(s)}{\sqrt{s}} \left|A_\ell^I(s)\right|^2. \tag{4.1}$$

In the case of pure elastic scattering, it is possible to write a particularly simple form of the unitarity condition by inverting Equation (2.46a). Thus

$$\text{Im}(A_\ell^I(s))^{-1} = -\frac{2k(s)}{\sqrt{s}}, \tag{4.2}$$

where

$$\frac{2k(s)}{\sqrt{s}} = \frac{\sqrt{(s-M^2-\mu^2)^2 - 4M^2\mu^2}}{s} \tag{4.3}$$

Unfortunately, the unitarity condition does not take the simple form for Channel III as it does for Channel I. However, from unitarity, it follows that in the region $4\mu^2 \leq t < 16\mu^2$, the phases of the amplitudes $B_\ell^{\pm}(t)$ are given by the phase shifts of the pion-pion scattering in the corresponding angular momentum and isospin states.[28,29] The

use of this phase condition permits the construction of a useful expression for Im $B_\ell^{\pm}(t)$ in the region below the threshold for four pion production. Consider the functions $f_\ell^I(t)$ which are the partial-wave amplitudes for the elastic scattering process, $\pi\pi \to \pi\pi$. In the elastic region $f_\ell^I(t)$ may be written

$$f_\ell^I(t) = \frac{\sqrt{t}}{2q} \exp(i\delta_\ell(t)) \sin\delta_\ell(t). \tag{4.4}$$

An expression for the partial-wave amplitude for $\pi\pi \to K\bar{K}$, $B_\ell^I(t)$, cannot be written down using the unitarity condition since an inelastic channel is open well below the physical threshold for this reaction. Since the exact behavior of this function is not crucial to this analysis, a reasonable guess will suffice. An expression might be written such as

$$B_\ell^I(t) = [\sqrt{(t-4\mu^2)(4M^2-t)}/t]^{2\ell+1} f_\ell^I(t), \tag{4.5}$$

where I = 0 or 1. This expression is considered "reasonable" since it obviously has the same phase as the pion-pion scattering amplitude in the region $4\mu^2 \le t \le 4M^2$ and it also has an appropriate threshold behavior. Since the expression

$$\sqrt{(t-4\mu^2)(4M^2-t)}/t$$

is real in the region of interest, the imaginary part of $B_\ell^I(t)$ in this region is written

$$\text{Im } B_\ell^I(t) = \left(\frac{\sqrt{(t-4\mu^2)(4M^2-t)}}{t}\right)^{2\ell+1} \text{Im} f_\ell^I(t). \tag{4.6}$$

Section 2. Effective Range Approximations

Channel I

In order to make use of the simple form of the unitarity condition for Channel I, it is also necessary to know the real part of the inverse amplitude in the physical region. These functions may be approximated in the low energy region from experimental data.

A resonance has not yet been observed in the S-wave scattering data for the pion-kaon interaction; thus a scattering length approximation of the form

$$\frac{2k}{\sqrt{s}} \cot\delta_o^I = \frac{1}{a_o^I} \tag{4.7}$$

is valid for energies well above the physical threshold. The left-hand side of Equation (4.7) is just the real part of the inverse amplitude as seen by inverting Equation (2.46a); therefore

$$\text{Re}(A_o^I(s))^{-1} = \frac{1}{a_o^{1/2}} . \tag{4.8}$$

The imaginary part of the S-wave amplitude can now be found by inverting Equations (4.2) and (4.8). Then

$$\text{Im } A_o^{1/2}(s) = \frac{\frac{2k}{\sqrt{s}}}{\left(\frac{1}{a_o^{1/2}}\right)^2 + \frac{4k^2}{s}} . \qquad (4.9)$$

In the P-wave scattering data, a resonance called the K^* has been observed at about 895 Mev. with a resonance width of about 50 Mev.[20] The "width" Γ is, by definition, the half-width at half-maximum. The K^* has an I-spin of 1/2, an ordinary spin of 1, and negative parity. These resonance data permit an effective range approximation for the P-wave of the form

$$\frac{2k^3}{\sqrt{s}} \cot\delta_1^{1/2}(s) = k^2 \text{Re}(A_1^{1/2}(s))^{-1} = a_1^{1/2}(s_r - s) \qquad (4.10)$$

which is valid for energies up to and slightly above the resonance position s_r. The imaginary part of the P-wave amplitude is found by inverting Equations (4.2) and (4.10) to give

$$\text{Im } A_1^I(s) = \frac{\frac{2k^5}{\sqrt{s}}}{(a_1^I(s_r - s))^2 + \frac{4k^6}{s}} . \qquad (4.11)$$

This function exhibits a resonance behavior and has its maximum value at $s = s_r$. The sharpness of this resonance should be comparable to the sharpness of the experimentally observed πK resonance. Since s is the

CM-total energy squared, the half-width at half-maximum of Im $A_1^I(s)$ should be on the order of Γ^2. The constant a_1^I of Equation (4.10) may be related to Γ in the following manner:

$$\text{Im } A_1^I(s_r) = \frac{\sqrt{s}}{2k(s_r)} , \tag{4.12}$$

and

$$\frac{1}{2} \text{ Im } A_1^I(s_r) = \frac{\dfrac{2k^5(s_{1/2})}{\sqrt{s_{1/2}}}}{(a_1^I\Gamma^2)^2 + \dfrac{4k^6(s_{1/2})}{s_{1/2}}} , \tag{4.13}$$

where the value of s for which Im $A_1^I(s)$ drops to one-half of its maximum value is denoted by $s_{1/2}$, and $s_r - s_{1/2} = \Gamma^2$. Equation (4.13) is easily solved as it stands for the constant a_1^I, however, if $s_{1/2}$ is not too different from s_r, $s_{1/2}$ can be replaced by s_r in this expression to give a considerably simplified result

$$a_1^I = \frac{1}{\Gamma^2} \frac{2k^3(s_r)}{\sqrt{s_r}} . \tag{4.14}$$

For Γ = 50 MeV, and $s_r = (890 \text{ MeV})^2$, the value of a_1^I is approximately 21.5.

Channel III

An expression for the imaginary part of the partial-wave amplitude in the physical region for Channel III was derived in the previous

section, Equation (4.6). The real part of the amplitude for the reaction $\pi\pi \to \pi\pi$ must be known in order to make use of this expression. A scattering length approximation for the P-wave amplitude can be written down from experimental data for the pion-pion interaction at energies not too far above the physical threshold, i.e. less than $16\mu^2$. The absence of a resonance in the S-wave allows an approximation of the form

$$\mathrm{Re}(f_o(t))^{-1} = \frac{1}{b_o} , \tag{4.15}$$

where $b_o = 0.75$. For the P-wave, there is a resonance at $t_r = 20.4\mu^2$ with a reduced width $b_1 = 19.$[14] Thus,

$$\mathrm{Re}(f_1(t))^{-1} = b_1 \frac{(t_r - t)}{(t-4\mu^2)} . \tag{4.16}$$

The imaginary part of the inverse of $f_\ell(t)$ can be found by writing Equation (4.4) in terms of the variable t. The result is

$$\mathrm{Im}(f_\ell(t))^{-1} = - \sqrt{t-4\mu^2/t}. \tag{4.17}$$

Equations (4.15) and (4.17) are combined and inverted to give

$$\mathrm{Im}f_o(t) = \frac{\sqrt{(t-4\mu^2)/t}}{(1/b_o)^2 + (t-4\mu^2/t)^2} \tag{4.18}$$

and Equations (4.16) and (4.17) are combined and inverted to give

$$\text{Im } f_1(t) = \frac{(t-4\mu^2)^2\sqrt{(t-4\mu^2)/t}}{b_1^2(t_r-t)^2 + \frac{(t-4\mu^2)^3}{t}}. \tag{4.19}$$

The functions given by Equations (4.18) and (4.19) are inserted into an expression for Im $B_\ell^I(t)$ which was derived in a previous section using the approximation that the phases of the amplitudes for Channel III, $\pi\pi \to K\bar{K}$, are given by the phase shifts of the $\pi\pi \to \pi\pi$ scattering in the corresponding angular momentum states. This expression is given by

$$\text{Im } B_\ell^I(t) = \left(\frac{\sqrt{(t-4\mu^2)(4M^2-t)}}{t}\right)^{2\ell+1} \text{Im } f_\ell^I(t). \tag{4.20}$$

Thus, the S and P-wave amplitudes for Channel III become

$$\text{Im } B_o(t) = \frac{\sqrt{(t-4\mu^2)(4M^2-t)}}{t} \frac{\sqrt{t-4\mu^2/t}}{[(1/b_o)^2 + (t-4\mu^2)/t]}, \tag{4.21}$$

$$\text{Im } B_1(t) = \left(\frac{\sqrt{(t-4\mu^2)(4M^2-t)}}{t}\right)^3 \left[\frac{(t-4^{\ 2})^2\sqrt{(t-4\mu^2)/t}}{b_1^2(t_r-t)^2 + (t-4\mu^2)^3/t}\right]. \tag{4.22}$$

Section 3. Introduction of Inelastic Scattering and the CDD Pole

In Chapter I, it was pointed out that the dispersion relation analysis of the previous section is arbitrary to the extent of CDD poles in the inverse amplitudes, and if a CDD pole of appropriate strength and position is inserted into the inverse amplitude solutions it can be made to behave like a stable or unstable particle. This

ambiguity provides a loophole in the inverse amplitude scheme for introducing these experimentally observed particles. It is also conceivable that CDD poles may appear in the solutions during the course of the analysis. However, in the case of purely elastic pion-pion scattering, no such poles have yet appeared. For example, Bransden and Moffat[17] found solutions for elastic pion-pion scattering exhibiting a sharp P-wave dynamical resonance at about 700 MeV. Their results are described by

$$\text{Im } f^{-1}(v) = -(v/(v+1))^{1/2}, \tag{4.23}$$

$$\text{Re}[vf^{-1}(v)] = A(v_R - v), \tag{4.24}$$

where v is the CM momentum squared, and v_R and A are the position and reduced width of the resonance. Equation (4.23), the unitary condition, served as input information and Equation (4.24) was obtained by a numerical interation scheme based on the inverse amplitude dispersion relations and the crossing equations. There is obviously no CDD pole in this inverse amplitude solution. Whether or not poles would appear in the analysis of elastic scattering of particles of non-equal masses is uncertain since very little work has been done in this case.

If contributions from inelastic intermediate states are included in the analysis, the results might be altered. In particular, Bransden, Gatland and Moffat[18] included inelastic intermediate states in the inverse amplitude dispersion relations for pion-pion scattering for given

models of the inelastic cross section. The models were calculated by representing the four-pion intermediate state as a combination of a three-pion resonance and a single pion. Interesting results were obtained using a small and slowly-varying inelastic cross section which lead to a resonant behavior of $R = \sigma_{tot}/\sigma_{el}$ where the real part of the P-wave phase shift passed through π in the inelastic region. The inclusion of this resonant R in the iteration scheme resulted in the appearance of a second P-wave resonance. When the pion-pion coupling constant was approximately equal to -0.1 and the three-pion decay coupling constant was approximately equal to 1, the position of the two di-pion resonances were about 600 MeV and 800 MeV. This result could account for the existence of two particles with the same quantum numbers, such as the ζ particle at 550-600 MeV and the ρ at 750-800 MeV, both with $I = 1$ and $J = 1^-$.

In a later paper, Gatland and Moffat[30] present a simple analytic approximation to this solution containing inelastic scattering which leads to the double resonance solution if the solution of the dispersion relations with only pure elastic scattering is known. When inelastic intermediate states are included, the original solution for pion-pion scattering is modified to read

$$\text{Im } f^{-1}(v) = -(v/(v+1))^{1/2}R(v), \tag{4.25}$$

$$\text{Re}[vf^{-1}(v)] = A(v_R - v) - \frac{v}{\pi} P \int_{v_T}^{\infty} \frac{dv'\sqrt{v'/(v'+1)}(R-1)}{(v'-v)} . \tag{4.26}$$

Above the inelastic threshold, v_T, $\delta = \delta_R + i\delta_I$. Now, it is assumed that δ_R passes through π at $v = v_\pi$ and that $\delta(\pi)$ is small. Then from scattering theory R may be written

$$R(v) - 1 = \frac{\delta_I}{(\delta_R-\pi)^2 + \delta_I^2}, \tag{4.27}$$

for the region $(\delta_R-\pi)^2 << \delta_I$. As δ_I is small, R has a resonant behavior and this resonance dominates the integral in Equation (4.26). Expanding δ_I and $(\delta_R-\pi)$ in powers of $(v-v_\pi)$ and keeping only the lower order terms, it follows that

$$\delta_I \approx \alpha, \tag{4.28a}$$

$$\delta_R - \pi \approx \beta(v-v_\pi), \tag{4.28b}$$

and

$$\sqrt{v/(v+1)}\,[R(v)-1] = \frac{\alpha}{\beta^2(v-v_\pi)^2 + \alpha^2}. \tag{4.29}$$

Substitution of the above value into the integral of Equation (4.26) gives

$$\frac{v}{\pi} P \int_{v_T}^{\infty} \frac{dv'\sqrt{v'/(v'+1)}\,(R-1)}{(v'-v)} = -\frac{v_\pi\beta(v-v_\pi)}{\beta^2(v-v_\pi)^2 + \alpha^2}. \tag{4.30}$$

It can also be shown from scattering theory that in this approximation, $\mathrm{Re}[vf^{-1}(v)]$ vanishes when $v = v_\pi$. Since the above expression also

vanishes at this point, it follows that $A(v_R-v)$ must also vanish. Thus $v_\pi = v_R$ (since $A\neq 0$).

The function $\mathrm{Re}[vf^{-1}(v)]$ has three zeros given by

$$(1)\quad v = v_\pi,$$

$$(2)\quad v = v_{R2} = v_\pi + \left[\frac{v_\pi}{\beta A} - \frac{\alpha^2}{\beta^2}\right]^{1/2}, \tag{4.31}$$

and

$$(3)\quad v = v_{R2} = v_\pi + \left[\frac{v_\pi}{\beta A} - \frac{\alpha^2}{\beta^2}\right]^{1/2},$$

Here (1) corresponds to $\delta_R = \pi$ (a minimum in σ_{el}), and (2) and (3) correspond to $\delta_R = \pi/2$ and $3\pi/2$, respectively, and give the positions of the two resonances in σ_{el}. The reduced width, which is the same for both resonances, is approximately $1/2A$. Since the reduced width in the pure elastic case is $1/A$, the total area and center of mass of the two resonances are approximately the same as for the single resonance. Thus the splitting of the resonance should have little effect on the inverse amplitude left cut which determines the constants v_R and A.

The analytic properties of the inverse amplitude obtained by this approximation are of considerable interest here. The phase shift, $\delta(v)$, is analytic in the cut plane with the cut beginning in the elastic threshold v_T. In view of this discontinuity, δ_I is written $\delta_I = \alpha = k(v-v_T)^{1/2}$, where k is an analytic function of v and is positive on the real axis. Then

$$f^{-1}(v) = \frac{A}{v}(v_R - v) - i\left(\frac{v}{v+1}\right)^{1/2} - \frac{1}{\beta(v_R - v) - ik(v - v_T)^{1/2}}, \quad (4.32)$$

which satisfies the reality condition $[f^{-1}(v)]^* = f^{-1}(v^*)$. This function has a CDD pole on the unphysical sheet (therefore not violating unitarity) at $v = v_p$ where

$$v_p = v_R - i\frac{\alpha}{\beta}. \quad (4.33)$$

The solution obtained here by the approximation technique is equivalent to inserting a CDD pole located on the unphysical sheet into the known solution of the elastic pion-pion scattering equations, providing the position and strength of this pole produces effects on the left cut that can be shown to be small. This technique, presented by Gatland and Moffat, for dealing with double resonances is not limited to pion-pion scattering, or to P-waves. All that is necessary is that there exists a part of the physical region in which the solution derived from the left cut contributions, $vf^{-1}(v)$, passes linearly through zero, that δ_I be small there and that the two resonances exhibited when CDD pole effects are added should appear as a single resonance when viewed from the left cut (or any other cuts which may be present). In the following section the particular case of interest here, pion-kaon scattering is discussed with this technique in mind.

Inelastic Pion-Kaon Scattering

Consider the P-wave amplitude $A_1(s)$ which assumes the form in the physical region

$$A_1(s) = \frac{\sqrt{s}\,(e^{2i\delta_1}-1)}{(2k)(2i)}\ , \tag{4.34}$$

where δ_1 is the P-wave phase shift.

Above the inelastic threshold s_T, the P-wave phase shift becomes complex with $Im\delta_1 > 0$ in virtue of unitarity. The imaginary part of $A_1(s)$ in the physical region can be written

$$Im\ A_1(s) = \frac{2k}{\sqrt{s}}\,|A_1(s)|^2 + \frac{\sqrt{s}}{2k}\left(\frac{1-e^{-4Im\delta_1}}{4}\right), \tag{4.35}$$

and unitarity implies that

$$Im\left(A_1(s)\right)^{-1} = -R\left(\frac{2k}{\sqrt{s}}\right)\ , \tag{4.36}$$

where R is the ratio of the total cross section (σ_{tot}) to the elastic cross section (σ_{el}).

Above the inelastic threshold δ_1 is written $\delta_1 = \delta_R + i\delta_I$. Now, suppose that δ_R passes through π at $s = s_\pi$ and that $\delta_I(s)$ is small, then R can be written in the form of Equation (4.27) for the region in which $(\delta_R-\pi)^2 << \delta_I$. Furthermore, the effective range approximation for $Re(k^2A_1^{-1}(s))$ gives a solution which passes linearly through zero at $\delta_1 = \pi$. The conditions necessary for applying the Gatland and Moffat approximation are fulfilled if the double resonance produced when the CDD pole is inserted has the same effects as the single resonance when viewed from the left and circular cuts.

Analysis

In the original discussion of CDD poles[14] their position and strength were arbitrary. However, for that analysis a very simple form of crossing (actually direct reflection) was used. Here, as pointed out in the previous section, partial wave coupling in the crossings equations may lead to some restrictions on the CDD pole. To start with, Equations (4.2) and (4.10) are modified to include a CDD pole at $s = s_p = s_r - i\tau$. Thus

$$\mathrm{Re}\left(A_1(s)\right)^{-1} = \frac{a_1(s_r - s)}{k^2} + \frac{\kappa(s - s_r)}{\tau^2 + (s - s_r)^2}\,, \tag{4.37}$$

$$\mathrm{Im}\left(A_1(s)\right)^{-1} = -\frac{2k}{\sqrt{s}} - \frac{\kappa\tau}{\tau^2 + (s - s_r)^2}\,, \tag{4.38}$$

where κ is the strength of the pole.

With Equations (4.27) and (4.36) it can be shown that the imaginary part of the P-wave phase shift is inversely proportional to κ and directly proportional to τ at $\mathrm{Re}\ \delta_1 = \pi$, and the slope of the real part of the phase shift as a function of s is inversely proportional to (κ). More precisely,

$$\mathrm{Im}\ \delta_1\Big|_{\mathrm{Re}\delta_1 = \pi} = \left(\frac{\tau}{\kappa}\right) \frac{2k(s_r)}{\sqrt{s_r}}\,, \tag{4.39}$$

$$\frac{d}{ds}\,\mathrm{Re}\delta_1\Big|_{\mathrm{Re}\delta_1 = \pi} = \left(\frac{1}{\kappa}\right) \frac{2k(s_r)}{\sqrt{s_r}}\,. \tag{4.40}$$

Equations (4.37) and (4.38) are inverted to give Im $A_1(s)$ on the physical cut and the results are inserted into the crossing equations to give Im $A_1(s)$ on the unphysical cuts. The dispersion relation, Equation (2.55), now determines $A_1^I(s)$ for all s and, in particular, Re $A_1^I(s)$ on the physical cut. When Equations (4.37) and (4.38) are inserted into the computer program, the resulting curves shown in Figures 13 and 14 were obtained. The data for these curves are found in Tables 1, 2, and 3.

The variable limits in the crossing equation produces a change of slope of Im $A_\ell^I(s)$ in the unphysical region at the reflected resonance position. When a CDD pole is present this gives a different behavior for Im $A_\ell^I(s)$ for $0 < s < (M-\mu)^2$. These changes on the left cut are not important in the dispersion integrals in the low energy physical region due to the subtractions. Their effect, if any, will be felt in the subtraction constants. Thus the consistency of the scheme with the CDD pole depends on leaving the P-wave subtraction constants unchanged.

Gatland[19] found that a pole in the inverse P-wave amplitude for $\pi\pi \to \pi\pi$ has only a very small effect on the contribution to the amplitudes from the unphysical cut for a wide range of pole strengths and distances off the real axis. In particular, for strengths ranging from 0.01 to 1 and positions from 0.5 to 0.01, the differences in the left cut contribution ranged from about one thousandth of 1 per cent to about one tenth of 1 per cent. Since this pole also has some effect on the amplitudes of $\pi K \to \pi K$, it is hoped that the effect will be small in this case also. The absorptive part of the amplitude in the physical

region of Channel III is shown in Figure 16 with no pole and with a pole of strength 10 and position 0.1. The values for the contribution from the circular cut when the pole is included in the calculation of Im $B_1(t)$ are not tabulated but the changes are on the order of 1 per cent for this pole. Although the effect is much greater than it was for the $\pi\pi \rightarrow \pi\pi$ amplitude, primarily due to the choice of functional form for Im $B_1(t)$, it is still quite small. And, as a matter of interest, the pole used here for purposes of illustration is much stronger than would be necessary to account for the experimental di-pion resonances at about 730 MeV and 800 MeV.

CHAPTER V

EVALUATION OF THE SUBTRACTION CONSTANTS

Before a scheme for evaluating the subtraction constants is presented, it will be convenient to take a closer look at the dispersion relation. Any computer program for the calculations necessary in the analysis must involve the evaluation of the three integrals which appear in the dispersion relation

$$\text{Re } A_\ell^I(s) = \alpha_\ell^I + \frac{(s-M^2)}{\pi} P \int_{(M+\mu)^2}^{\infty} \frac{ds' \text{ Im } A^I(s')}{(s'-M^2)(s'-s)} + \frac{(s-M^2)}{\pi} \int_{-\infty}^{(M-\mu)^2} \frac{ds' \text{ Im } A_\ell^I(s')}{(s'-M^2)(s'-s)}$$

$$+ \frac{2(s-M^2)}{\pi} \text{Re} \int_{-M^2}^{-\mu^2} \frac{d\lambda \; 2s_+ M_\ell^I(s_+)}{(s_+-M^2-{}^2-2\,)(s_+-M^2)(s_+-s)} . \qquad (5.1)$$

The three integrals are best discussed separately and for convenience, they will be labeled in the following way:

$R_\ell^I(s)$ will stand for the integral over the physical cut.

$C_\ell^I(s)$ will stand for the integral over the circular cut.

$L_\ell^I(s)$ will stand for the integral over the unphysical cut along the real axis.

The evaluation of the contribution from the physical cut is straightforward. The integrand of $R_\ell^I(s)$ has a simple pole at $s' = s$

for values of s in the physical region. This singularity can be removed from the integrand by adding and subtracting a term of the form

$$\frac{(s-M^2)}{\pi}\int_{(M+\mu)^2}^{\infty}\frac{ds'\ \mathrm{Im}\ A_\ell^I(s)}{(s-M^2)(s'-s)} \cong \frac{\mathrm{Im}\ A_\ell^I(s)}{\pi}\ln\left(\frac{N-s}{s-(M+\mu)^2}\right), \tag{5.2}$$

where N is a large number. Then $R_\ell^I(s)$ may be written

$$R_\ell^I(s) = \frac{s-M^2}{\pi}\int_{(M+\mu)^2}^{N} ds'\ \frac{[\mathrm{Im}\ A_\ell^I(s')/(s'-M^2) - \mathrm{Im}\ A_\ell^I(s)/(s-M^2)]}{(s'-s)}$$

$$+\ \frac{\mathrm{Im}\ A_\ell^I(s)}{\pi}\ln\left(\frac{N-s}{s-(M+\mu)^2}\right). \tag{5.3}$$

The integrand is now an analytic function of s' even at s' = s. The computer, of course, cannot evaluate the integrand in this form when s' = s. It can, however, evaluate it for s' as near to s as the programmer desires. A computer program using either Simpson's rule or the trapezoidal rule can be employed to evaluate this integral, provided a conditional statement is included in the program which prevents the computer from evaluating the integrand at s' = s.

Section 1. Analytic Evaluation of the Integrals Over s' for the Unphysical Cuts

Unfortunately, the evaluation of the contributions of the unphysical cuts is not as straightforward as it is for the right cut.

When the crossing equations are employed for evaluating Im $A_\ell^I(s')$ on the left cut and $M_\ell^I(s_+)$ on the circular cut, both $L_\ell^I(s)$ and $C_\ell^I(s)$ contain double integrations. A computer program can be written to approximate the double integrals, of course, but the integrations over s' can be carried out analytically upon interchange of the order of integration. The calculations are shown in detail in the following two sections.

The Left Cut

When the expressions for Im $A_\ell^I(s')$ from the crossing equations are substituted into the integral over the left cut, it becomes necessary to divide the integral over s' into two sections, one integral running from $-\infty$ to 0 and the other integral running from 0 to $(M-\mu)^2$. The expressions for Im $A_\ell^I(s')$ are given by

$$\text{Im } A_\ell^I(s) = \frac{1}{4k^2(s)} \int_{2M^2+2\mu^2-s}^{(M^2-\mu^2)^2/s} du\, P_\ell\left(1 + \frac{2M^2+2\mu^2-u-s}{2k^2(s)}\right) \sum_{I'} \alpha_{II'} \left[\text{Im } A_0^{I'}(u)\right.$$

(for $0<s<(M-\mu)^2$)

$$\left. + 3\left(1 + \frac{2M^2+2\mu^2-u-s}{2p^2(u)}\right) \text{Im } A_1^{I'}(u)\right], \qquad (5.4)$$

$$\text{Im } A_\ell^I(s) = \frac{-1}{4k^2(s)} \int_{(M+\mu)^2}^{2M^2+2\mu^2-s} du\, P_\ell\left(1 + \frac{2M^2+2\mu^2-u-s}{2k^2(s)}\right) \sum_{I'} \alpha_{II'} \left[\text{Im } A_o^{I'}(u)\right.$$

(for $s<0$)

$$+ 3\left[1 + \frac{2M^2+2\mu^2-u-s}{2p^2(u)}\right] \text{Im } A_1^{I'}(u)\Big], \tag{5.5}$$

$$k^2(s) = \left(s - (M-\mu)^2\right)\left(s - (M+\mu)^2\right)/4s,$$

$$p^2(u) = \left(u - (M-\mu)^2\right)\left(u - (M+\mu)^2\right)/4u, \tag{5.6}$$

Then

$$L_\ell^I(s) = \frac{s - M^2}{\pi} \int_0^{(M-\mu)^2} ds' \int_{2M^2+2\mu^2-s'}^{(M^2-\mu^2)^2/s'} du\, P_\ell\left[1 + \frac{2M^2+2\mu^2-u-s'}{2k^2(s')}\right] \frac{1}{4k^2(s')(s'-M^2)(s'-s)}$$

$$\times \left[\text{Im } A_o^{1/2}(u) + 3\left[1 + \frac{2M^2+2\mu^2-u-s'}{2p^2(u)}\right] \text{Im } A_1^{1/2}(u)\right].$$

$$- \frac{s - M^2}{\pi} \int_{-\infty}^{0} ds' \int_{(M+\mu)^2}^{2M^2+2\mu^2-s'} du\, P_\ell\left[1 + \frac{2M^2+2\mu^2-u-s'}{2k^2(s')}\right] \frac{1}{4k^2(s')(s'-M^2)(s'-s)}$$

$$\times \left[\text{Im } A_o^{1/2}(u) + 3\left[1 + \frac{2M^2+2\mu^2-u-s'}{2p^2(u)}\right] \text{Im } A_1^{1/2}(u)\right]. \tag{5.7}$$

If the following constants and functions of u are defined, the expressions for $L_\ell^I(s)$ can be simplified somewhat.

$$a = (M-\mu)^2, \quad b = (M+\mu)^2, \quad c = M^2 + \mu^2, \tag{5.8}$$

$$f(u) = \text{Im } A_o^{1/2}(u) + \frac{3(2p^2(u)+2c-u)}{2p^2(u)} \text{Im } A_1^{1/2}(u) \tag{5.9}$$

$$g(u) = \frac{3 \text{ Im } A_1^{1/2}(u)}{2p^2(u)} . \tag{5.10}$$

Then,

$$L_\ell^I(s) = \frac{s-M^2}{\pi} \int_0^a ds' \int_{2c-s'}^{ab/s'} du \frac{s'[f(u)-s'g(u)]}{(s'-M^2)(s'-s)(s'-a)(s'-b)} P_\ell\left[1+\frac{2s'(2c-u-s')}{(s'-a)(s'-b)}\right]$$
$$- \frac{s-M^2}{\pi} \int_{-\infty}^0 ds' \int_b^{2c-s'} du \frac{s'[f(u)-s'g(u)]}{(s'-M^2)(s'-s)(s'-a)(s'-b)} P_\ell\left[1+\frac{2s'(2c-u-s')}{(s'-a)(s'-b)}\right]. \tag{5.11}$$

If the order of integration is interchanged, it is possible to carry out the integration over s' analytically, leaving only the integration over u for the computer. In order to interchange the order of integration, the limits must be adjusted so that the same area is covered. This area is shown in Figure 10. It is easily verified from this figure that the same area can be covered with the following interchange:

$$\int_0^b ds' \int_{2c-s'}^{ab/s'} du - \int_{-\infty}^0 ds' \int_b^{2c-s'} du \longrightarrow \int_{2c}^{\infty} du \int_0^{ab/u} ds' + \int_b^{2c} du \int_{2c-u}^{ab/u} ds'$$

$$- \int_{2c}^{\infty} du \int_{-\infty}^{2c-u} ds' \; - \int_{b}^{2c} du \int_{-\infty}^{0} ds'.$$

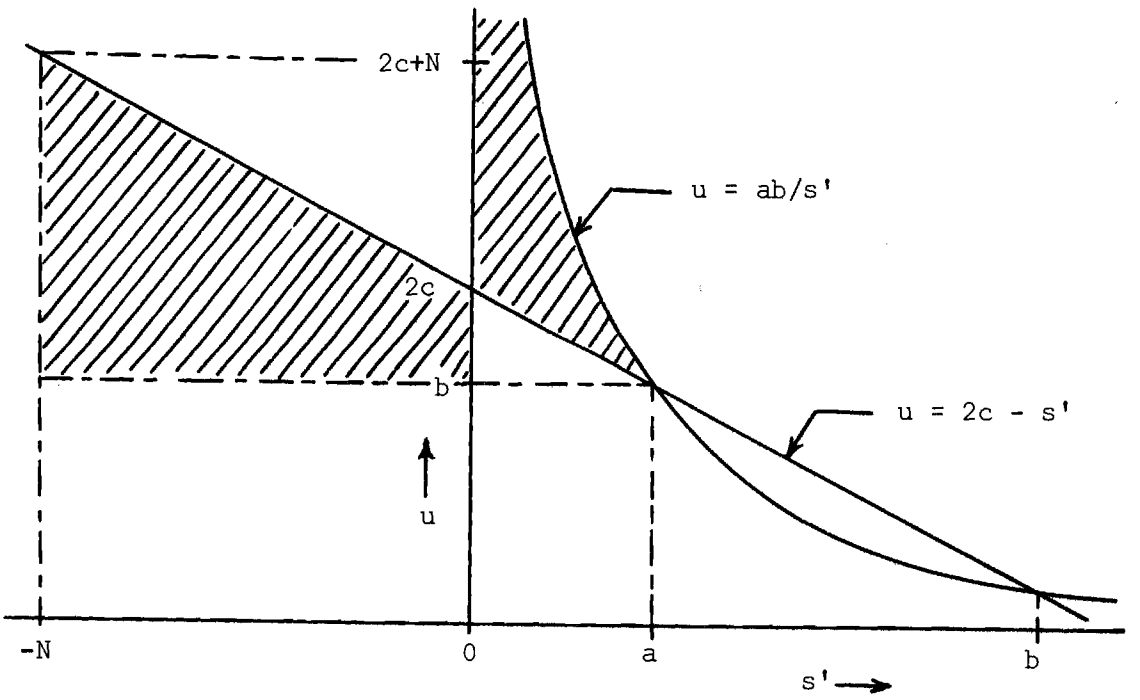

Figure 10. The s'-u Plane. The Shaded Areas Are the Areas of Integration for $L_{\ell}^{I}(s)$.

The integrations over s' can now be carried out explicitly. The results can be written in terms of the integrals defined below.

$$I_1(x,y) = \int_{y}^{x} \frac{ds'(s')}{(s'-a)(s'-b)(s'-M^2)(s'-s)} = \frac{a \ln\frac{(y-a)}{(x-a)}}{(b-a)(s-a)(M^2-a)} \qquad (5.12)$$

$$+ \frac{b \ln\frac{(y-b)}{(x-b)}}{(a-b)(s-b)(M^2-b)} + \frac{s \ln\frac{(y-s)}{(x-s)}}{(a-s)(b-s)(M^2-s)} + \frac{M^2 \ln\frac{(y-M^2)}{(x-M^2)}}{(b-M^2)(a-M^2)(s-M^2)},$$

$$I_2(x,y) = \int_y^x \frac{ds'\,(s')^2}{(s'-a)(s'-b)(s'-M^2)(s'-s)} = \frac{a^2\ln\frac{(y-a)}{(x-a)}}{(b-a)(s-a)(M^2-a)} \qquad (5.13)$$

$$+ \frac{b^2\ln\frac{(y-b)}{(x-b)}}{(a-b)(s-b)(M^2-b)} + \frac{s^2\ln\frac{(y-s)}{(x-s)}}{(a-s)(b-s)(M^2-s)} + \frac{M^4\ln\frac{(y-M^2)}{(x-M^2)}}{(a-M^2)(b-M^2)(s-M^2)},$$

$$I_3(x,y) = \int_y^x \frac{ds'\,(s')^2}{(s'-a)^2(s'-b)^2(s'-M^2)(s'-s)} = \frac{s^2\ln\frac{(y-s)}{(x-s)}}{(M^2-s)(a-s)^2(b-s)^2}$$

$$+ \frac{b}{(s-M^2)(a-M^2)^2(b-M^2)^2} + \frac{a^2\left[\frac{1}{(y-a)} - \frac{1}{(x-a)}\right]}{(a-s)(a-M^2)(a-b)^2} + \frac{b^2\left[\frac{1}{(y-b)} - \frac{1}{(x-b)}\right]}{(b-s)(b-M^2)(b-a)^2}$$

$$+ \left[\frac{M^4\ln\frac{(y-M^2)}{(x-M^2)}}{(s-a)(M^2-a)(a-b)^2} + \frac{b}{(s-b)(M^2-b)(a-b)^2} + \frac{s}{(M^2-s)(s-a)^2(b-s)}\right.$$

$$\left. + \frac{M^2}{(s-M^2)(a-M^2)^2(b-M^2)}\right] \frac{a\ln\frac{(y-a)}{(x-a)}}{(a-b)} + \left[\frac{a}{(s-b)(M^2-b)(a-b)^2}\right.$$

$$+ \frac{a}{(s-a)(M^2-a)(a-b)^2} + \frac{s}{(a-s)(M^2-s)(s-b)^2}$$

$$\left. + \frac{M^2}{(s-M^2)(a-M^2)(b-M^2)^2}\right] \frac{b\ln\frac{(y-b)}{(x-b)}}{(b-a)}, \qquad (5.14)$$

$$I_4(x,y) = \int_y^x \frac{ds'(s')^3}{(s'-a)^2(s'-b)^2(s'-M^2)(s'-s)} = \frac{s^3\ln\frac{(y-s)}{(x-s)}}{(M^2-s)(a-s)^2(b-s)^2}$$

$$+\frac{M^6\ln\frac{(y-M^2)}{(x-M^2)}}{(s-M^2)(a-M^2)(b-M^2)}+\frac{a^3\left[\frac{1}{(y-a)}-\frac{1}{(x-a)}\right]}{(a-s)(s-M^2)(a-b)^2}+\frac{b^3\left[\frac{1}{(y-b)}-\frac{1}{(x-b)}\right]}{(b-s)(b-M^2)(b-a)^2}$$

$$+\frac{s^2(M^2-a)}{(M^2-s)(s-a)(s-b)}+\frac{M^4(s-a)}{(s-M^2)(a-M^2)(b-M^2)}-\frac{b^2(M^2-a)(s-a)}{(a-b)^2(M^2-b)(s-b)}$$

$$-\frac{ab}{(a-b)^2}\Bigg]\frac{a\ln\frac{(y-a)}{(x-a)}}{(M^2-a)(s-a)(b-a)}+\Bigg[\frac{s^2(M^2-b)}{(M^2-s)(s-a)(s-b)}+\frac{M^4(s-b)}{(s-M^2)(a-M^2)(b-M^2)}$$

$$-\frac{a^2(M^2-b)(s-b)}{(a-b)^2(M^2-a)(s-a)}-\frac{ab}{(a-b)^2}\Bigg]\frac{b\ln\frac{(y-b)}{(x-b)}}{(M^2-b)(s-b)(a-b)}, \qquad (5.15)$$

$$I_5(x,y)=\int_y^x\frac{ds'(s')^4}{(s'-a)^2(s'-b)^2(s'-M^2)(s'-s)}=\frac{s^4\ln\frac{(y-s)}{(x-s)}}{(M^2-s)(a-s)^2(b-s)^2}$$

$$+\frac{M^8\ln\frac{(y-M^2)}{(x-M^2)}}{(s-M^2)(a-M^2)^2(b-M^2)^2}+\frac{a^4\left[\frac{1}{(y-a)}-\frac{1}{(x-a)}\right]}{(a-s)(a-M^2)(a-b)^2}+\frac{b^4\left[\frac{1}{(y-b)}-\frac{1}{(x-b)}\right]}{(b-s)(b-M^2)(b-a)^2}$$

$$+\Bigg[\frac{s^3(M^2-a)}{(M^2-s)(s-a)(s-b)}+\frac{M^6(s-a)}{(s-M^2)(a-M^2)(b-M^2)}-\frac{b^3(s-a)(M^2-a)}{(M^2-b)(s-b)(a-b)^2}$$

$$-\frac{a^2b}{(a-b)^2}\Bigg]\frac{a\ln\frac{(y-a)}{(x-a)}}{(M^2-a)(s-a)(b-a)}+\Bigg[\frac{s^3(M^2-b)}{(M^2-s)(s-b)(s-a)}-\frac{ab^2}{(a-b)^2}$$

$$+\frac{M^6(s-b)}{(s-M^2)(a-M^2)(b-M^2)}-\frac{a^3(s-b)(M^2-b)}{(a-b)^2(M^2-a)(s-a)}\Bigg]\frac{b\ln\frac{(y-b)}{(x-b)}}{(M^2-b)(s-b)(a-b)}. \qquad (5.16)$$

Finally, the function $L_o^I(s)$ and $L_1^I(s)$ may be written

$$L_o^I(s) = \frac{s - M^2}{\pi} \int_b^{2c} du\{f(u)[I_1(ab/u,2c-u) - I_1(0,-N)]$$

$$- g(u)[I_2(ab/u,2c-u) - I_2(0,-N)]\}$$

$$+ \frac{s - M^2}{\pi} \int_{2c}^{2c+N} du\{f(u)[I_1(ab/u,0) - I_1(2c-u,-N)]$$

$$- g(u)[I_2(ab/u,0) - I_2(2c-u,-N)]\}, \quad (5.17)$$

$$L_1^I(s) = L_o^I(s) + \frac{2(s-M^2)}{\pi} \left[\int_b^{2c} du\{f(u)[(2c-u)(I_3(ab/u,2c-u) - \right.$$

$$I_3(0,-N)) - (I_4(ab/u,ac-u) - I_4(0,-N))]$$

$$- g(u)[(2c-u)(I_4(ab/u,2c-u) - I_4(0,-N))$$

$$+ (I_5(ab/u,2c-u) - I_5(0,-N))]\}$$

$$+ \int_{2c}^{2c+N} du\{f(u)[(2c-u)(I_3(ab/u,0) - I_3(2c-u,-N)) - (I_4(ab/u,0)$$

$$- I_4(2c-u,-N))] - g(u)[(2c-u)(I_4(ab/u,0) - I_4(2c-u,-N))$$

$$\left. + (I_5(ab/u,0) - I_5(2c-u,-N))]\} \right]. \quad (5.18)$$

The integrand is a well-behaved function of u in the regions of integration, and the integrals can be evaluated by computer using any standard method. The limits of $-\infty$ and ∞ are, of course, replaced by -N and N,

where N is a cutoff consistent with the effective range approximations used for Im $A_\ell^I(u)$. A realistic cutoff should be between $50\mu^2$ and $60\mu^2$. Note that in evaluating the contribution from the left cut, the effects of Channel III are neglected. The introduction of the CDD pole does not affect the contribution from Channel III, and including it adds an unnecessary complication to the calculations. In addition, it is assumed that Im $A_\ell^{1/2}(u)$ is approximately equal to Im $A_\ell^{3/2}(u)$. This assumption is consistent with the experimentally observed evidence that the masses of the different charge states of the K^* differ by a very small percentage.

The Circular Cut

The contribution from the circular cut, $C_\ell^I(s)$ can be evaluated in a manner similar to that of $L_\ell^I(s)$. As in the case of $L_\ell^I(s)$, the function $C_\ell^I(s)$ is obtained by evaluating a double integral. The double integral arises when the discontinuity across the circular cut, $M_\ell^I(s_+)$, is put into the integral expression for $C_\ell^I(s)$. Before these integrals can be evaluated; however, the real part of the integrand must be found. The function, $M_\ell^I(s_+)$, is a complex function of s_+. Its real and imaginary parts are given by

$$\text{Re } M_\ell^I(s_+) = \frac{1}{-4\lambda}\int_{4\mu^2}^{-4\lambda} dt\, P_\ell\left(1+\frac{t}{2\lambda}\right)\left[\frac{\text{Im}}{\sqrt{6}}\, B_o(t) + \frac{3}{2}\,\xi^I\,\frac{\left(\frac{t}{2}+2\lambda\right)\text{Im } B_1(t)}{\sqrt{(t-4\mu^2)(4M^2-t)}}\right], \quad (5.19)$$

$$\text{Im } M_\ell^I(s_+) = \frac{1}{-4\lambda}\int_{4\mu^2}^{-4\lambda} dt\, P_\ell\left(1+\frac{t}{2\lambda}\right)\frac{3}{2}\,\xi^I\sqrt{(M^2+\lambda)(-\mu^2-\lambda)}\;\frac{\text{Im } B_1(t)}{\sqrt{(t-4\mu^2)(4M^2-t)}}\,. \quad (5.20)$$

Then the real part of the integrand of $C_\ell^I(s)$ is given by

$$\mathrm{Re}\left[\frac{2s_+(\mathrm{Re}M_\ell^I(s_+) + i\mathrm{Im}M_\ell^I(s_+))}{(s_+-M^2-\mu^2-2\lambda)(s_+-M^2)(s_+-s)}\right]. \tag{5.21}$$

If a change of variables is made and the following constants are defined, the integrand can be simplified considerably.

$$x = M^2 + \mu^2 + 2\lambda, \tag{5.22a}$$

$$y(x) = \sqrt{[(M^2-\mu^2) + x][(M^2-\mu^2) - x]}, \tag{5.22b}$$

$$A = \frac{(M^2-\mu^2)^2 + M^4}{2M^2}, \quad B = \frac{(M^2-\mu^2)^2 + s^2}{2s}, \tag{5.22c}$$

$$C = M^2 + \mu^2, \quad D = \frac{M^2s + (M^2-\mu^2)^2}{4sM^2}, \quad E = \frac{(s+M^2)(M^2-\mu^2)^2}{4sM^2}, \tag{5.22d}$$

$$F = \frac{sM^2 - (M^2-\mu^2)^2}{4sM^2}, \quad G(t) = \left(\frac{t}{2} - M^2-\mu^2\right)F - E. \tag{5.22e}$$

Then the contribution of the circular cut can be written

$$C_\ell^I(s) = \frac{2(s-M^2)}{\pi}\int_{-(M^2-\mu^2)}^{(M^2-\mu^2)} dx\left[\frac{F\ \mathrm{Re}\ M_\ell^I(s_+(x))}{(x-A)(x-B)} + \frac{(Dx-E)\mathrm{Im}\ M_\ell^I(s_+(x))}{y(x)(x-A)(x-B)}\right]. \tag{5.23}$$

When Re M_ℓ^I and Im M_ℓ^I are substituted into the above integral equation, there is a double integral of the form shown below.

$$\int_{-(M^2-\mu^2)}^{(M^2-\mu^2)} dx \int_{4\mu^2}^{2(C-x)} dt$$

The order of integration may be interchanged if the limits of integration are adjusted so that the same area is covered. The area is shown in Figure 11.

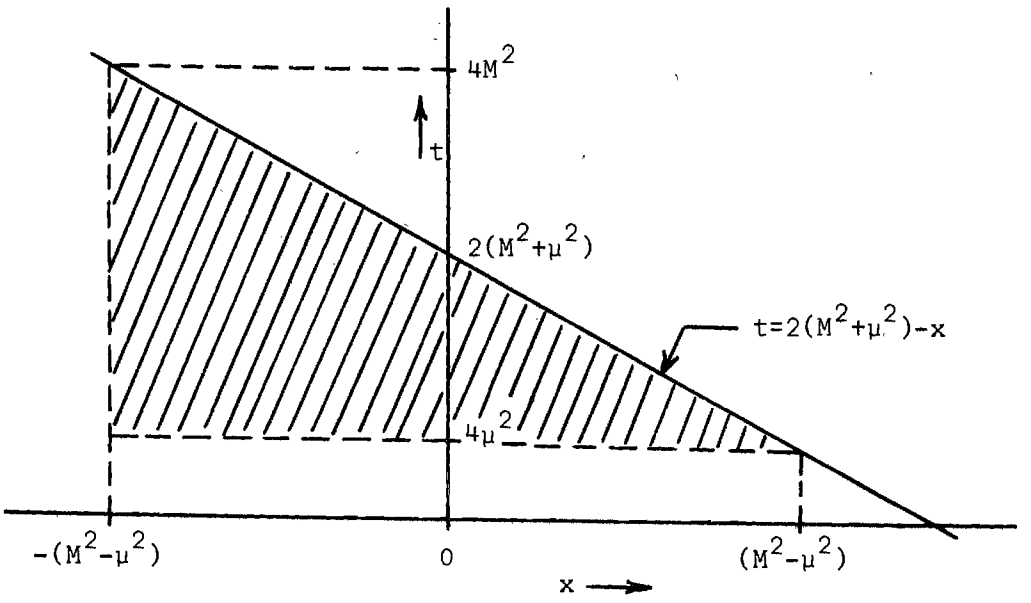

Figure 11. The x-t Plane. The Shaded Area is the Area of Integration for $C_\ell^I(s)$.

From the figure, it is easily verified that the correct limits are shown below.

$$\int_{-(M^2-\mu^2)}^{(M^2-\mu^2)} dx \int_{4\mu^2}^{2(C-x)} dt \longrightarrow \int_{4\mu^2}^{4M^2} dt \int_{-(M^2-\mu^2)}^{C-t/2} dx$$

With this interchange of the order of integration, $C_\ell^I(s)$ can be written

$$C_\ell^I(s) = \frac{s - M^2}{\pi} \int_{4\mu^2}^{4M^2} dt \int_{-(M^2-\mu^2)}^{C-t/2} dx\, P_\ell\left[1 - \frac{1}{(C-x)}\right] \frac{1}{(C-x)(A-x)(B-x)} \times$$

$$\left\{F\left[\text{Im } B_o(t) + \frac{3}{2}\,\xi^I\left(\frac{t}{2} - C + x\right) \text{Im } B_1(t)\right]\right.$$

$$\left. + \frac{3}{2}\,(Dx-E)\,\xi^I \text{Im } B_1(t)\right\} . \qquad (5.24)$$

The integration over x can be carried out explicitly using the following results:

$$J_1(t) = \int_{-(M^2-\mu^2)}^{C-t/2} \frac{dx}{(C-x)(A-x)(B-x)} = \frac{1}{(C-A)(B-A)} \ln \frac{A + M^2 - \mu^2}{A - C + t/2}$$

$$+ \frac{1}{(A-B)(C-B)} \ln \frac{B + M^2 - \mu^2}{B - C + t/2} + \frac{1}{(A-C)(B-C)} \ln \frac{C + M^2 - \mu^2}{t/2}, \qquad (5.25)$$

$$J_2(t) = \int_{-(M^2-\mu^2)}^{C-t/2} \frac{x\,dx}{(C-x)(A\,x)(B-x)} = \frac{A}{(C-A)(B-A)} \ln \frac{A + M^2 - \mu^2}{A - C + t/2}$$

$$+ \frac{B}{(A-B)(C-B)} \ln \frac{B + M^2 - \mu^2}{B - C + t/2} + \frac{C}{(A-C)(B-C)} \ln \frac{C + M^2 - \mu^2}{t/2}, \qquad (5.26)$$

$$J_3(t) = \int_{-(M^2-\mu^2)}^{C-t/2} \frac{dx}{(C-x)^2(A-x)(B-x)} = \frac{A}{(C-A)^2(B-A)} \ln \frac{A + M^2 - \mu^2}{A - C + t/2}$$

$$+ \frac{1}{(C-B)^2(A-B)} \ln \frac{B + M^2 - \mu^2}{B - C + t/2} + \frac{(2C-A-B)}{(A-C)^2(B-C)^2} \ln \frac{C + M^2 - \mu^2}{t/2}$$

$$+ \frac{(4M^2-t)}{(A-C)(B-C)2M^2t} , \qquad (5.27)$$

$$J_4(t) = \int_{-(M^2-\mu^2)}^{C-t/2} \frac{x\, dx}{(C-x)^2(A-x)(B-x)} = \frac{A}{(C-A)^2(B-A)} \ln \frac{A + M^2 - \mu^2}{A - C + t/2}$$

$$+ \frac{B}{(C-B)^2(A-B)} \ln \frac{B + M^2 - \mu^2}{B - C + t/2} + \frac{(C^2-AB)}{(C-A)^2(C-B)^2} \ln \frac{C + M^2 - \mu^2}{t/2}$$

$$+ \frac{C(4M^2-t)}{(A-C)(B-C)2M^2t} . \qquad (5.28)$$

The $C_\ell^I(s)$ can be written in terms of these functions of t.

$$C_0^I(s) = \frac{s - M^2}{\pi} \int_{4\mu^2}^{4M^2} dt \left\{ \left[F \text{ Im } B_o(t) + \frac{3}{2} \xi^I \frac{G(t) \text{ Im } B_1(t)}{\sqrt{(t-4\mu^2)(4M^2-t)}} \right] J_1(t) \right.$$

$$\left. + \frac{3}{2} \xi^I \frac{H \text{ Im } B_1(t)}{\sqrt{(t-4\mu^2)(4\mu^2-t)}} J_2(t) \right\} , \qquad (5.29)$$

$$C_1^I(s) = C_o^I(s) - \frac{(s-M^2)}{\pi} \int_{4\mu^2}^{4M^2} t\, dt \quad F \text{ Im } B_o(t) + \frac{\frac{3}{2} \xi^I \text{Im } B_1(t)}{\sqrt{(t-4\mu^2)(4M^2-t)}} \Bigg] J_3(t)$$

$$+ \frac{\frac{3}{4}\xi^I \text{Im } B_1(t)}{\sqrt{(t-4\mu^2)(4M^2-t)}} J_4(t) \Bigg\} . \qquad (5.30)$$

The contribution from the circular cut is now in a convenient form for computer evaluation. The integrand is well-behaved in the region of integration, thus it can be evaluated by one of the standard methods.

In order to introduce the CDD pole into the calculations, the functions, $(\text{Im } A_1^{1/2}(s))^{-1}$ and $(\text{Re } A_1^{1/2}(s))^{-1}$ must be in the form shown in Equations (4.37) and (4.38), i.e.,

$$(\text{Im } A_1^{1/2}(s))^{-1} = - \frac{2k}{\sqrt{s}} - \frac{\kappa\tau}{\tau^2 + (s-s_r)^2} , \qquad (5.31)$$

$$(\text{Re } A_1^{1/2}(s))^{-1} = \frac{a_1(s_r-s)}{k^2} + \frac{\kappa(s-s_r)}{\tau^2 + (s-s_r)^2} . \qquad (5.32)$$

These are the only changes necessary to introduce the CDD pole in the pion-kaon amplitude. Since Im $B_o(t)$ and Im $B_1(t)$ are not affected by this pole, $C_\ell^I(s)$ is also unaffected. This function is affected, however, by a pole in the pion-pion inverse amplitudes, and these effects may be determined by introducing a pole of strength η at $t_p = t_r - i\xi$, in the pion-pion inverse amplitude. The real and imaginary parts of the inverse amplitude are then written

$$(\text{Im } f_1(t))^{-1} = - \sqrt{\frac{t-4\mu^2}{t}} - \frac{\eta\xi}{\xi^2 + (t_r-t)^2} , \qquad (5.33)$$

$$(\text{Re } f_1(t))^{-1} = \frac{b_1(t_r-t)}{(t-4^2)} + \frac{\eta(t-t_r)}{\xi^2 + (t_r-t)^2} . \qquad (5.34)$$

Section 2. The Calculation of Subtraction Constants from Consistency Requirements

Expressions for Im $A_\ell^I(s)$ and Im $B_\ell^I(t)$ were written down in Section 2 of Chapter IV for values of s and t above the physical threshold but below the threshold for inelastic scattering. Im $A_\ell^I(s)$ on the left cut along the real axis and $M_\ell^I(s)$ on the circular cut are calculated from the crossing equations, Equations (3.27), (3.28) and (3.29) in Section 2 of Chapter III. For these calculations, the effects of the cut along the real axis below $s = -50\mu^2$ are neglected. Recall from a previous section that the further out on the unphysical cut, the shorter the range of the interaction forces; thus the effects of this portion of the cut on the partial-wave amplitudes in the low energy physical region should be slowly varying with energy and easily absorbed in the subtraction constants.

Since the discontinuities of the partial-wave amplitudes across the cuts are now known, the dispersion relation, Equation (5.1), can be employed to calculate the amplitudes for all values of s. A consistency requirement is imposed in order that the subtraction constants α_ℓ^I can be determined. The scheme is shown in block diagram in Figure 12 on page 91. The real and imaginary part of the amplitudes for Channel I and the imaginary part of the amplitudes for Channel III are input for a computer program. The computer calculates the real part of the amplitude for Channel I for s greater than $(M+\mu)^2$. The real part of the

inverse amplitude is then calculated by inverting Re $A_\ell^I(s)$ and Im $A_\ell^I(s)$. This procedure should not change the experimentally observed scattering length or the resonance position. This is equivalent to requiring that $\mathrm{Re}(A_\ell^I(s))^{-1}$ iterate into itself. The subtraction constants are then determined.

The input functions and the equations necessary for a computer calculation are summarized below.

Input Functions

$$\mathrm{Im}(A_o^{1/2}(s))^{-1} = \frac{-\sqrt{(s-(M+\mu)^2)(s-(M-\mu)^2)}}{s}, \tag{5.35}$$

$$\mathrm{Im}(A_1^{1/2}(s))^{-1} = \frac{-\sqrt{(s-(M+\mu)^2)(s-(M-\mu)^2)}}{s} - \frac{\kappa\tau}{\tau^2+(s-s_r)^2}, \tag{5.36}$$

$$\mathrm{Re}(A_o^{1/2}(s))^{-1} = \frac{1}{a_o^{1/2}}, \tag{5.37}$$

$$\mathrm{Re}(A_1^{1/2}(s))^{-1} = \frac{a_1(s_r-s)}{k^2} + \frac{\kappa(s-s_r)}{\tau^2+(s-s_r)^2}, \tag{5.38}$$

$$q(t) = \frac{\sqrt{(t-4\mu^2)(4M^2-t)}}{t}, \tag{5.39}$$

$$\mathrm{Im}\ B_o(t) = q(t)\left[\frac{\sqrt{(t-4\mu^2)/t}}{(1/b_o)^2+(t-4\mu^2)/t}\right], \tag{5.40}$$

$$\mathrm{Im}\ B_1(t) = q^3(t)\left[\frac{-\mathrm{Im}f_1^{-1}(t)}{(\mathrm{Re}f_1^{-1}(t))^2+(\mathrm{Im}f_1^{-1}(t))^2}\right], \tag{5.41}$$

$$\mathrm{Im} f_1^{-1}(t) = -\sqrt{\frac{t-4\mu^2}{t}} - \frac{\eta\xi}{\xi^2 + (t_r-t)^2} , \tag{5.42}$$

$$\mathrm{Re} f_1^{-1}(t) = \frac{b_1(t_r-t)}{(t-4\mu^2)} + \frac{\eta(t-t_r)}{\xi^2 + (t_r-t)^2} , \tag{5.43}$$

where $a_o^{1/2} = 4.0$, $a_1^{1/2} = 21.5$, $s_r = 41\mu^2$, $b_o = 0.75$, $b_1 = 19$, and $t_r = 20.4\mu^2$. The value of a_o is determined by trial in the computer calculation. The value given here is simply the best value for which the calculated values of Re $A_o^{1/2}(s)$ and the input values of Re $A_o^{1/2}(s)$ are comparable. In any case, the value of a_o is of little importance in the final analysis. The values of $a_1^{1/2}$ and s_r are determined from experimental resonance data from reference 20. The resonance position, s_r, is expressed in the CM system and has units of energy squared. The reduced width, $a_1^{1/2}$ is dimensionless and is related to the resonance width, Γ, by

$$a_1^{1/2} = \frac{1}{\Gamma^2} \frac{2k^3(s_r)}{\sqrt{s_r}} . \tag{5.44}$$

The values for b_o, the reduced width, b_1, and the resonance position, t_r, for the pion-pion interaction are obtained from reference 30. The values of κ, τ, η, and ξ are set equal to zero for the evaluation of the subtraction constants with no CDD poles in the inverse amplitudes and their values are varied to observe the effects of the pole on the subtraction constants. If the pion-pion scattering amplitude is indeed a split resonance, the values of η and ξ will be determined by the

desired spacing of the two parts of the resonance and the widths of these resonances, and they will not be variable in this analysis. The values of κ and τ are the important variables of this analysis.

Equations for Computer Calculations

$$\underset{\text{(on right cut)}}{\text{Im } A_\ell^I(s)} = \frac{-\text{Im } A_\ell^I(s)^{-1}}{(\text{Im } A_\ell^I(s)^{-1})^2 + (\text{Re } A_\ell^I(s)^{-1})^2}, \tag{5.45}$$

$$[\text{Re } A_\ell^I(s)]_{\text{input}} = \frac{\text{Re } A_\ell^I(s)^{-1}}{(\text{Im } A_\ell^I(s)^{-1})^2 + (\text{Re } A_\ell^I(s)^{-1})^2} \tag{5.46}$$

$$R_\ell^I(s) = \frac{s-M^2}{\pi} \int_{(M+\mu)^2}^{N} ds' \frac{[\text{Im } A_\ell^I(s')/(s'-M^2) - \text{Im } A_\ell^I(s)/(s-M^2)]}{(s'-s)} \tag{5.47}$$

$$\frac{\text{Im } A_\ell^I(s)}{\pi} \ln \left[\frac{N - s}{s - (M+\mu)^2}\right],$$

$C_\ell^I(s) \rightarrow$ See Equations (5.29), (5.30),

$L_\ell^I(s) \rightarrow$ See Equations (5.17), (5.18),

$$\alpha_\ell^I = [\text{Re } A^I(s)]_{\text{input}} - R_\ell^I(s) - C_\ell^I(s) - L_\ell^I(s). \tag{5.48}$$

If the subtraction constants are evaluated for many values of s, small variations are introduced in their values since the effects of the unphysical cuts are not constant. The value of s for which the subtraction

constants are determined is arbitrarily picked to be $s = s_r$.

Accuracy of the Computer Program

The variations in the subtraction constants produced by the CDD pole were found to be quite small and it was possible that those variations could have been in the same range of significant figures as the inaccuracies introduced by the approximation methods of the computer programs. For this reason, it is worthwhile to mention here some of the details concerning the accuracy of the computer programs. The two primary sources of error in the computer programs were the substitution of finite limits of integration for infinite ones, and the use of the trapezoidal rule for evaluating the integrals. Much of the error introduced by the choice of a finite limit of integration was absorbed in the subtraction constants. The limits were extended until the error was reduced to less than one part in 10 for $R_o(s)$, one part in 100 for $R_1(s)$ and about one part in 200 for $L_\ell(s)$. There are no infinite limits in the calculation of $C_\ell(s)$. The larger error in $R_o(s)$ was considered acceptable since the effects of the CDD pole on the S-wave amplitudes were not of special interest. The accuracy of the trapezoidal rule for evaluating the integral of a function of $f(x)$ depends on the number of rectangles, N, into which the area under the curve, $f(x)$, has been divided. It also depends on $f(x)$, of course, since rapidly varying functions require larger values of N than slowly varying functions. Each computer program in this thesis in which an integral was to be evaluated was run with varying values of N. The value of N was increased until the variations in the computer output for that integral were on the

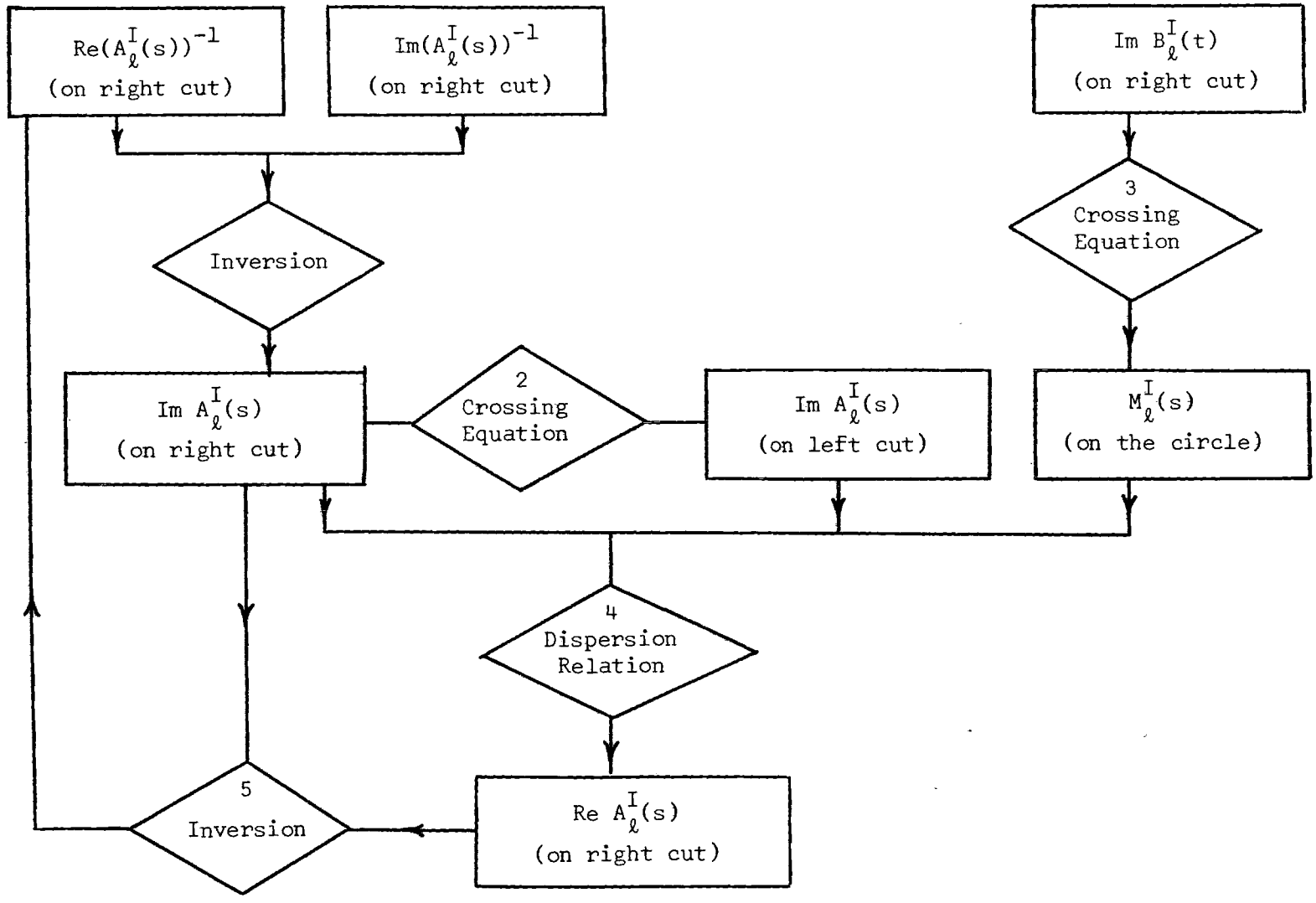

Figure 12. Block Diagram for the Consistency Requirements

order of one part in 1,000,000. The value of N necessary to obtain this degree of accuracy was different for different integrals, but values from 100-200 were sufficient for most integrations involving Im $A_o^{1/2}(s)$ and values from 200-500 were sufficient for most integrations involving Im $A_1^{1/2}(s)$. The very sharp resonance peak in Im $A_1^{1/2}(s)$ accounts for the larger value of N necessary to achieve the desired accuracy.

The effects of the computer program on the S-wave amplitudes are shown in Figure 13. The subtraction constants are chosen so that the input and output values of the S-wave amplitudes are the same at $s = 4\mu^2$. The maximum variation between input and output is about one part in ten in the region of interest. The effects of the computer program on the P-wave amplitudes are too small to appear on the graphs in Figure 14, although they are noticeable in the tabulation of computer input and output data, Table 2. The subtraction constants are again chosen so that input equals output at $s = 4\mu^2$. The maximum variation in the region of interest is about one part per 100.

Section 3. Appendix Guide

All computer programs used in the calculations for this thesis are shown in Appendix B. The primary function of the programs is the evaluation of the subtraction constants with and without a CDD pole in the inverse amplitude. Both the strength and position of the pole may be varied in order to observe the effects of the pole on the subtraction constants. It was noted previously in this thesis that a pole in the pion-kaon inverse amplitudes affects only $R_1^I(s)$ and $L_\ell^I(s)$ while a pole in the pion-pion inverse amplitude affects only $C_\ell^I(s)$. For this reason,

much computer time can be saved by dividing the program into several sections. An added incentive for this division is the many long and tedious algebraic expressions which must be included in the evaluation of $L_\ell^I(s)$ and $C_\ell^I(s)$.

In the first program $R_o^{1/2}(s)$ and $[\text{Re } A_o^{1/2}(s)]_{\text{input}}$ are evaluated for values of s from $(M+\mu)^2$ to about $60\mu^2$. This program is not changed by a CDD pole in either the pion-pion or the pion-kaon inverse amplitudes. The next program evaluates $R_1^{1/2}(s)$ and $[\text{Re } A_1^{1/2}(s)]_{\text{input}}$ for s in the same range. This program includes a CDD pole in the inverse P-wave amplitude for pion-kaon scattering. The third program evaluates $C_\ell^I(s)$ with a pole in the pion-pion inverse P-wave amplitude. The fourth program and the fifth program calculate $L_\ell^I(s)$ with the pion-kaon pole. The contribution from the cut from 0 to $(M-\mu)^2$ is handled separately from the cut from -N to 0. The last two programs are necessary in the calculation of the subtraction constants, and they are not included primarily for interest. The P-wave phase shifts are calculated from the expression

$$\frac{2k^3}{\sqrt{s}} \cot\delta_1^I(s) = k^2 \, \text{Re}(A_1^I(s))^{-1}, \tag{5.49}$$

and the absorptive parts of the amplitudes on the left cut are calculated from the crossing equations.

A sample of the computer output from each program is included at the end of the program.

CHAPTER VI

SUMMARY OF RESULTS AND CONCLUSIONS

It was necessary to determine the subtraction constants, α_ℓ^I, before the introduction of a CDD pole into the inverse amplitude solutions. The consistency of the scheme used in this thesis for handling split resonances, if a single resonance solution is known, depends upon the introduction of a CDD pole leaving these constants unchanged. The constants were calculated from the equation

$$\alpha_\ell^I = \mathrm{Re}A_\ell^I(s) - R_\ell^I(s) - C_\ell^I(s) - L_\ell^I(s), \tag{6.1}$$

for $s = s_r = 40.96$. The first three terms on the right side of the equation, $\mathrm{Re}A_\ell^I(s)$, $R_\ell^I(s)$, and $C_\ell^I(s)$, were each calculated from a separate computer program, and the last term, $L_\ell^I(s)$, was calculated from two separate programs which differed by only a few calculations. These programs are shown in full in Appendix B. The values of the subtraction constants which were obtained from these calculations are

$$\alpha_o^{1/2} = 0.8942, \quad \alpha_o^{3/2} = 0.7312, \tag{6.2a}$$

$$\alpha_1^{1/2} = -0.0451, \quad \alpha_1^{3/2} = 0.0089. \tag{6.2b}$$

The CDD pole was introduced into the original inverse amplitude by modifying the original solution

$$\text{Re } A_1^{-1}(s) = a_1(s_r - s)/k^2, \tag{6.3}$$

$$\text{Im } A_1^{-1}(s) = -\frac{2k}{\sqrt{s}}, \tag{6.4}$$

to include a CDD pole of strength κ at $s_p = s_r = i\tau$. Then

$$\text{Re } A_1^{-1}(s) = a_1(s_r - s)/k^2 + \frac{\kappa(s - s_r)}{(s_r - s)^2 + \tau^2}, \tag{6.5}$$

$$\text{Im } A_1^{-1}(s) = -\frac{2k}{\sqrt{s}} - \frac{\kappa\tau}{(s_r - s)^2 + \tau^2}. \tag{6.6}$$

The contribution to the pion-kaon amplitude from the discontinuity across the circular cut, $C_\ell^I(s)$, is not affected by the introduction of this pole. However, a pole could be inserted into the pion-pion inverse amplitude, $f_1^{-1}(v)$, to account for the ζ and the ρ di-pion resonances. The position and strength of the pole necessary to agree with the experimental data has already been determined by Gatland and Moffat[30] and they have shown that its effects on the contribution to the pion-pion amplitude from the unphysical cut are negligible. Such a pole was not included in the calculations since it has little effect on the present problem. This simply means that it is possible that the pion-pion scattering amplitude has a double resonance solution while the pion-kaon scattering amplitude does not.

The functions, $R_1^I(s)$, $L_o^I(s)$ and $L_1^I(s)$, were recalculated using the modified form of Im $A_1(s)$. The function, $R_0^I(s)$, is not affected by the pole in the P-wave inverse amplitude. The strength of the pole was varied until Im $A_1(s)$ showed two resonance peaks. As the strength of the pole increased, the single resonance decreased in height and became broader. At a strength of about μ^2, the resonance split, and at a strength of about 10 μ^2, the two resonance peaks were separated by more than 200 MeV. The function, $R_1(s)$, is shown in Figure 14, both with and without a CDD pole. The strength of the pole is 10 μ^2 for the example given. The imaginary part of the pole position τ also has an effect on $R_1(s)$. As the pole approaches the real axis the resonance peaks are increased in height and decreased in width. However, these effects are small. In any case, the point of interest here is the splitting effect on $R_1(s)$. With a proper choice of pole strength and position it is possible to create solutions which have the masses and resonances widths of any pair of experimentally observed resonances, provided the corresponding effects on the left cut contributions, $L_1(s)$, are negligible. Poles of strengths varying from zero to 100 μ^2 and positions, τ, varying from one to 10^{-5} μ^2, were inserted into the computer program for $L_1(s)$. The variations in $L_1^I(s)$ due to both strength and position were quite small. In particular, a pole for which $\kappa = 10$ μ^2 and $\tau = 10^{-3}$ μ^2 changed $L_1(s)$ by less than one tenth of 1 per cent. The functions $L_o(s)$ and $L_1(s)$ are shown graphically in Figure 17, but the effects of the CDD pole for any of the above range of strengths and positions are too small to appear on this scale. It is of interest to

note, however, that the effects of the pole increases as the pole moves nearer to real axis. This implies that inelastic contributions should be small since the imaginary part of the phase shift at $\mathrm{Re}\delta_1 = \pi$, is directly proportional to τ,

$$\mathrm{Im}\delta_1\Big|_{\mathrm{Re}\delta_1=\pi} = \frac{\tau}{\kappa}\frac{2k(s_r)}{\sqrt{s_r}} . \tag{6.7}$$

In addition, the effects on $L_1(s)$ due to the pole are reduced as the strength of the pole, κ, is reduced as expected. Since the slope of the real part of the P-wave phase shift is inversely proportional to κ, the real part of the phase shift should be sharply increasing as it passes through π, i.e.

$$\frac{d}{ds}\mathrm{Re}\delta_1\Big|_{\mathrm{Re}\delta_1=\pi} = \left(\frac{1}{\kappa}\right)\frac{2k(s_r)}{\sqrt{s_r}} . \tag{6.8}$$

In conclusion, a split resonance solution can be produced from a single resonance solution for pion-kaon scattering without violating unitarity. Since the crossing equations for the scattering amplitudes of any two particles of unequal masses have the same general form as the crossing equations for pion-kaon scattering, the technique presented here applies equally well to all scattering problems involving particles of unequal masses, provided the spin cases are the same. The technique should also apply for particles with non-zero spin, but until the effects of spin on the problem have been investigated, some caution should be exercised in generalizing the results to particles with spin.

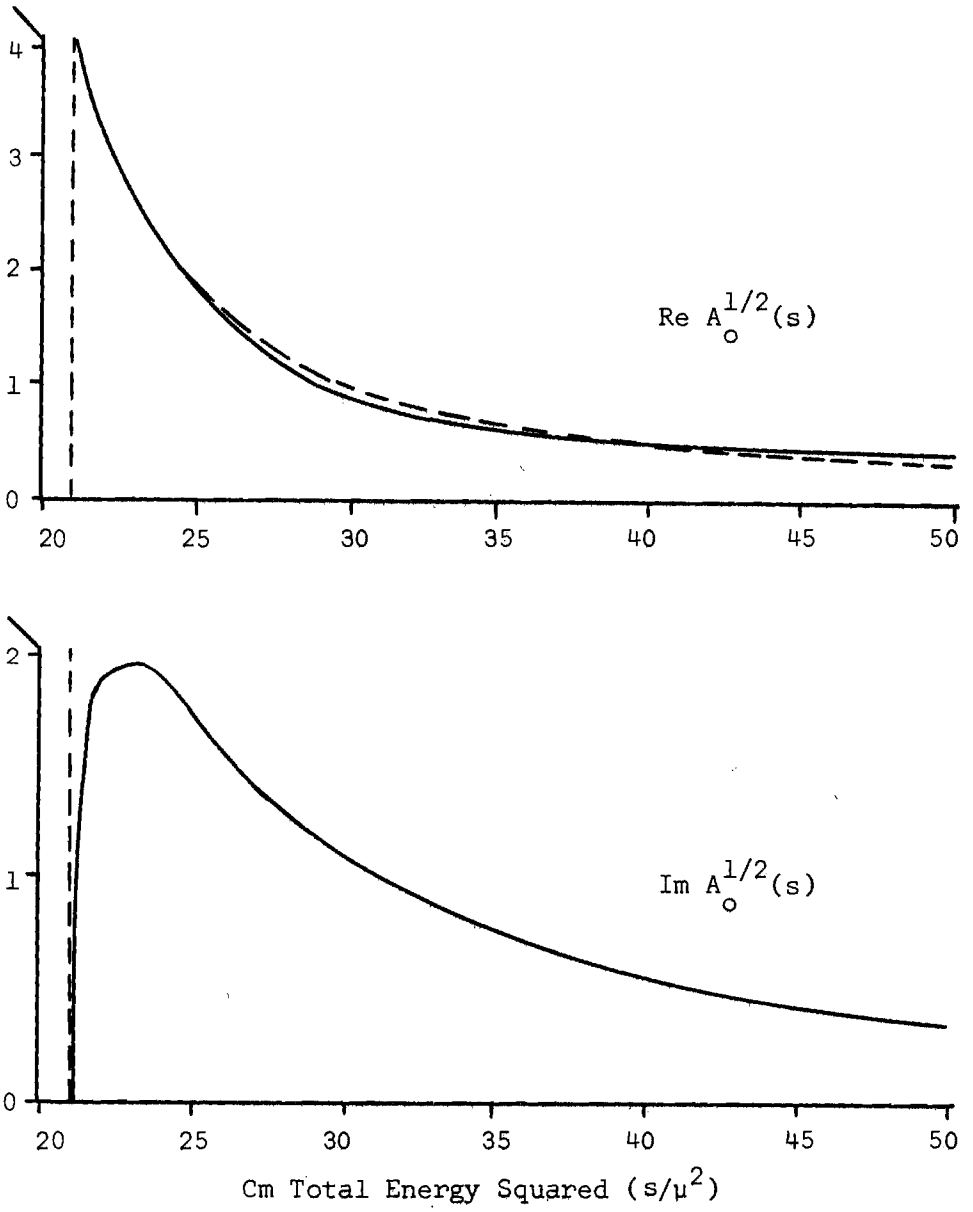

Figure 13. The S-Wave Amplitudes in the Physical Region of Channel I. The Effects of a CDD Pole in the P-Wave Inverse Amplitudes Are Not Apparent on This Scale. The Broken Line Shows the Effects of the Computer Program on Re $A_o^{1/2}(s)$.

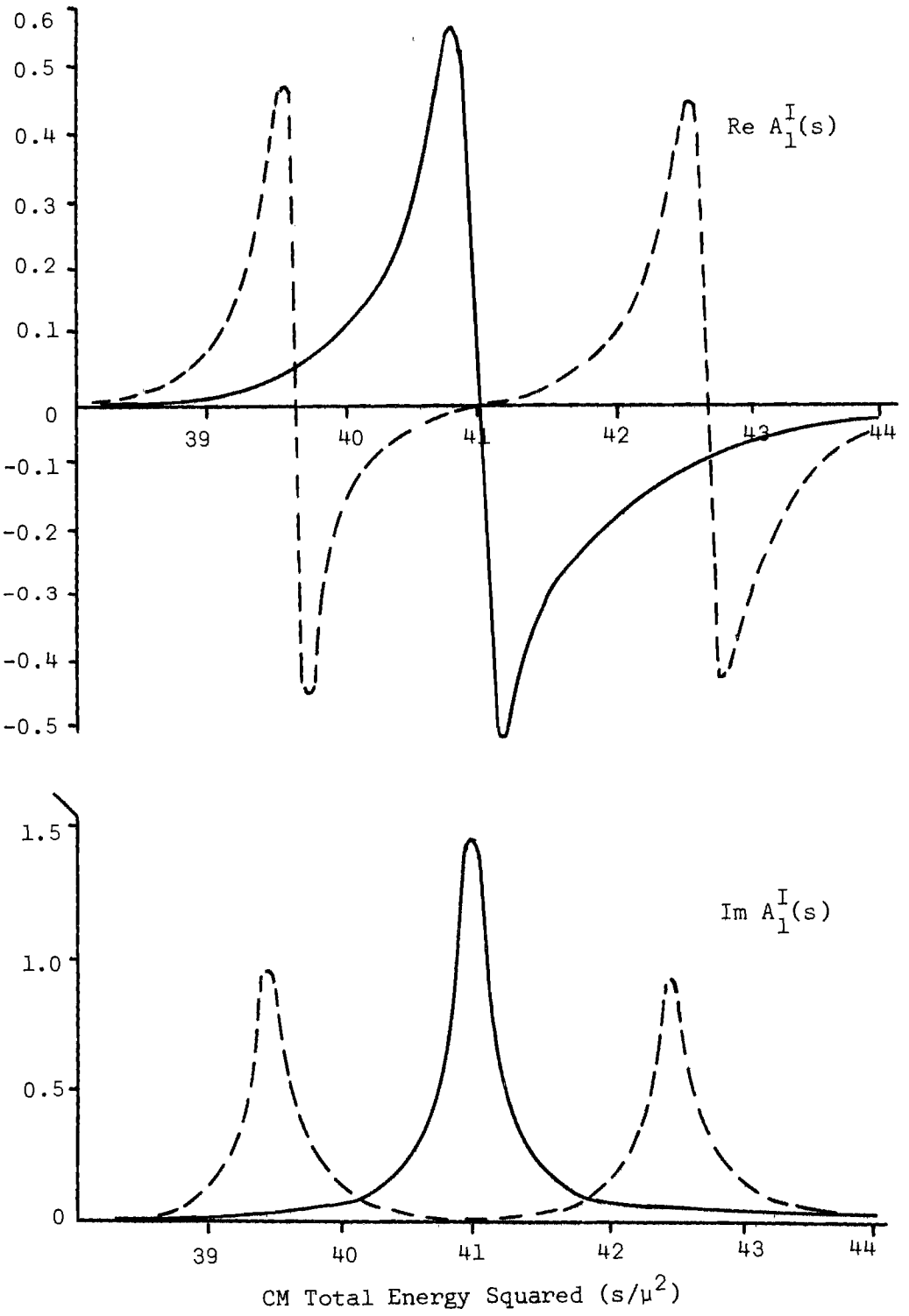

Figure 14. The P-Wave Amplitudes Without CDD Pole (Solid Line) and with CDD Pole (Broken Line)

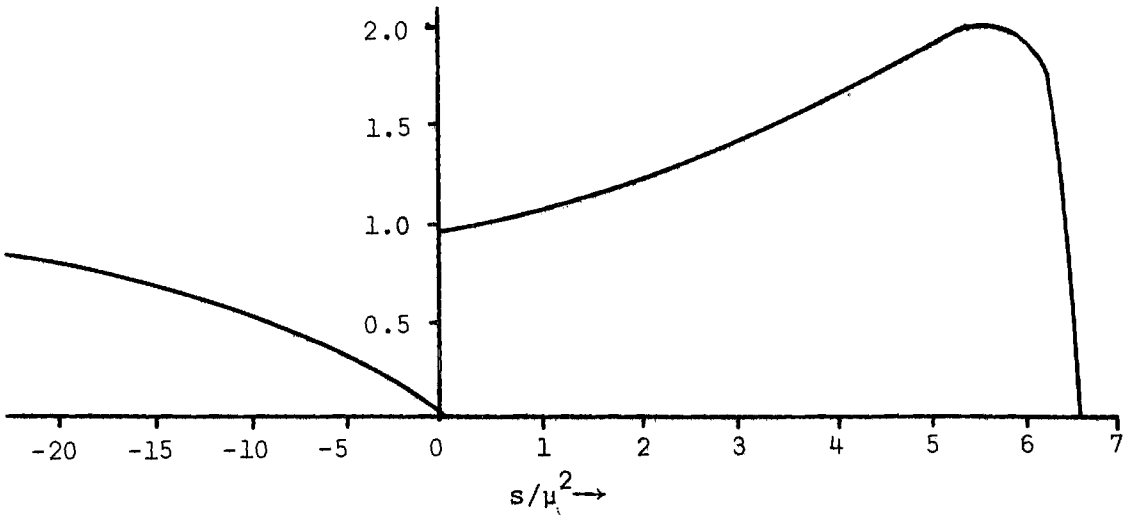

Figure 15a. The Absorptive Part of the S-Wave Amplitude in the Unphysical Region of Channel I. The Curves Are Calculated from the Crossing Equation. The Effects of the CDD Pole Are Negligible on this Scale.

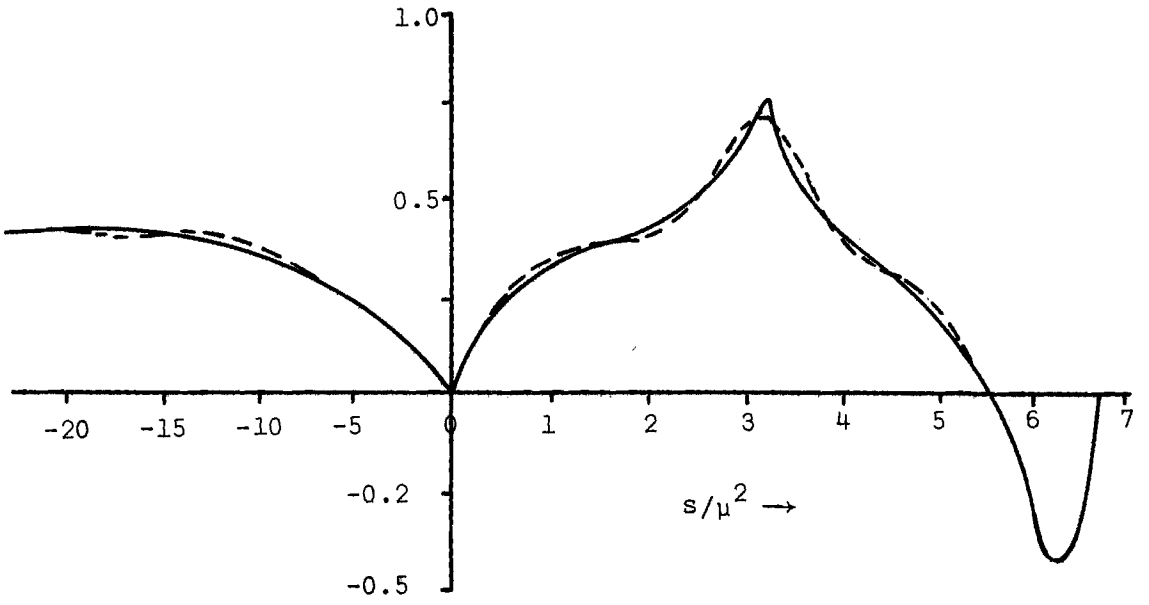

Figure 15b. The Absorptive Part of the P-Wave Amplitude in the Unphysical Region of Channel I. The Curves Are Calculated from the Crossing Equation. The Broken Line Shows the Effects of the CDD Pole.

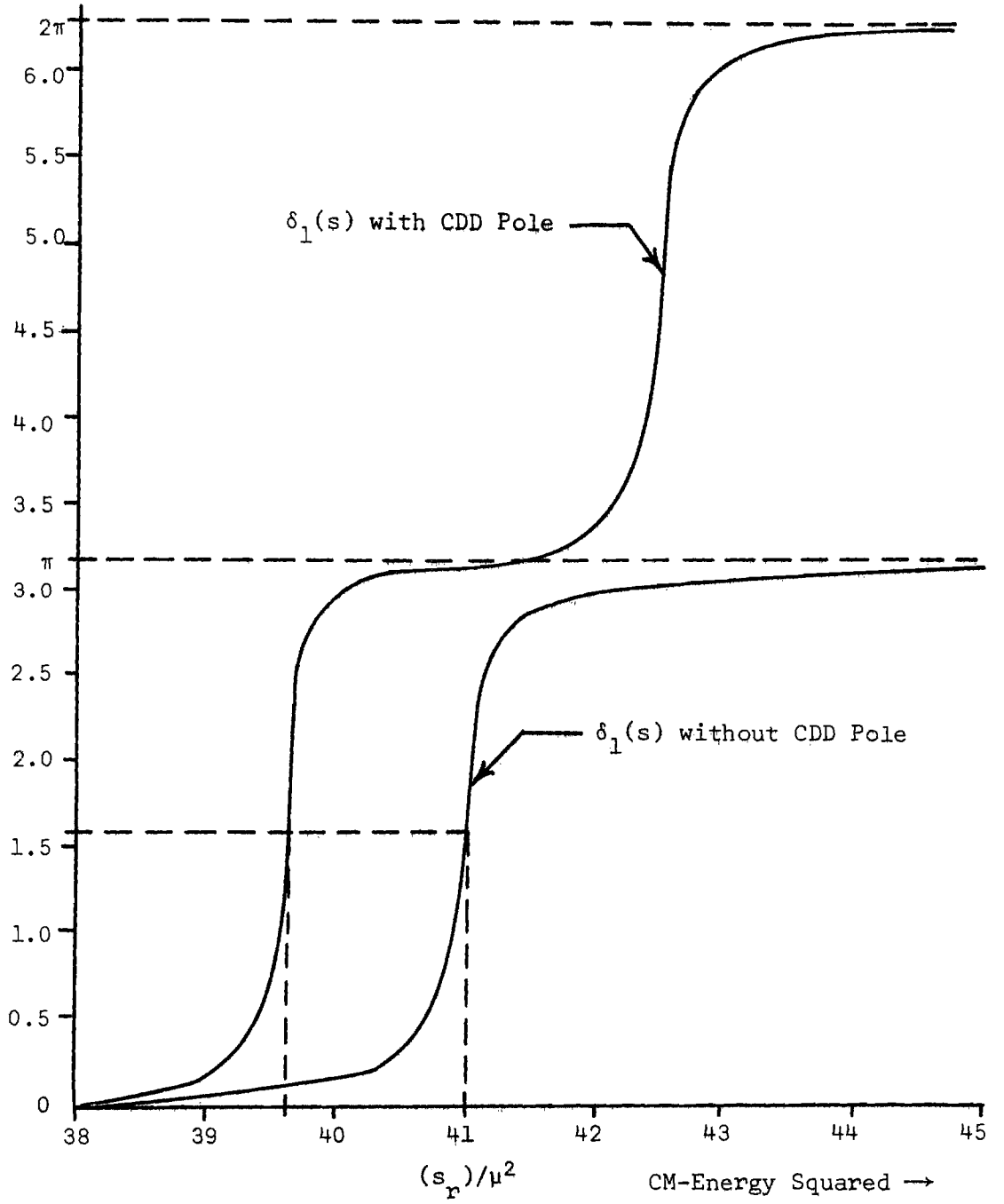

Figure 16. P-Wave Phase Shifts with and without CDD Pole. The Value of s for Which the Phase Shift Goes Through $\pi/2$ is Usually Defined to be the $(\text{Mass})^2$ of the Resonance. The Mass-Squared of the Resonance Position before the CDD Pole is Given by s_r.

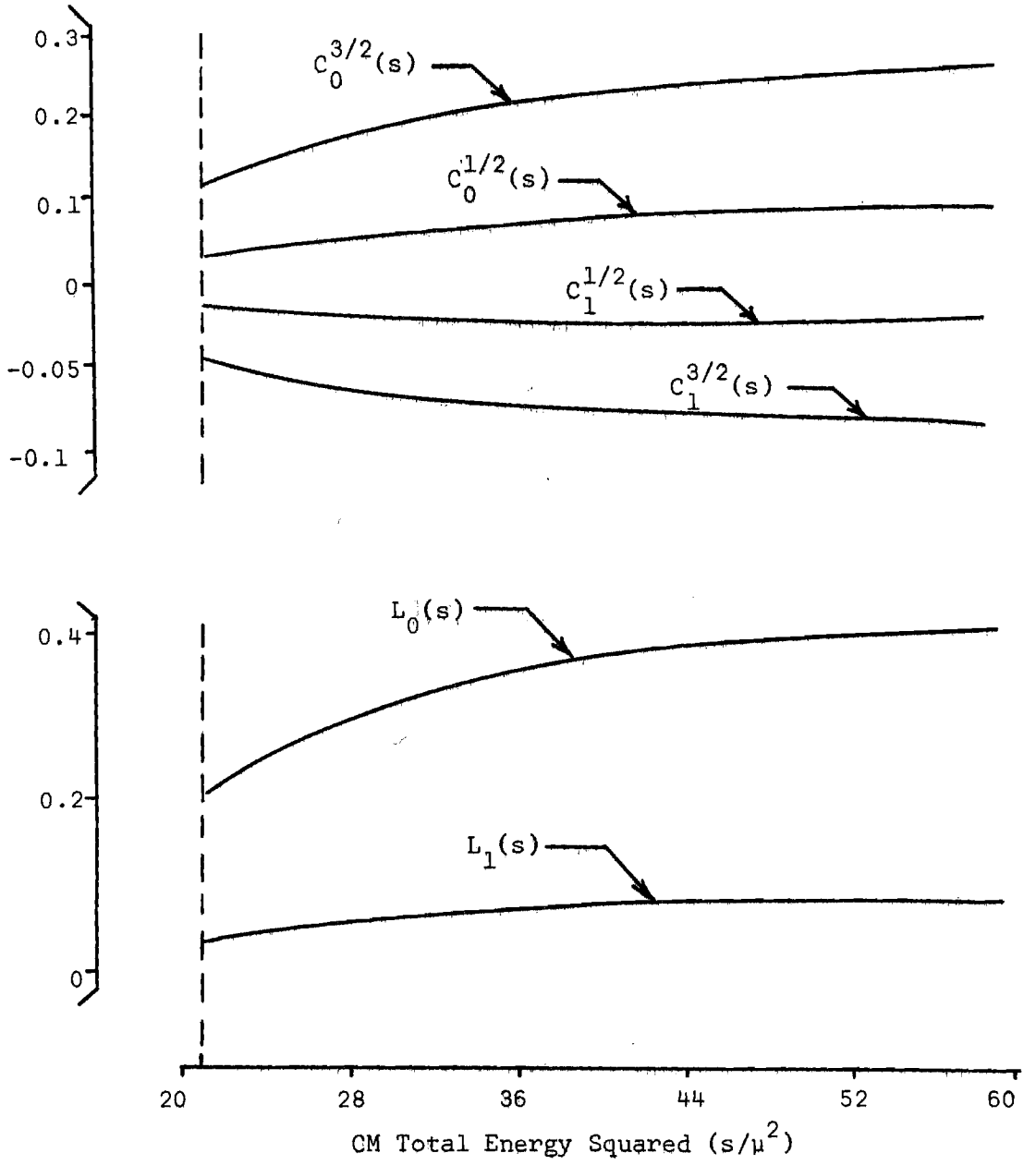

Figure 17. Contributions to the Real Part of the Amplitude from the Circular Cut and from the Left Cut. (The Effects of the CDD Pole Are of Insufficient Magnitude to Display on this Scale.)

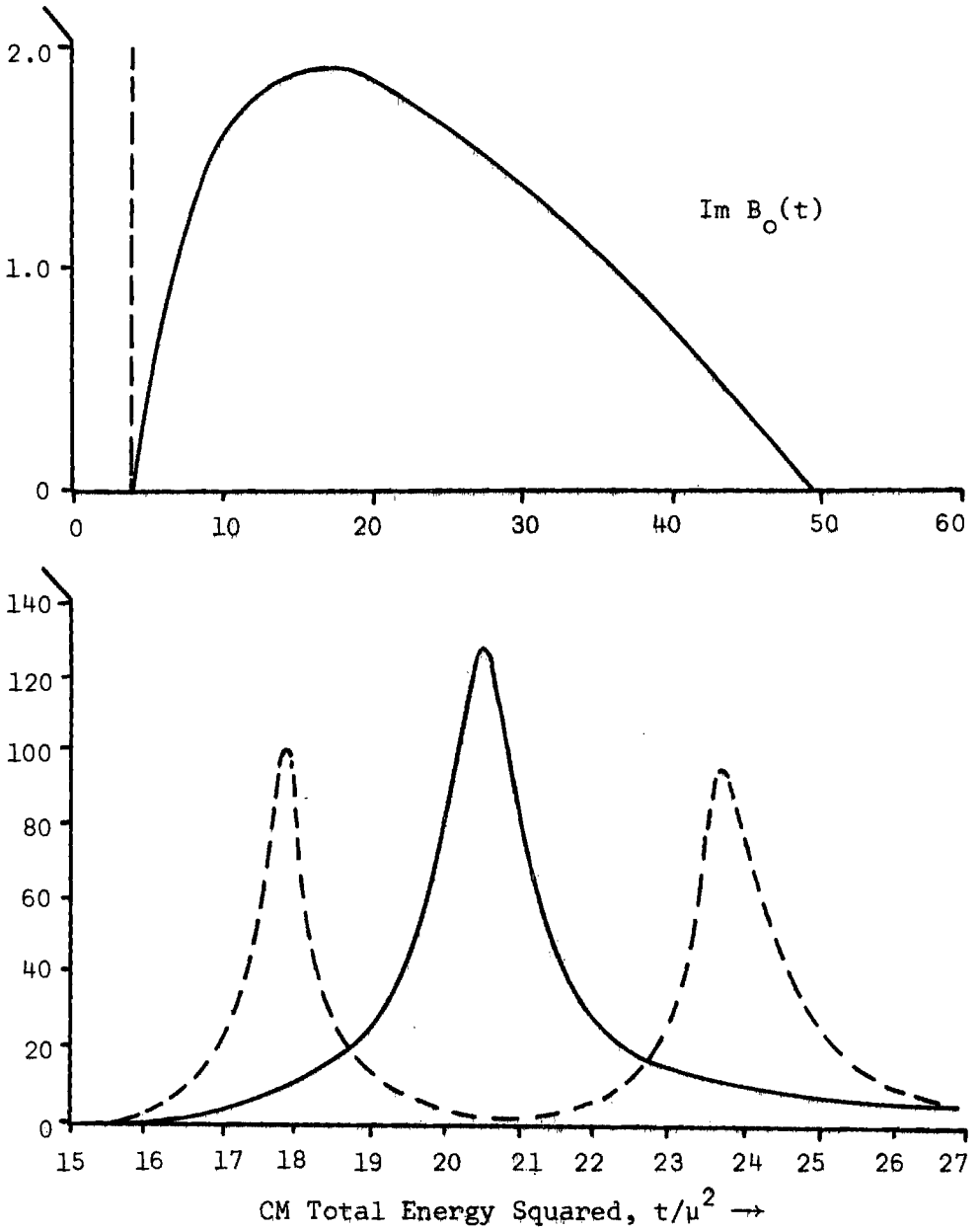

Figure 18. The Absorptive Parts of the S-Wave and the P-Wave Amplitudes in the Physical Region of Channel III. The P-Wave Amplitude is Shown with a CDD Pole in the Pion-Pion → Pion-Pion Inverse Amplitude (Broken Line) and Without the Pion (Solid Line).

Table 1. S-Wave Amplitudes With and Without CDD Pole

$(\kappa = 10, \tau = 10^{-3})$

$\alpha_o^{1/2} = 0.8942, \quad \alpha_o^{3/2} = 0.7312$

s	Input Functions		$R_o(s)$	$C_o^{1/2}(s)$	$C_o^{3/2}(s)$	$L_o(s)$	With Pole $L_o(s)$	$ReA_o^{1/2}(s)$	With Pole $ReA_o^{1/2}(s)$
	$ReA_o(s)$	$ImA_o(s)$							
21	3.2630	1.5508	2.0074	0.0316	0.1170	0.2210	0.2210	3.1542	3.1542
22	2.3059	1.9765	1.0573	0.0351	0.1273	0.2340	0.2340	2.2206	2.2206
23	1.8046	1.9904	0.5542	0.0383	0.1368	0.2470	0.2469	1.7337	1.7336
24	1.4966	1.9356	0.2695	0.0413	0.1457	0.2578	0.2577	1.4628	1.4627
25	1.2884	1.8691	0.0557	0.0441	0.1539	0.2687	0.2686	1.2627	1.2626
26	1.1383	1.8049	-0.1239	0.0467	0.1616	0.2779	0.2778	1.0949	1.0948
27	1.0251	1.7463	-0.2416	0.0491	0.1688	0.2871	0.2870	0.9888	0.9887
28	0.9369	1.6940	-0.3157	0.0514	0.1755	0.2956	0.2955	0.9255	0.9254
29	0.8661	1.6475	-0.3938	0.0537	0.1817	0.3031	0.3030	0.8570	0.8569
30	0.8080	1.6060	-0.4573	0.0554	0.1876	0.3101	0.3100	0.8024	0.8023
31	0.7596	1.5689	-0.5261	0.0573	0.1931	0.3171	0.3170	0.7425	0.7424
32	0.7187	1.5357	-0.5719	0.0590	0.1983	0.3232	0.3231	0.7045	0.7044
33	0.6836	1.5057	-0.5999	0.0607	0.2032	0.3294	0.3293	0.6844	0.6843
34	0.6532	1.4785	-0.6361	0.0622	0.2078	0.3349	0.3348	0.6552	0.6551
35	0.6266	1.4539	-0.6783	0.0637	0.2122	0.3404	0.3403	0.6200	0.6199
36	0.6031	1.4314	-0.7064	0.0651	0.2163	0.3453	0.3452	0.5982	0.5981
37	0.5823	1.4107	-0.7319	0.0664	0.2203	0.3503	0.3502	0.5790	0.5789
38	0.5637	1.3918	-0.7468	0.0677	0.2240	0.3547	0.3546	0.5698	0.5697
39	0.5469	1.3742	-0.7685	0.0688	0.2275	0.3592	0.3591	0.5537	0.5536
40	0.5318	1.3581	-0.7962	0.0700	0.2309	0.3632	0.3631	0.5312	0.5311
41	0.5180	1.3430	-0.8145	0.0710	0.2341	0.3672	0.3671	0.5180	0.5179
42	0.5055	1.3291	-0.8245	0.0721	0.2372	0.3709	0.3708	0.5127	0.5126
43	0.4940	1.3160	-0.8411	0.0731	0.2401	0.3746	0.3745	0.5008	0.5007
44	0.4834	1.3039	-0.8560	0.0740	0.2429	0.3780	0.3779	0.4902	0.4901
45	0.4737	1.2924	-0.8765	0.0749	0.2456	0.3814	0.3813	0.4740	0.4739
46	0.4647	1.2817	-0.8898	0.0758	0.2481	0.3845	0.3844	0.4647	0.4646
47	0.4563	1.2716	-0.8970	0.0766	0.2506	0.3877	0.3876	0.4615	0.4614
48	0.4485	1.2621	-0.9093	0.0774	0.2529	0.3905	0.3904	0.4528	0.4527
49	0.4413	1.2531	-0.9258	0.0782	0.2552	0.3934	0.3933	0.4400	0.4399
50	0.4345	1.2447	-0.9374	0.0789	0.2574	0.3960	0.3959	0.4317	0.4316

Table 2. P-Wave Amplitudes Without CDD Pole

$(\alpha_1^{1/2} = -0.0451)$

$(\alpha_1^{3/2} = 0.0089)$

s	Input Functions		$R_1(s)$	$C_1^{1/2}(s)$	$C_1^{3/2}(s)$	$L_1(s)$	Re $A_1^{1/2}(s)$
	Re $A_1^{1/2}(s)$	Im $A_1^{1/2}(s)$					
35.0	0.0230	0.0003	0.0265	-0.0321	-0.0827	0.0680	0.0173
35.5	0.0260	0.0004	0.0295	-0.0323	-0.0832	0.0687	0.0208
36.0	0.0297	0.0005	0.0332	-0.0325	-0.0838	0.0694	0.0250
36.5	0.0342	0.0007	0.0377	-0.0327	-0.0843	0.0701	0.0300
37.0	0.0398	0.0010	0.0433	-0.0329	-0.0848	0.0708	0.0361
37.5	0.0471	0.0014	0.0507	-0.0331	-0.0853	0.0715	0.0440
38.0	0.0568	0.0020	0.0603	-0.0333	-0.0858	0.0721	0.0540
38.5	0.0704	0.0031	0.0740	-0.0335	-0.0862	0.0727	0.0681
39.0	0.0910	0.0052	0.0946	-0.0337	-0.0867	0.0734	0.0892
39.5	0.1254	0.0100	0.1286	-0.0338	-0.0871	0.0740	0.1237
40.0	0.1943	0.0245	0.1967	-0.0340	-0.0875	0.0746	0.1922
40.5	0.3944	0.1075	0.3981	-0.0341	-0.0879	0.0752	0.3941
41.0	-0.4341	1.4091	-0.4305	-0.0343	-0.0883	0.0758	-0.4341
41.5	-0.3586	0.0892	-0.3474	-0.0344	-0.0886	0.0764	-0.3505
42.0	-0.1993	0.0266	-0.1957	-0.0346	-0.0890	0.0770	-0.1984
42.5	-0.1393	0.0130	-0.1356	-0.0348	-0.0893	0.0775	-0.1380
43.0	-0.1082	0.0078	-0.1043	-0.0350	-0.0897	0.0780	-0.1063
43.5	-0.0891	0.0053	-0.0853	-0.0351	-0.0900	0.0785	-0.0870
44.0	-0.0763	0.0039	-0.0726	-0.0352	-0.0904	0.0790	-0.0739
44.5	-0.0671	0.0030	-0.0634	-0.0353	-0.0907	0.0796	-0.0642
45.0	-0.0602	0.0025	-0.0564	-0.0354	-0.0910	0.0801	-0.0569
45.5	-0.0547	0.0020	-0.0510	-0.0355	-0.0913	0.0806	-0.0510
46.0	-0.0504	0.0019	-0.0467	-0.0357	-0.0916	0.0810	-0.0465
46.5	-0.0468	0.0015	-0.0431	-0.0358	-0.0918	0.0815	-0.0425
47.0	-0.0438	0.0013	-0.0401	-0.0359	-0.0921	0.0820	-0.0391
47.5	-0.0414	0.0012	-0.0376	-0.0360	-0.0923	0.0825	-0.0362
48.0	-0.0392	0.0011	-0.0354	-0.0361	-0.0926	0.0830	-0.0336
48.5	-0.0373	0.0010	-0.0335	-0.0362	-0.0928	0.0834	-0.0314
49.0	-0.0356	0.0009	-0.0318	-0.0363	-0.0931	0.0838	-0.0294
49.5	-0.0342	0.0008	-0.0304	-0.0364	-0.0933	0.0842	-0.0277
50.0	-0.0330	0.0008	-0.0293	-0.0365	-0.0936	0.0845	-0.0264

Table 3. P-Wave Amplitudes with CDD Pole

($\kappa = 10$, $\tau = 10^{-3}$, $\alpha_1^{1/2} = -0.0451$)

($\alpha_1^{3/2} = 0.0089$)

s	Input Functions		$R_1(s)$	$C_1^{1/2}(s)$	$C_1^{3/2}(s)$	$L_1(s)$	Re $A_1^{1/2}(s)$
	Re $A_1^{1/2}(s)$	Im $A_1^{1/2}(s)$					
35.0	0.0237	0.0003	0.0277	-0.0321	-0.0827	0.0680	0.0185
35.5	0.0271	0.0004	0.0312	-0.0323	-0.0832	0.0687	0.0225
36.0	0.0313	0.0006	0.0355	-0.0325	-0.0838	0.0694	0.0273
36.5	0.0367	0.0008	0.0411	-0.0327	-0.0843	0.0701	0.0334
37.0	0.0437	0.0012	0.0484	-0.0329	-0.0848	0.0708	0.0412
37.5	0.0537	0.0018	0.0588	-0.0331	-0.0853	0.0715	0.0521
38.0	0.0689	0.0029	0.0748	-0.0333	-0.0858	0.0721	0.0685
38.5	0.0958	0.0058	0.1035	-0.0335	-0.0862	0.0727	0.0976
39.0	0.1602	0.0164	0.1756	-0.0337	-0.0867	0.0734	0.1702
39.5	0.5714	0.2473	0.5230	-0.0338	-0.0871	0.0740	0.5181
40.0	-0.2077	0.0285	-0.1816	-0.0340	-0.0875	0.0746	-0.1861
40.5	-0.0573	0.0022	-0.0502	-0.0341	-0.0879	0.0752	-0.0542
41.0	0.0000	0.0000	0.0060	-0.0343	-0.0883	0.0758	0.0024
41.5	0.0568	0.0022	0.0647	-0.0344	-0.0886	0.0764	0.0616
42.0	0.1871	0.0237	0.2109	-0.0346	-0.0890	0.0770	0.2082
42.5	-0.5157	1.2959	-0.7471	-0.0348	-0.0893	0.0775	-0.7495
43.0	-0.2422	0.0403	-0.2211	-0.0350	-0.0897	0.0780	-0.2232
43.5	-0.1415	0.0136	-0.1329	-0.0351	-0.0900	0.0785	-0.1346
44.0	-0.1040	0.0073	-0.0983	-0.0352	-0.0904	0.0790	-0.0996
44.5	-0.0841	0.0058	-0.0793	-0.0353	-0.0907	0.0796	-0.0801
45.0	-0.0716	0.0035	-0.0672	-0.0354	-0.0910	0.0801	-0.0676
45.5	-0.0629	0.0027	-0.0588	-0.0355	-0.0913	0.0806	-0.0588
46.0	-0.0565	0.0022	-0.0525	-0.0357	-0.0916	0.0810	-0.0523
46.5	-0.0516	0.0018	-0.0477	-0.0358	-0.0918	0.0815	-0.0471
47.0	-0.0477	0.0016	-0.0438	-0.0359	-0.0921	0.0820	-0.0428
47.5	-0.0444	0.0014	-0.0406	-0.0360	-0.0923	0.0825	-0.0392
48.0	-0.0418	0.0012	-0.0378	-0.0361	-0.0926	0.0830	-0.0360
48.5	-0.0395	0.0011	-0.0355	-0.0362	-0.0928	0.0834	-0.0334
49.0	-0.0376	0.0010	-0.0336	-0.0363	-0.0931	0.0838	-0.0312
49.5	-0.0359	0.0009	-0.0319	-0.0364	-0.0933	0.0842	-0.0292
50.0	-0.0344	0.0008	-0.0304	-0.0365	-0.0936	0.0845	-0.0275

Table 4. Absorptive Part of S and P-Wave Amplitudes on the Left Cut with and without CDD Pole

$\kappa = 10, \quad \tau = 10^{-3}$

s	Im $A_o(s)$	Im $A_o(s)$ With CDD Pole	Im $A_1(s)$	Im $A_1(s)$ With CDD Pole
6.40	0.6994	0.6994	-0.0593	-0.0593
6.10	1.7502	1.7502	-0.0785	-0.0785
5.80	1.9421	1.9421	-0.0369	-0.0369
5.50	1.9704	1.9704	-0.0009	-0.0009
5.20	1.9426	1.9426	0.0264	0.0264
4.60	1.8351	1.8351	0.0626	0.0626
4.00	1.7139	1.7139	0.0831	0.0831
3.40	1.5959	1.5953	0.0952	0.0958
2.80	1.4099	1.4102	0.1350	0.1364
2.20	1.3350	1.3375	0.0957	0.0966
1.60	1.2527	1.2489	0.0814	0.0799
1.00	1.1609	1.1646	0.0705	0.0732
0.40	1.0547	1.0558	0.0509	0.0519
0.01	0.9413	0.9413	0.0004	0.0004
-0.01	0.0009	0.0009	0.0009	0.0009
-0.50	0.0044	0.0044	0.0044	0.0044
-1.00	0.0883	0.0883	0.0841	0.0841
-2.00	0.1632	0.1632	0.1483	0.1483
-3.00	0.2301	0.2301	0.2000	0.2000
-4.00	0.2901	0.2901	0.2413	0.2413
-5.00	0.3439	0.3439	0.2743	0.2743
-6.00	0.3925	0.3925	0.3003	0.3003
-7.00	0.4363	0.4363	0.3207	0.3207
-8.00	0.4761	0.4761	0.3364	0.3363
-9.00	0.5122	0.5122	0.3484	0.3484
-10.00	0.5452	0.5452	0.3572	0.3572
-11.00	0.5753	0.5754	0.3635	0.3636
-12.00	0.6031	0.6035	0.3678	0.3681
-13.00	0.6292	0.6449	0.3708	0.3862
-14.00	0.6746	0.6708	0.3936	0.3888
-15.00	0.7125	0.6944	0.4081	0.3897
-16.00	0.7369	0.7352	0.4095	0.4079
-17.00	0.7595	0.7592	0.4092	0.4091
-18.00	0.7801	0.7795	0.4078	0.4073
-19.00	0.7995	0.8000	0.4055	0.4021
-20.00	0.8174	0.8172	0.4024	0.4021

Table 5. P-Wave Phase Shifts with CDD Pole and without CDD Pole

$\kappa = 10$ and $\kappa = 10^{-3}$

s	Without CDD Pole $\delta_1(s)$	With CDD Pole $\delta_1(s)$
35.0	0.0132	0.0138
35.5	0.0152	0.0159
36.0	0.0175	0.0186
36.5	0.0203	0.0220
37.0	0.0239	0.0265
37.5	0.0285	0.0329
38.0	0.0346	0.0426
38.5	0.0432	0.0598
39.0	0.0561	0.1014
39.5	0.0776	0.4058
40.0	0.1205	3.0072
40.5	0.2457	3.1047
41.0	1.5708	3.1631
41.5	2.8793	3.1787
42.0	3.0038	3.2659
42.5	3.0464	5.0935
43.0	3.0679	6.1189
43.5	3.0808	6.1878
44.0	3.0894	6.2128
44.5	3.0955	6.2260
45.0	3.1001	6.2343
45.5	3.1037	6.2400
46.0	3.1065	6.2442
46.5	3.1089	6.2473
47.0	3.1108	6.2499
47.5	3.1124	6.2520
48.0	3.1138	6.2538
48.5	3.1150	6.2550
49.0	3.1160	6.2560
49.5	3.1168	6.2568
50.0	3.1174	6.2574

APPENDIX A

THE CONNECTION BETWEEN $A^{\pm}$ AND $A^{1/2,3/2}$

In the I-spin space of the kaon, the transition amplitude has the form

$$A_{\beta\alpha} = A^{(+)}\delta_{\beta\alpha} + A^{(-)}\frac{1}{2}[\tau_\beta,\tau_\alpha]. \tag{1}$$

For reaction I, there are two independent isospin states, T = 1/2 and T = 3/2. The operator for the total I-spin has the form

$$\vec{T} = \frac{1}{2}\vec{\tau} + \vec{t}_\pi, \tag{2}$$

where $\frac{1}{2}\vec{\tau}$ is the kaon I-spin operator and $\vec{t}_\pi$ is the pion I-spin operator. Then,

$$\vec{T}\cdot\vec{T} = \left(\frac{1}{2}\vec{\tau} + \vec{t}_\pi\right)\cdot\left(\frac{1}{2}\vec{\tau} + t_\pi\right) \tag{3}$$

or,

$$T(T+1) = \frac{1}{2}\left(\frac{3}{2}\right) + 1(2) + \vec{t}_\pi\cdot\vec{\tau}\,. \tag{4}$$

Solving for $\vec{t}_\pi\cdot\vec{\tau}$ we obtain

$$\vec{t}_\pi\cdot\vec{\tau} = T(T+1) - 11/4. \tag{5}$$

For $T = \frac{1}{2}$, $\vec{t}_\pi \cdot \vec{\tau} = -2$, and for $T = \frac{3}{2}$, $\vec{t}_\pi \cdot \vec{\tau} = 1$, i.e. $\vec{t}_\pi \cdot \vec{\tau}$ is an operator which has eigenvalues -2 and 1 when $T = \frac{1}{2}$ and $\frac{3}{2}$, respectively. We can use the above operator to find projection operators $P_{1/2}$ and $P_{3/2}$ which project out the eigenfunctions for $T = \frac{1}{2}$ and $\frac{3}{2}$. Then

$$P_{1/2}\Psi_{1/2} = \Psi_{1/2} \text{ and } P_{1/2}\Psi_{3/2} = 0, \tag{6}$$

$$P_{3/2}\Psi_{1/2} = 0 \text{ and } P_{3/2}\Psi_{3/2} = \Psi_{3/2}. \tag{7}$$

These projection operators can be written as a linear combination of the operator $\vec{t}_\pi \cdot \vec{\tau}$, for example

$$P_{1/2} = a + b(\vec{t}_\pi \cdot \vec{\tau}), \tag{8}$$

$$P_{1/2} = c + d(\vec{t}_\pi \cdot \vec{\tau}). \tag{9}$$

Equation (8) operating first on $\Psi_{1/2}$ and then on $\Psi_{3/2}$ gives the two equations for a and b

$$\begin{aligned} a - 2b &= 1, \\ a + b &= 0. \end{aligned} \tag{10}$$

Solving these two equations simultaneously gives

$$a = 1/3 \quad \text{and} \quad b = -1/3. \tag{11}$$

Thus,

$$P_{1/2} = \frac{1 - \vec{t}_\pi \cdot \vec{\tau}}{3} . \tag{12}$$

Then we let Equation (9) operate first on $\Psi_{1/2}$ and then on $\Psi_{3/2}$ to give

$$\begin{aligned} c - 2d &= 0, \\ c + d &= 1. \end{aligned} \tag{13}$$

The simultaneous solution of these two equations gives

$$c = 2/3 \quad \text{and} \quad d = 1/3. \tag{14}$$

The projection operator $P_{3/2}$ can now be written

$$P_{3/2} = \frac{2 + \vec{t}_\pi \cdot \vec{\tau}}{3} . \tag{15}$$

We now need a representation for the operator $\vec{t}_\pi$. A convenient one is

$$[(t_\pi)_a]_{ij} = -i\epsilon_{ija} \qquad a = 1,2,3. \tag{16}$$

Then we may write

$$(P_{1/2})_{\beta\alpha} = (\delta_{\beta\alpha} + i\epsilon_{\beta\alpha i}\tau_i)/3,$$

or,

$$(P_{1/2})_{\beta\alpha} = (\delta_{\beta\alpha} + \frac{1}{2}[\tau_\beta,\tau_\alpha])/3, \tag{17}$$

and

$$(P_{3/2})_{\beta\alpha} = (2\delta_{\beta\alpha} - \frac{1}{2}[\tau_\beta,\tau_\alpha])/3. \tag{18}$$

We can now rewrite $A_{\beta\alpha}$ as

$$A_{\beta\alpha} = A^{(+)}(P_{1/2}+P_{3/2})_{\beta\alpha} + A^{(-)}(2P_{1/2}-P_{3/2})_{\beta\alpha}. \tag{19}$$

Rearranging the above expression we obtain

$$A_{\beta\alpha} = (P_{1/2})_{\beta\alpha}(A^{(+)} + 2A^{(-)}) + (P_{3/2})_{\beta\alpha}(A^{(+)} - A^{(-)}). \tag{20}$$

Thus,

$$\begin{aligned} A^{1/2} &= A^{(+)} + 2A^{(-)}, \\ A^{3/2} &= A^{(+)} - A^{(-)}. \end{aligned} \tag{21}$$

The connection between $A^{\pm}$ and $A^{1/2,3/2}$ for Channels II and III may be found in a similar manner.

APPENDIX B

The Computer Program

The computer program is divided into four parts:

(1) the input functions calculated from experimental data, Re $A_\ell(s)$ and Im $A_\ell(s)$,

(2) the contribution to Re $A_\ell(s)$ from the integral over the right cut in the dispersion relation, $R_\ell(s)$,

(3) the contribution from the circular cut, $C_\ell^I(s)$, and

(4) the contribution from the left cut, $L_\ell(s)$.

In order to keep the computer time to a minimum, the S and P-wave parts of $R_\ell(s)$ are programmed separately since only $R_1(s)$ is affected by the introduction of the CDD pole. The contribution from the left cut is also divided into two parts, the contribution from the cut from $0 < s < (M-\mu)^2$ and the contribution from the cut from $-\infty < s < 0$.

The following list which shows the relationship between the symbols used within the body of the thesis and the corresponding symbols used in the computer program is helpful in following the program. The meaning of the many additional symbols used in the program should be clear within the program.

MU = pion mass

M = kaon mass

BO = $1/b_o$, AO = $1/a_o$

C01, C03, C11, C13 = $C_o^{1/2}(s)$, $C_o^{1/2}(s)$, $C_1^{1/2}(s)$, $C_1^{1/2}(s)$

RO1, R11 = $R_o(s)$, $R_1(s)$

LO1 + KO1 = $L_o(s)$

L11 + K11 = $L_1(s)$

IMAO, IMA1 = $ImA_o^{1/2}(u)$, $ImA_1^{1/2}(u)$

IMBO, IMB1 = $ImB_o(t)$, $ImB_1(t)$

AR = $Re(A_1(x))^{-1}$

KX = $Im(A_1(x))^{-1}$.

Each part of the computer program is shown as it was run on the computer. The language used here is Algol and only the format statements have been omitted. A sample of the computer output data is shown immediately following each program, in Tables 6, 7, 8(a), 8(b), 8(c), 8(d), 9(a), 9(b), 10, 11, 12(a), 12(b), 12(c), 12(d), 13(a), 13(b), 13(c), 13(d), 14 and 15.

The Contribution from the Right Cut for the S-Wave

```
REAL PROCEDURE FO(Y)    ;
      VALUE Y    ;
      REAL Y    ;
      BEGIN
      IF ABS(Y-S)< (DELTAX/4) THEN
      FO ← (1/2)×(FO(Y+DELTAX) + FO(Y-DELTAX))  ELSE
FO ← (IMAO - IMAOS)/(Y-S)    ;
      END FO    ;
COMMENT      N IS ASSUMED TO BE EVEN      ;
WRITE    (FOUT)     ;
MU←1        ;
M←(0.495/0.14)×MU    ;
MU2← MU×MU    ;
M2 ← M × M    ;
S0← M2    ;
MMU ← 4×M2×MU2    ;
C ← M2 + MU2    ;
PI ← 3.14159    ;
N ← 500    ;
MIN ← (M+MU)*2    ;
DELTAX ← (200×MU2 - MIN)/N    ;
WRITE (FOUT,F02)    ;
B1 ← 0.25    ;
FOR S ← 21.0 STEP 1 UNTIL 51 DO
BEGIN
SSOPI ← (S - S0)/PI    ;
LOGS ← LN((200×MU2-S)/(S- MIN))    ;
KS ← SQRT((S-C)*2-MMU)/S    ;
IMAOS ← KS/(B1*2 + KS*2)×(1/(S-S0))    ;
INTO1 ← 0    ;
FOR J ← 1 STEP 1 UNTIL N DO
   BEGIN
X ← MIN + (J-0.5)×DELTAX    ;
K ← SQRT(ABS((X-C)*2 - MMU))/X    ;
IMAO ← K/(B1*2 + K*2)×(1/(X-S0))    ;
INTO1 ← INTO1 + FO(X)×DELTAX    ;
   END    ;
G01 ← 0.8×LN((200-S0)/(200-S))/PI          ;
R01 ← SSOPI×(INTO1 + IMAOS×LOGS) + G01    ;
WRITE (FOUT,F03,S,R01)    ;
END    ;
WRITE (FOUT,F04,B1)    ;
END     .
```

Table 6. Contribution from Right Cut
Without CDD Pole (S-Wave)

S= 2.1000000@+01	R01= 2.0073861@+00
S= 2.2000000@+01	R01= 1.0573233@+00
S= 2.3000000@+01	R01= 5.5419735@-01
S= 2.4000000@+01	R01= 2.6944764@-01
S= 2.5000000@+01	R01= 5.5663623@-02
S= 2.6000000@+01	R01=-1.2394368@-01
S= 2.7000000@+01	R01=-2.4164242@-01
S= 2.8000000@+01	R01=-3.1565980@-01
S= 2.9000000@+01	R01=-3.9375324@-01
S= 3.0000000@+01	R01=-4.5726652@-01
S= 3.1000000@+01	R01=-5.2613068@-01
S= 3.2000000@+01	R01=-5.7187148@-01
S= 3.3000000@+01	R01=-5.9986942@-01
S= 3.4000000@+01	R01=-6.3605879@-01
S= 3.5000000@+01	R01=-6.7825632@-01
S= 3.6000000@+01	R01=-7.0641685@-01
S= 3.7000000@+01	R01=-7.3192324@-01
S= 3.8000000@+01	R01=-7.4682851@-01
S= 3.9000000@+01	R01=-7.6852876@-01
S= 4.0000000@+01	R01=-7.9623231@-01
S= 4.1000000@+01	R01=-8.1450127@-01
S= 4.2000000@+01	R01=-8.2450206@-01
S= 4.3000000@+01	R01=-8.4107437@-01
S= 4.4000000@+01	R01=-8.5603697@-01
S= 4.5000000@+01	R01=-8.7647648@-01
S= 4.6000000@+01	R01=-8.8978925@-01
S= 4.7000000@+01	R01=-8.9695859@-01
S= 4.8000000@+01	R01=-9.0926593@-01
S= 4.9000000@+01	R01=-9.2582896@-01
S= 5.0000000@+01	R01=-9.3674108@-01
S= 5.1000000@+01	R01=-9.4718351@-01

The Contribution from the Right Cut for the P-Wave Without CDD Pole

```
REAL PROCEDURE FI(YY)    ;
      VALUE YY    ;
      REAL  YY    ;
      BEGIN
      IF ABS(YY-S)< DELTAX/4 THEN
      FI ← (FI(YY+DELTAX) + FI(YY-DELTAX))/2  ELSE
FI ← (IMA1/(YY-S0) - IMA1S/(S-S0))/(YY-S)    ;
      END FI    ;
COMMENT      N IS ASSUMED TO BE EVEN      ;
WRITE   (FOUT)     ;
MU←1       ;
M←(0.495/0.14)×MU    ;
MU2← MU×MU    ;
M2 ← M × M    ;
A1 ← 21.5    ;
SR ← 40.96×MU2    ;
S0← M2    ;
PI ← 3.14159    ;
C ← M2 + MU2    ;
MMU ← 4×M2×MU2    ;
N ← 250    ;
DELTAX ← (100×MU2 - (M+MU)↑2)/(4×N)    ;
WRITE (FOUT,F01)    ;
FOR S ← 35 STEP 0.10 UNTIL 48 DO
BEGIN
KS ← SQRT((S-C)↑2 - MMU)/(S)    ;
KSQ ← S×(KS↑2)/4    ;
ARS ← A1×(SR - S)    ;
IMA1S ← (KSQ↑2)×KS/(ARS↑2 + (KS×KSQ)↑2)    ;
SSOPI ← (S - S0)/PI    ;
LOGS ← LN((100×MU2-S)/(S-(M+MU)↑2))    ;
INT11 ← 0    ;
FOR J ← 1 STEP 1 UNTIL 4×N DO
   BEGIN
X ← (M+MU)↑2 + (J -0.5)×DELTAX    ;
AR1 ← A1×(SR-X)    ;
KX ← SQRT(ABS((X-C)↑2 - MMU))/(X)    ;
KXSQ ← X×(KX↑2)/4    ;
IMA1 ← KXSQ↑2×KX/(AR1↑2 + (KXSQ×KX)↑2)    ;
INT11 ←  INT11 + FI(X)×DELTAX    ;
   END    ;
R11 ← SSOPI×INT11 + IMA1S×LOGS/PI    ;
END   .
```

Table 7. Contribution from Right Cut Without Pole (P-Wave)

S= 3.5000000@+01	R11= 2.6471671@-02
S= 3.5100000@+01	R11= 2.7047430@-02
S= 3.5200000@+01	R11= 2.7639009@-02
S= 3.5300000@+01	R11= 2.8246693@-02
S= 3.5400000@+01	R11= 2.8880770@-02
S= 3.5500000@+01	R11= 2.9543665@-02
S= 3.5600000@+01	R11= 3.0225689@-02
S= 3.5700000@+01	R11= 3.0927886@-02
S= 3.5800000@+01	R11= 3.1662771@-02
S= 3.5900000@+01	R11= 3.2434190@-02
S= 3.6000000@+01	R11= 3.3229587@-02
S= 3.6100000@+01	R11= 3.4049639@-02
S= 3.6200000@+01	R11= 3.4911381@-02
S= 3.6300000@+01	R11= 3.5820330@-02
S= 3.6400000@+01	R11= 3.6748939@-02
S= 3.6500000@+01	R11= 3.7730082@-02
S= 3.6600000@+01	R11= 3.8767040@-02
S= 3.6700000@+01	R11= 3.9841344@-02
S= 3.6800000@+01	R11= 4.0952995@-02
S= 3.6900000@+01	R11= 4.2133656@-02
S= 3.7000000@+01	R11= 4.3389125@-02
S= 3.7100000@+01	R11= 4.4693988@-02
S= 3.7200000@+01	R11= 4.6048512@-02
S= 3.7300000@+01	R11= 4.7496218@-02
S= 3.7400000@+01	R11= 4.9047226@-02
S= 3.7500000@+01	R11= 5.0665560@-02
S= 3.7600000@+01	R11= 5.2351950@-02
S= 3.7700000@+01	R11= 5.4168445@-02
S= 3.7800000@+01	R11= 5.6132914@-02
S= 3.7900000@+01	R11= 5.8192647@-02
S= 4.0800000@+01	R11= 6.4472498@-01
S= 4.0900000@+01	R11= 5.9480879@-01
S= 4.1000000@+01	R11=-4.3047969@-01
S= 4.1100000@+01	R11=-6.2956814@-01
S= 4.1200000@+01	R11=-5.8138085@-01
S= 4.1300000@+01	R11=-5.1598446@-01
S= 4.1400000@+01	R11=-4.2215961@-01
S= 4.1500000@+01	R11=-3.4741387@-01
S= 4.1600000@+01	R11=-3.0030059@-01
S= 4.1700000@+01	R11=-2.6795840@-01
S= 4.1800000@+01	R11=-2.3628217@-01
S= 4.1900000@+01	R11=-2.1337628@-01
S= 4.2000000@+01	R11=-1.9568556@-01
S= 4.2100000@+01	R11=-1.7962641@-01
S= 4.2200000@+01	R11=-1.6532023@-01
S= 4.2300000@+01	R11=-1.5387009@-01
S= 4.2400000@+01	R11=-1.4440673@-01

The Contribution to the Right Cut for the P-Wave With CDD Pole

```
REAL PROCEDURE FI(YY)    ;
      VALUE YY    ;
      REAL  YY    ;
      BEGIN
      IF ABS(YY-S)< DELTAX/4 THEN
      FI ← (FI(YY+DELTAX) + FI(YY-DELTAX))/2  ELSE
FI ← (IMA1 - IMA1S)/((YY-S)×(YY-S0))  ;
      END FI    ;
COMMENT      N IS ASSUMED TO BE EVEN      ;
WRITE    (FOUT)     ;
MU←1        ;
M←(0.495/0.14)×MU    ;
MU2← MU×MU    ;
M2 ← M × M    ;
A1 ← 21.5    ;
SR ← 40.96×MU2    ;
S0← M2    ;
PI ← 3.14159   ;
C ← M2 + MU2    ;
MMU ← 4×M2×MU2    ;
TAU ← 0.000001    ;
N ← 250    ;
DELTAX ← (100×MU2 - (M+MU)*2)/(4×N)    ;
WRITE (FOUT,F01)    ;
FOR I ← 1 STEP 1 UNTIL 5 DO
    BEGIN
KAPPA ← 10*(-I)    ;
WRITE (FOUT,F03,KAPPA,TAU)    ;
FOR S ← 37 STEP 0.25 UNTIL 45 DO
BEGIN
KS ← SQRT((S-C)*2 - MMU)/(S)    ;
KSQ ← S×(KS*2)/4    ;
Q ← KAPPA×TAU/(TAU*2 + (S-SR)*2)    ;
ARS ← A1×(SR - S)    ;
NARS ← ARS + Q×(S-SR)×KSQ    ;
NKS ← KS + Q×TAU    ;
IMA1S ← (KSQ*2)×NKS/(NARS*2 +(NKS×KSQ)*2)    ;
SSOPI ← (S - S0)/PI    ;
```

The Contribution to the Right Cut for the P-Wave With CDD Pole
(Continued)

```
LOGS ← LN((100×MU2-S)/(S-(M+MU)*2))    ;
INT11 ← 0    ;
FOR J ← 1 STEP 1 UNTIL 4×N DO
   BEGIN
X ← (M+MU)*2 + (J -0.5)×DELTAX    ;
QX← KAPPA×TAU/(TAU*2 + (X-SR)*2)    ;
AR1 ← A1×(SR-X)    ;
KX ← SQRT(ARS((X-C)*2 - MMU))/(X)    ;
KXSQ ← X×(KX*2)/4    ;
NKX ← KX + QX×TAU    ;
NAR1 ← AR1 + QX×(X-SR)×KXSQ    ;
IMA1 ← KXSQ*2×NKX/(NAR1*2 + (KXSQ×NKX)*2)    ;
INT11 ←  INT11 + FI(X)×DELTAX    ;
   END    ;
R11 ← SSOPI×INT11 + IMA1S×LOGS/PI    ;
REA1 ← S×ARS×(KS*2)/(ARS*2+4×(S*2)×(KS*6))    ;
WRITE (FOUT,FO2,S,REA1,R11)    ;
END    ;
    END    ;
END    .
```

Table 8(a). The Contribution from the Right Cut for the P-Wave With CDD Pole

($\kappa = 10$, $\tau = 10^{-1}$)

S= 3.7000000@+01	R11= 4.8833958@-02
S= 3.7250000@+01	R11= 5.3706695@-02
S= 3.7500000@+01	R11= 5.9631032@-02
S= 3.7750000@+01	R11= 6.6938354@-02
S= 3.8000000@+01	R11= 7.6425370@-02
S= 3.8250000@+01	R11= 8.9182675@-02
S= 3.8500000@+01	R11= 1.0740954@-01
S= 3.8750000@+01	R11= 1.3668902@-01
S= 3.9000000@+01	R11= 1.8951933@-01
S= 3.9250000@+01	R11= 3.1671252@-01
S= 3.9500000@+01	R11= 6.7939797@-01
S= 3.9750000@+01	R11=-9.1518525@-02
S= 4.0000000@+01	R11=-1.1954977@-01
S= 4.0250000@+01	R11=-6.9466290@-02
S= 4.0500000@+01	R11=-3.6099090@-02
S= 4.0750000@+01	R11=-9.3778806@-03
S= 4.1000000@+01	R11= 1.5096440@-02
S= 4.1250000@+01	R11= 4.1623302@-02
S= 4.1500000@+01	R11= 7.6306230@-02
S= 4.1750000@+01	R11= 1.3104485@-01
S= 4.2000000@+01	R11= 2.4882158@-01
S= 4.2250000@+01	R11= 6.0432762@-01
S= 4.2500000@+01	R11= 1.1043294@-01
S= 4.2750000@+01	R11=-2.3756703@-01
S= 4.3000000@+01	R11=-1.7954365@-01
S= 4.3250000@+01	R11=-1.4385430@-01
S= 4.3500000@+01	R11=-1.2008579@-01
S= 4.3750000@+01	R11=-1.0394628@-01
S= 4.4000000@+01	R11=-9.1708111@-02
S= 4.4250000@+01	R11=-8.2378548@-02
S= 4.4500000@+01	R11=-7.5014557@-02
S= 4.4750000@+01	R11=-6.8967671@-02
S= 4.5000000@+01	R11=-6.4034431@-02

Table 8(b). The Contribution from the Right Cut for the P-Wave With CDD Pole

($\kappa = 10$, $\tau = 10^{-2}$)

S= 3.7000000@+01	R11= 4.9175722@-02
S= 3.7250000@+01	R11= 5.4072004@-02
S= 3.7500000@+01	R11= 6.0018746@-02
S= 3.7750000@+01	R11= 6.7358093@-02
S= 3.8000000@+01	R11= 7.6858345@-02
S= 3.8250000@+01	R11= 8.9607515@-02
S= 3.8500000@+01	R11= 1.0777940@-01
S= 3.8750000@+01	R11= 1.3669498@-01
S= 3.9000000@+01	R11= 1.8888004@-01
S= 3.9250000@+01	R11= 3.1651225@-01
S= 3.9500000@+01	R11= 8.1578330@-01
S= 3.9750000@+01	R11=-2.8672475@-01
S= 4.0000000@+01	R11=-1.5970283@-01
S= 4.0250000@+01	R11=-8.7394123@-02
S= 4.0500000@+01	R11=-4.7209970@-02
S= 4.0750000@+01	R11=-1.8134018@-02
S= 4.1000000@+01	R11= 7.2342184@-03
S= 4.1250000@+01	R11= 3.3908728@-02
S= 4.1500000@+01	R11= 6.7933852@-02
S= 4.1750000@+01	R11= 1.2118331@-01
S= 4.2000000@+01	R11= 2.3569476@-01
S= 4.2250000@+01	R11= 6.5482853@-01
S= 4.2500000@+01	R11=-9.8740454@-02
S= 4.2750000@+01	R11=-2.8355849@-01
S= 4.3000000@+01	R11=-1.9296432@-01
S= 4.3250000@+01	R11=-1.4940163@-01
S= 4.3500000@+01	R11=-1.2298405@-01
S= 4.3750000@+01	R11=-1.0562151@-01
S= 4.4000000@+01	R11=-9.2838650@-02
S= 4.4250000@+01	R11=-8.3201891@-02
S= 4.4500000@+01	R11=-7.5650468@-02
S= 4.4750000@+01	R11=-6.9492536@-02
S= 4.5000000@+01	R11=-6.4473223@-02

Table 8(c). The Contribution from the Right Cut for the P-Wave With CDD Pole

($\kappa = 10$, $\tau = 10^{-3}$)

S= 3.7000000@+01	R11= 4.9341250@-02
S= 3.7250000@+01	R11= 5.4256138@-02
S= 3.7500000@+01	R11= 6.0225307@-02
S= 3.7750000@+01	R11= 6.7593555@-02
S= 3.8000000@+01	R11= 7.7128825@-02
S= 3.8250000@+01	R11= 8.9923076@-02
S= 3.8500000@+01	R11= 1.0815508@-01
S= 3.8750000@+01	R11= 1.3713322@-01
S= 3.9000000@+01	R11= 1.8941053@-01
S= 3.9250000@+01	R11= 3.1724923@-01
S= 3.9500000@+01	R11= 8.3309422@-01
S= 3.9750000@+01	R11=-3.1252389@-01
S= 4.0000000@+01	R11=-1.6467276@-01
S= 4.0250000@+01	R11=-8.9823203@-02
S= 4.0500000@+01	R11=-4.8819684@-02
S= 4.0750000@+01	R11=-1.9433355@-02
S= 4.1000000@+01	R11= 6.0658397@-03
S= 4.1250000@+01	R11= 3.2770691@-02
S= 4.1500000@+01	R11= 6.6712911@-02
S= 4.1750000@+01	R11= 1.1972487@-01
S= 4.2000000@+01	R11= 2.3349248@-01
S= 4.2250000@+01	R11= 6.5591235@-01
S= 4.2500000@+01	R11=-1.3970694@-01
S= 4.2750000@+01	R11=-2.8803180@-01
S= 4.3000000@+01	R11=-1.9425002@-01
S= 4.3250000@+01	R11=-1.4995608@-01
S= 4.3500000@+01	R11=-1.2330025@-01
S= 4.3750000@+01	R11=-1.0582841@-01
S= 4.4000000@+01	R11=-9.2998100@-02
S= 4.4250000@+01	R11=-8.3334371@-02
S= 4.4500000@+01	R11=-7.5766154@-02
S= 4.4750000@+01	R11=-6.9598017@-02
S= 4.5000000@+01	R11=-6.4570341@-02

Table 8(d). The Contribution from the Right Cut for the P-Wave with Weak CDD Pole

($\kappa = -1$, $\tau = 10^{-3}$)

S= 3.7000000@+01	R11= 4.3991354@-02
S= 3.7250000@+01	R11= 4.7515023@-02
S= 3.7500000@+01	R11= 5.1562277@-02
S= 3.7750000@+01	R11= 5.6224956@-02
S= 3.8000000@+01	R11= 6.1733458@-02
S= 3.8250000@+01	R11= 6.8291040@-02
S= 3.8500000@+01	R11= 7.6227735@-02
S= 3.8750000@+01	R11= 8.6144919@-02
S= 3.9000000@+01	R11= 9.8619232@-02
S= 3.9250000@+01	R11= 1.1494929@-01
S= 3.9500000@+01	R11= 1.3683192@-01
S= 3.9750000@+01	R11= 1.6679698@-01
S= 4.0000000@+01	R11= 2.1885874@-01
S= 4.0250000@+01	R11= 3.0814061@-01
S= 4.0500000@+01	R11= 5.2632768@-01
S= 4.0750000@+01	R11= 1.4052868@+00
S= 4.1000000@+01	R11= 4.9949090@-01
S= 4.1250000@+01	R11=-2.8738507@-01
S= 4.1500000@+01	R11=-2.9106245@-01
S= 4.1750000@+01	R11=-2.2142045@-01
S= 4.2000000@+01	R11=-1.7817733@-01
S= 4.2250000@+01	R11=-1.4784453@-01
S= 4.2500000@+01	R11=-1.2656769@-01
S= 4.2750000@+01	R11=-1.1084083@-01
S= 4.3000000@+01	R11=-9.8580909@-02
S= 4.3250000@+01	R11=-8.9061719@-02
S= 4.3500000@+01	R11=-8.1324054@-02
S= 4.3750000@+01	R11=-7.4991648@-02
S= 4.4000000@+01	R11=-6.9583910@-02
S= 4.4250000@+01	R11=-6.4971861@-02
S= 4.4500000@+01	R11=-6.0992088@-02
S= 4.4750000@+01	R11=-5.7493116@-02
S= 4.5000000@+01	R11=-5.4447489@-02

The Contribution of the Circular Cut

(A CDD Pole in the P-wave amplitude for $\pi K \to \pi K$ does not alter this program; however, a pole in the P-wave of $\pi\pi \to \pi\pi$ requires some minor changes.)

```
REAL PROCEDURE L(XX,P,Q,R)    ;
     VALUE XX,P,Q,R    ;
     REAL XX,P,Q,R    ;
     BEGIN
     L ← LN(ABS((P+M2-MU2)/(P-C+XX/2)))/((Q-P)×(R-P))    ;
     END L    ;
MU←1       ;
M←(0.495/0.14)×MU    ;
MU2← MU×MU    ;
M2 ← M × M    ;
B0←  1/0.75    ;
B1 ← 19    ;
TR← 20.4 × MU2    ;
S0← M2    ;
PI ← 3.14159    ;
AA ← (M2-MU2)*2    ;
A ← (AA + (S0*2))/(2×S0)    ;
C← M2 + MU2    ;
N ← 100    ;
WRITE    (FOUT,FU1)    ;
FOR S ← 21.0 STEP 1 UNTIL 50 DO
BEGIN
B ← (AA + (S*2))/(2×S)    ;
D← (S×S0 + AA)/(4×S0×S)    ;
E← (S+S0)×AA/(4×S0×S)    ;
F← (S×S0 - AA)/(4×S0×S)    ;
H← F + D    ;
SS0PI ← (S - S0)/PI    ;
     PART01 ← 0  ;  PART03 ← 0  ;  PART11 ← 0  ;  PART13 ← 0
DT ← 4×(M2 - MU2)/N    ;
FOR I ← 1 STEP 1 UNTIL N DO
     BEGIN
T ← 4×MU2 + (I-0.5)×DT    ;
G← (T/2-M2-MU2)×F - E    ;
TM ← (T - 4×MU2)    ;
QT ← SQRT((TM)×(4×M2 - T))/T    ;
TM2 ← TM×TM    ;
DUM1 ← SQRT(TM/T)    ;
DUM12 ← DUM1×DUM1    ;
```

The Contribution of the Circular Cut
(Continued)

```
DUM2 ← B1×B1×(TR=T)×(TR=T)   ;
IMB0 ← QT×(DUM1/(B0×B0 + DUM12))   ;
IMB1 ← QT×QT/T× (DUM1×TM2/(DUM12×TM2 + DUM2))   ;
LA ← L(T,A,B,C)   ;   LB ← L(T,B,A,C)   ;   LC ← L(T,C,A,B)
DUM3 ← LA + LB + LC   ;
DUM4  ← A×LA + B×LB + C×LC   ;
G101 ← (F×IMB0 + 6×G×IMB1)×DUM3   ;
G201← (6×H×IMB1)×DUM4   ;
F01← G101 + G201   ;
G103 ← (F×IMB0 + (-3  )×G×IMB1)×DUM3   ;
G203 ← -3×H×IMB1×DUM4   ;
F03 ← G103 + G203   ;
DUM5 ← LA/(C-A) + LB/(C-B) + (2×C-A-B)×LC/((C-A)×(C-B))
HI← DUM5 + (4×M2-T)/((C-A)×(C-B)×2×M2×T )   ;
G111 ← (F×T×IMB0 + 6×G×T×IMB1) × HI   ;
DUM6  ← A×LA/(C-A) + B×LB/(C-B)   ;
DUM7 ← ((C*2-A×B)×LC + C×(4×M2-T)/(2×M2×T))/((C-A)×(C-B))
G211← (6×H×T×IMB1)×(DUM6 + DUM7 )   ;
F11← G111 + G211   ;
G113 ← (F×T×IMB0 -(3  )×G×T×IMB1) × HI   ;
G213← (-3×H×T×IMB1)×(DUM6 + DUM7 )   ;
F13← G113 + G213   ;
     PART01 ← PART01 + F01   ;
     PART03 ← PART03 + F03   ;
     PART11 ← PART11 + F11   ;
     PART13 ← PART13 + F13   ;
     END   ;
C01 ← SSOPI×PART01×DT   ;
C03 ← SSOPI×PART03×DT   ;
C11 ← C01 - SSOPI×PART11×DT   ;
C13 ← C03 - SSOPI×PART13×DT   ;
WRITE(FOUT,FO2,S,C01,C03,C11,C13) ;
END   ;
END   .
```

Table 9. Contribution of Circular Cut Without CDD Pole

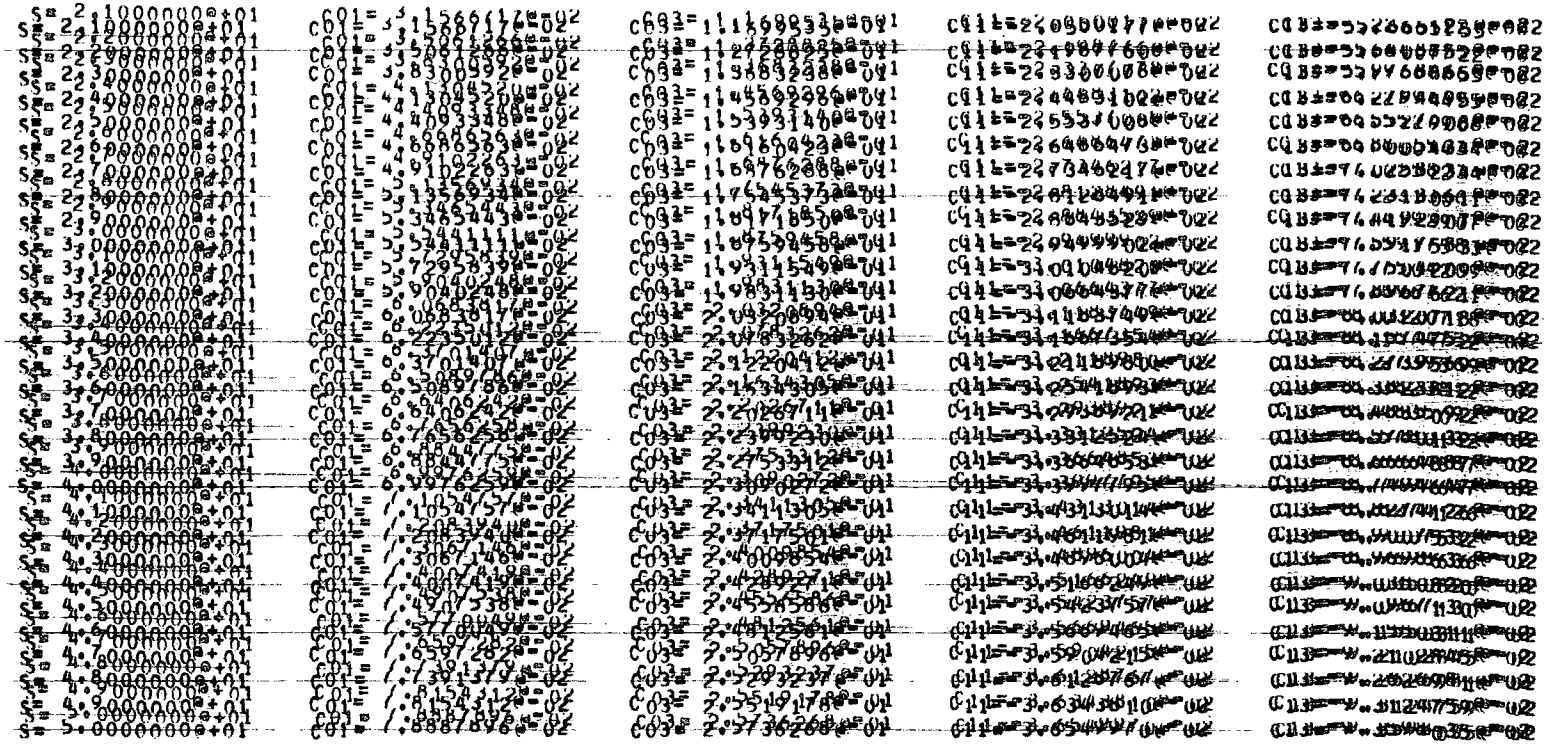

Contribution from Cut Along Real Axis from $0 < s < (M-\mu)^2$

```
REAL PROCEDURE P1(K,V,W,R)    ;
      VALUE K,V,W,R    ;
      REAL K,V,W,R    ;
      BEGIN
      P1←K×LN(ABS((2×C-U-K)/(A2×B2/U-K)))/((V-K)×(W-K)×(R-K))
      END P1;
REAL PROCEDURE P2(KK,VV,RR,WW)    ;
      VALUE KK,VV,RR,WW    ;
      REAL KK,VV,RR,WW    ;
      BEGIN
      P2←KK×LN(ABS((A2×B2/U-KK)/(-KK)))/((VV-KK)×(RR-KK)×(WW-KK))
      END P2;
WRITE (FOUT,F05)    ;
MU ← 1    ;
MU2 ← 1    ;
M ← (0.495/0.140)× MU    ;
M2 ← M × M    ;
SR ← 40.96    ;
S0 ← M2    ;
C ← M2 + MU2    ;
PI ← 3.14159    ;
NN ←  500    ;
N ← 100    ;
A1 ← 21.5    ;
B2 ← (M+MU)↑2    ;
A2 ← (M-MU)↑2        ;
B1 ← 0.25    ;
S02 ← S0×S0    ;
AB ← A2 -B2    ;
S0A ← S0 - A2    ;
S0B ← S0 - B2    ;
S0AB ← S0A×S0B    ;
AB2 ← AB×AB    ;
DU1 ← (2×C - B2)/N    ;
DU2 ← (100 - 2×C)/NN    ;
TAU ← 1.0    ;
KAPPA ← 0    ;
WRITE (FOUT,F07,KAPPA,TAU)    ;
FOR S ← 21.0 STEP 2 UNTIL 51 DO
BEGIN
SA ← S - A2    ;
SB ← S - B2    ;
S0S ← S0 - S    ;
SAB ← SA×SB    ;
S2  ← S×S    ;
DUM3 ← (S×S0A/SAB - S0×SA/S0AB)/S0S    ;
DUM4 ← B2/AB2 + B2×SA×S0A/(S0B×SB×AB2)    ;
DUM5 ← (S×S0B/SAB - S0×SB/S0AB)/S0S    ;
DUM6 ← A2/AB2 + A2×SB×S0B/(S0A× SA× AB2)    ;
```

Contribution from Cut Along Real Axis from $0 < s < (M-\mu)^2$
(Continued)

```
DUM7 ← (S2×S0A/SAB - S02×SA/S0AB)/S0S    ;
DUM8 ← A2×B2/AB2 + B2×B2×SA×S0A/(S0B×SB×AB2)    ;
DUM9 ← (S2×S0B/SAB - S02×SB/S0AB)/S0S    ;
DUM10 ← A2×B2/AB2 + A2×A2×SB×S0B/(S0A×SA×AB2)    ;
DUM11 ← S2×S×S0A/(SAB×S0S) - S02×S0×SA/(S0AB×S0S)    ;
DUM12← (B2/AB2)×(A2×A2 + B2×B2×SA×S0A/(SB×S0B))    ;
DUM13 ← S2×S×S0B/(SAB×S0S) - S02×S0×SB/(S0AB×S0S)    ;
DUM14 ← (A2/AB2)×(B2×B2 + A2×A2×SB×S0B/(SA×S0A))    ;
SS0PI ← (S-S0)/PI    ;
SUM11 ← 0    ;    SUM01 ← 0    ;
FOR I ← 1 STEP 1 UNTIL N DO
     BEGIN
U ← B2 + (I-0.5)×DU1    ;
KU ← SQRT(ABS((C-U)*2-4×M2×MU2))/U    ;
KUSQ ← (KU*2)×U/4    ;
AR ← A1×(SR - U)    ;
NAR ← AR +Q×(U-SR)×KUSQ    ;
NKU ← KU + Q×TAU    ;
Q ← KAPPA×TAU/(TAU*2 + (U-SR)*2)    ;
DUM2 ← (3/2)×NKU×(KUSQ ) /(NAR*2  + (NKU×KUSQ)*2)    ;
DUM1  ← KU/(B1*2+KU*2) +  DUM2×(U×(KU*2)/2+2×C-U)    ;
P1A ← P1(A2,B2,S,S0)    ;    P1B ← P1(B2,A2,S,S0)    ;
P1S ← P1(S,S0,A2,B2)    ;    P1S0← P1(S0,S,A2,B2)    ;
G1 ← P1A + P1B + P1S + P1S0    ;
G2 ← A2×P1A + B2×P1B + S×P1S + S0×P1S0    ;
D1 ← S×P1S/SAB + S0×P1S0/S0AB    ;
E1 ← P1A×(DUM3 - DUM4) + P1B×(DUM5 - DUM6)    ;
J1 ← A2×A2/(AB2×S0A×SA)×(1/(2×C-U-A2) - 1/(A2×B2/U-A2))
K1 ← B2×B2/(AB2×S0B×SB)×(1/(2×C-U-B2) - 1/(A2×B2/U-B2))
G3 ← D1 + E1 + J1 + K1    ;
D3 ← S2×P1S/SAB + S02×P1S0/S0AB    ;
E3 ← P1A×(DUM7 - DUM8) + P1B×(DUM9 - DUM10)    ;
G4 ← A2×J1 + B2×K1 + E3 + D3    ;
D5 ← S2×S×P1S/SAB + S02×S0×P1S0/S0AB    ;
E5 ← P1A×(DUM11 - DUM12) + P1B×(DUM13 - DUM14)    ;
G5 ← D5 + E5 + A2*2×J1 + B2*2×K1    ;
G01 ← DUM1×G1 - DUM2×G2    ;
G11 ← DUM1×((2×C-U)×G3-G4) - DUM2×((2×C-U)×G4-G5)    ;
SUM01 ← SUM01 + G01    ;
SUM11 ← SUM11 + G11    ;
     END    ;
H01 ← SUM01×DU1    ;
H11 ← SUM11×DU1    ;
SUM02 ← 0    ;    SUM12 ← 0    ;
FOR II ← 1 STEP 1 UNTIL NN DO
     BEGIN
U ← 2×C + (II-0.5)×DU2    ;
```

Contribution from Cut Along Real Axis from $0 < s < (M-\mu)^2$
(Continued)

```
AR ← A1×(SR - U)    ;
KU ← SQRT(ABS((C-U)*2-4×M2×MU2))/U    ;
KUSQ ← (KU*2)×U/4    ;
Q ← KAPPA×TAU/(TAU*2 + (U-SR)*2)    ;
NAR ← AR + Q×(U-SR)×KUSQ    ;
NKU ← KU + Q×TAU    ;
DUM2 ← (3/2)×NKU×(KUSQ ) /(NAR*2  + (NKU×KUSQ)*2)    ;
DUM1  ← KU/(B1*2+KU*2) +  DUM2×(U×(KU*2)/2+2×C-U)    ;
P2A ← P2(A2,B2,S,S0)    ;    P2B ← P2(B2,A2,S,S0)    ;
P2S ← P2(S,S0,A2,B2)    ;    P2S0← P2(S0,S,A2,B2)    ;
H1 ← P2A + P2B + P2S + P2S0    ;
H2 ← A2×P2A + B2×P2B + S×P2S + S0×P2S0    ;
D2 ← S×P2S/SAB + S0×P2S0/S0AB    ;
E2 ← P2A×(DUM3 - DUM4) + P2B×(DUM5 - DUM6)    ;
J2 ← A2×A2/(AB2×S0A×SA)×(1/(A2×B2/U - A2) + 1/A2)    ;
K2 ← B2×B2/(AB2×S0B×SB)×(1/(A2×B2/U - B2) + 1/B2)    ;
H3 ← D2 + E2 + J2 + K2    ;
D4 ← S2×P2S/SAB + S02×P2S0/S0AB    ;
E4 ← P2A×(DUM7 - DUM8) + P2B×(DUM9 - DUM10)    ;
H4 ← A2×J2 + B2×K2 + D4 + E4    ;
D6 ← S2×S×P2S/SAB + S02×S0×P2S0/S0AB    ;
E6 ← P2A×(DUM11 - DUM12) + P2B×(DUM13 - DUM14)    ;
H5 ← D6 + E6 + A2*2×J2 + B2*2×K2    ;
G02 ← DUM1×H1 - DUM2×H2    ;
G12 ← DUM1×((2×C-U)×H3-H4) - DUM2×((2×C-U)×H4-H5)    ;
SUM02 ← SUM02 + G02    ;
SUM12 ← SUM12 + G12    ;
    END    ;
H02 ← SUM02×DU2    ;
H12 ← SUM12×DU2    ;
L01 ← SSOPI×(H01 - H02)    ;
L11 ← SSOPI×2×(H11 - H12) + L01    ;
WRITE (FOUT,FN6,S,L01,L11)    ;
END    ;
END    .
```

Table 10. Contribution of Cut Along Left Real Axis for $0 < s < (M-\mu)^2$ Without CDD Pole

KAPPA= 0.0000000@+00		TAU= 1.0000000@+00
S= 2.1000000@+01	L01= 1.7071218@-01	L11= 7.8046307@-03
S= 2.3000000@+01	L01= 1.8827975@-01	L11= 8.7383804@-03
S= 2.5000000@+01	L01= 2.0247197@-01	L11= 9.5116146@-03
S= 2.7000000@+01	L01= 2.1418026@-01	L11= 1.0162425@-02
S= 2.9000000@+01	L01= 2.2400653@-01	L11= 1.0717737@-02
S= 3.1000000@+01	L01= 2.3237216@-01	L11= 1.1197128@-02
S= 3.3000000@+01	L01= 2.3958116@-01	L11= 1.1615169@-02
S= 3.5000000@+01	L01= 2.4585845@-01	L11= 1.1982927@-02
S= 3.7000000@+01	L01= 2.5137407@-01	L11= 1.2308960@-02
S= 3.9000000@+01	L01= 2.5625898@-01	L11= 1.2599988@-02
S= 4.1000000@+01	L01= 2.6061570@-01	L11= 1.2861362@-02
S= 4.3000000@+01	L01= 2.6452562@-01	L11= 1.3097394@-02
S= 4.5000000@+01	L01= 2.6805422@-01	L11= 1.3311601@-02
S= 4.7000000@+01	L01= 2.7125476@-01	L11= 1.3506876@-02
S= 4.9000000@+01	L01= 2.7417101@-01	L11= 1.3685622@-02
S= 5.1000000@+01	L01= 2.7683928@-01	L11= 1.3849854@-02

Table 11. Contribution of Cut Along Left Real Axis for $0 < s < (M-\mu)^2$ With CDD Pole

KAPPA= 1.0000000@+01		TAU= 1.0000000@-02
S= 2.1000000@+01	L01= 1.7068244@-01	L11= 7.8113339@-03
S= 2.3000000@+01	L01= 1.8824657@-01	L11= 8.7458136@-03
S= 2.5000000@+01	L01= 2.0243595@-01	L11= 9.5196417@-03
S= 2.7000000@+01	L01= 2.1414187@-01	L11= 1.0170945@-02
S= 2.9000000@+01	L01= 2.2396612@-01	L11= 1.0726672@-02
S= 3.1000000@+01	L01= 2.3233001@-01	L11= 1.1206418@-02
S= 3.3000000@+01	L01= 2.3953750@-01	L11= 1.1624766@-02
S= 3.5000000@+01	L01= 2.4581347@-01	L11= 1.1992791@-02
S= 3.7000000@+01	L01= 2.5132791@-01	L11= 1.2319060@-02
S= 3.9000000@+01	L01= 2.5621178@-01	L11= 1.2610298@-02
S= 4.1000000@+01	L01= 2.6056755@-01	L11= 1.2871858@-02
S= 4.3000000@+01	L01= 2.6447663@-01	L11= 1.3108059@-02
S= 4.5000000@+01	L01= 2.6800446@-01	L11= 1.3322417@-02
S= 4.7000000@+01	L01= 2.7120430@-01	L11= 1.3517830@-02
S= 4.9000000@+01	L01= 2.7411992@-01	L11= 1.3696702@-02
S= 5.1000000@+01	L01= 2.7678760@-01	L11= 1.3861049@-02

Table 11. Contribution of Cut Along Left Real Axis for $0 < s < (M-\mu)^2$ (Continued)

KAPPA= 1.0000000@+01		TAU= 1.0000000@-03
S= 2.1000000@+01	L01= 1.7067419@-01	L11= 7.8131150@-03
S= 2.3000000@+01	L01= 1.8823736@-01	L11= 8.7477854@-03
S= 2.5000000@+01	L01= 2.0242596@-01	L11= 9.5217682@-03
S= 2.7000000@+01	L01= 2.1413122@-01	L11= 1.0173199@-02
S= 2.9000000@+01	L01= 2.2395491@-01	L11= 1.0729034@-02
S= 3.1000000@+01	L01= 2.3231832@-01	L11= 1.1208872@-02
S= 3.3000000@+01	L01= 2.3952539@-01	L11= 1.1627299@-02
S= 3.5000000@+01	L01= 2.4580099@-01	L11= 1.1995393@-02
S= 3.7000000@+01	L01= 2.5131512@-01	L11= 1.2321722@-02
S= 3.9000000@+01	L01= 2.5619869@-01	L11= 1.2613013@-02
S= 4.1000000@+01	L01= 2.6055421@-01	L11= 1.2874622@-02
S= 4.3000000@+01	L01= 2.6446305@-01	L11= 1.3110865@-02
S= 4.5000000@+01	L01= 2.6799067@-01	L11= 1.3325262@-02
S= 4.7000000@+01	L01= 2.7119032@-01	L11= 1.3520710@-02
S= 4.9000000@+01	L01= 2.7410576@-01	L11= 1.3699613@-02
S= 5.1000000@+01	L01= 2.7677328@-01	L11= 1.3863990@-02
KAPPA= 1.0000000@+01		TAU= 1.0000000@-04
S= 2.1000000@+01	L01= 1.7067330@-01	L11= 7.8133073@-03
S= 2.3000000@+01	L01= 1.8823637@-01	L11= 8.7479983@-03
S= 2.5000000@+01	L01= 2.0242488@-01	L11= 9.5219978@-03
S= 2.7000000@+01	L01= 2.1413007@-01	L11= 1.0173443@-02
S= 2.9000000@+01	L01= 2.2395370@-01	L11= 1.0729289@-02
S= 3.1000000@+01	L01= 2.3231706@-01	L11= 1.1209137@-02
S= 3.3000000@+01	L01= 2.3952409@-01	L11= 1.1627572@-02
S= 3.5000000@+01	L01= 2.4579965@-01	L11= 1.1995674@-02
S= 3.7000000@+01	L01= 2.5131374@-01	L11= 1.2322010@-02
S= 3.9000000@+01	L01= 2.5619728@-01	L11= 1.2613306@-02
S= 4.1000000@+01	L01= 2.6055277@-01	L11= 1.2874920@-02
S= 4.3000000@+01	L01= 2.6446158@-01	L11= 1.3111168@-02
S= 4.5000000@+01	L01= 2.6798918@-01	L11= 1.3325569@-02
S= 4.7000000@+01	L01= 2.7118881@-01	L11= 1.3521021@-02
S= 4.9000000@+01	L01= 2.7410423@-01	L11= 1.3699928@-02
S= 5.1000000@+01	L01= 2.7677174@-01	L11= 1.3864308@-02

Contribution from Cut Along Left Real Axis from $-\infty < s < 0$

```
REAL PROCEDURE P1(K,V,W,R)    ;
      VALUE K,V,W,R    ;
      REAL K,V,W,R    ;
      BEGIN
      P1←K×LN(ABS((30 + K)/  K          ))/((V-K)×(W-K)×(R-K))
      END P1;
REAL PROCEDURE P2(KK,VV,RR,WW)    ;
      VALUE KK,VV,RR,WW    ;
      REAL KK,VV,RR,WW    ;
      BEGIN
       P2←KK×LN(ABS((KK-2×C+U)/(30+KK)))/((VV-KK)×(RR-KK)×(WW-KK))
      END P2;
WRITE (FOUT,F05)    ;
MU ← 1    ;
MU2 ← 1    ;
M ← (0.495/0.140)× MU    ;
M2 ← M × M    ;
SR ← 40.96    ;
S0 ← M2    ;
C ← M2 + MU2    ;
PI ← 3.14159    ;
NN ← 400    ;
N ← 100    ;
A1 ← 21.5    ;
B2 ← (M+MU)*2    ;
A2 ← (M-MU)*2    ;
B1 ← 0.25    ;
S02 ← S0×S0    ;
AB ← A2 -B2    ;
S0A ← S0 - A2    ;
S0B ← S0 - B2    ;
S0AB ← S0A×S0B    ;
AB2 ← AB×AB    ;
DU1 ← (2×C - B2)/N    ;
DU2 ← ( 60 - 2×C)/NN    ;
TAU ← 1    ;
KAPPA ← 0    ;
WRITE (FOUT,F07,KAPPA,TAU)    ;
FOR S ← 21.0 STEP 2 UNTIL 51 DO
BEGIN
SA ← S - A2    ;
SB ← S - B2    ;
S0S ← S0 - S    ;
SAB ← SA×SB    ;
S2 ← S×S    ;
DUM3 ← (S×S0A/SAB - S0×SA/S0AB)/S0S    ;
DUM4 ← B2/AB2 + B2×SA×S0A/(S0B×SB×AB2)    ;
DUM5 ← (S×S0B/SAB - S0×SB/S0AB)/S0S    ;
DUM6 ← A2/AB2 + A2×SB×S0B/(S0A× SA× AB2)    ;
```

Contribution from Cut Along Left Real Axis from $-\infty < s < 0$
(Continued)

```
DUM7 ← (S2×S0A/SAB - S02×SA/S0AB)/S0S    ;
DUM8 ← A2×B2/AB2 + B2×B2×SA×S0A/(S0B×SB×AB2)    ;
DUM9 ← (S2×S0B/SAB - S02×SB/S0AB)/S0S    ;
DUM10 ← A2×B2/AB2 + A2×A2×SB×S0B/(S0A×SA×AB2)    ;
DUM11 ← S2×S×S0A/(SAB×S0S) - S02×S0×SA/(S0AB×S0S)    ;
DUM12← (B2/AB2)×(A2×A2 + B2×B2×SA×S0A/(SB×S0B))    ;
DUM13 ← S2×S×S0B/(SAB×S0S) - S02×S0×SB/(S0AB×S0S)    ;
DUM14 ← (A2/AB2)×(B2×B2 + A2×A2×SB×S0B/(SA×S0A))    ;
SS0PI ← (S-S0)/PI    ;
SUM11 ← 0    ;    SUM01 ← 0    ;
FOR I ← 1 STEP 1 UNTIL N DO
      BEGIN
U ← B2 + (I-0.5)×DU1    ;
KU ← SQRT(ABS((C-U)*2-4×M2×MU2))/U    ;
AR ← A1×(SR - U)    ;
Q ← KAPPA×TAU/(TAU*2 + (U-SR)*2)    ;
KUSQ ← (KU*2)×U/4    ;
NAR ← AR +Q×(U-SR)×KUSQ    ;
NKU ← KU + Q×TAU    ;
DUM2 ← (3/2)×NKU×(KUSQ ) /(NAR*2  + (NKU×KUSQ)*2)    ;
DUM1  ← KU/(B1*2+KU*2) +  DUM2×(U×(KU*2)/2+2×C-U)    ;
P1A ← P1(A2,B2,S,S0)    ;    P1B ← P1(B2,A2,S,S0)    ;
P1S ← P1(S,S0,A2,B2)    ;    P1S0← P1(S0,S,A2,B2)    ;
G1 ← P1A + P1B + P1S + P1S0    ;
G2 ← A2×P1A + B2×P1B + S×P1S + S0×P1S0    ;
D1 ← S×P1S/SAB + S0×P1S0/S0AB    ;
E1 ← P1A×(DUM3 - DUM4) + P1B×(DUM5 - DUM6)    ;
J1 ← A2×A2/(AB2×S0A×SA)×(1/(A2) - 1/(30+A2))    ;
K1 ← B2×B2/(AB2×S0B×SB)×(1/(B2) - 1/(30+B2))    ;
G3 ← D1 + E1 + J1 + K1    ;
D3 ← S2×P1S/SAB + S02×P1S0/S0AB    ;
E3 ← P1A×(DUM7 - DUM8) + P1B×(DUM9 - DUM10)    ;
G4 ← A2×J1 + B2×K1 + E3 + D3    ;
D5 ← S2×S×P1S/SAB + S02×S0×P1S0/S0AB    ;
E5 ← P1A×(DUM11 - DUM12) + P1B×(DUM13 - DUM14)    ;
G5 ← D5 + E5 + A2*2×J1 + B2*2×K1    ;
G01 ← DUM1×G1 - DUM2×G2    ;
G11 ← DUM1×((2×C-U)×G3-G4) - DUM2×((2×C-U)×G4-G5)    ;
SUM01 ← SUM01 + G01    ;
SUM11 ← SUM11 + G11    ;
      END    ;
H01 ← SUM01×DU1    ;
H11 ← SUM11×DU1    ;
SUM02 ← 0    ;    SUM12 ← 0    ;
FOR II ← 1 STEP 1 UNTIL NN DO
      BEGIN
U ← 2×C + (II-0.5)×DU2    ;
```

Contribution from Cut Along Left Real Axis from $-\infty < s < 0$
(Continued)

```
AR ← A1×(SR - U)      ;
Q ← KAPPA×TAU/(TAU*2 + (U-SR)*2)    ;
KU ← SQRT(ABS((C-U)*2-4×M2×MU2))/U    ;
KUSQ ← (KU*2)×U/4    ;
NAR ← AR +Q×(U-SR)×KUSQ    ;
NKU ← KU + Q×TAU    ;
DUM2 ← (3/2)×NKU×(KUSQ ) /(NAR*2  + (NKU×KUSQ)*2)    ;
DUM1  ← KU/(B1*2+KU*2) +  DUM2×(U×(KU*2)/2+2×C-U)    ;
P2A ← P2(A2,B2,S,S0)    ;    P2B ← P2(B2,A2,S,S0)    ;
P2S ← P2(S,S0,A2,B2)    ;    P2S0← P2(S0,S,A2,B2)    ;
H1 ← P2A + P2B + P2S + P2S0    ;
H2 ← A2×P2A + B2×P2B + S×P2S + S0×P2S0    ;
D2 ← S×P2S/SAB + S0×P2S0/S0AB    ;
E2 ← P2A×(DUM3 - DUM4) + P2B×(DUM5 - DUM6)    ;
J2 ← A2×A2/(AB2×S0A×SA)×(1/(2×C-U-A2) + 1/(30+A2) )    ;
K2 ← B2×B2/(AB2×S0B×SB)×(1/(2×C-U-B2) + 1/(30+B2) )    ;
H3 ← D2 + E2 + J2 + K2    ;
D4 ← S2×P2S/SAB + S02×P2S0/S0AB    ;
E4 ← P2A×(DUM7 - DUM8) + P2B×(DUM9 - DUM10)    ;
H4 ← A2×J2 + B2×K2 + D4 + E4    ;
D6 ← S2×S×P2S/SAB + S02×S0×P2S0/S0AB    ;
E6 ← P2A×(DUM11 - DUM12) + P2B×(DUM13 - DUM14)    ;
H5 ← D6 + E6 + A2*2×J2 + B2*2×K2    ;
G02 ← DUM1×H1 - DUM2×H2    ;
G12 ← DUM1×((2×C-U)×H3-H4) - DUM2×((2×C-U)×H4-H5)    ;
SUM02 ← SUM02 + G02    ;
SUM12 ← SUM12 + G12    ;
     END    ;
H02 ← SUM02×DU2    ;
H12 ← SUM12×DU2    ;
K01 ←-SS0PI×(H01 - H02)    ;
      K11← - 2×SS0PI×(H11 - H12) + K01    ;
WRITE (FOUT,F06,S,K01,K11)    ;
END    ;
END    .
```

Table 12. Contribution of Cut Along Left Real Axis for s < 0
Without CDD Pole

KAPPA= 0.0000000@+00		TAU= 1.0000000@+00
S= 2.1000000@+01	K01= 5.0315161@-02	K11= 3.0339367@-02
S= 2.3000000@+01	K01= 5.8681744@-02	K11= 3.5269436@-02
S= 2.5000000@+01	K01= 6.6180810@-02	K11= 3.9661940@-02
S= 2.7000000@+01	K01= 7.2945407@-02	K11= 4.3603183@-02
S= 2.9000000@+01	K01= 7.9081854@-02	K11= 4.7161436@-02
S= 3.1000000@+01	K01= 8.4676308@-02	K11= 5.0391497@-02
S= 3.3000000@+01	K01= 8.9799446@-02	K11= 5.3337938@-02
S= 3.5000000@+01	K01= 9.4509872@-02	K11= 5.6037424@-02
S= 3.7000000@+01	K01= 9.8856644@-02	K11= 5.8520435@-02
S= 3.9000000@+01	K01= 1.0288118@-01	K11= 6.0812531@-02
S= 4.1000000@+01	K01= 1.0661872@-01	K11= 6.2935332@-02
S= 4.3000000@+01	K01= 1.1009946@-01	K11= 6.4907254@-02
S= 4.5000000@+01	K01= 1.1334941@-01	K11= 6.6744094@-02
S= 4.7000000@+01	K01= 1.1639116@-01	K11= 6.8459487@-02
S= 4.9000000@+01	K01= 1.1924438@-01	K11= 7.0065264@-02
S= 5.1000000@+01	K01= 1.2192630@-01	K11= 7.1571749@-02

Table 13. Contribution of Cut Along Left Real Axis for s < 0
With CDD Pole

KAPPA= 1.0000000@+01		TAU= 1.0000000@-02
S= 2.1000000@+01	K01= 5.0308450@-02	K11= 3.0331198@-02
S= 2.3000000@+01	K01= 5.8673661@-02	K11= 3.5259692@-02
S= 2.5000000@+01	K01= 6.6171435@-02	K11= 3.9650731@-02
S= 2.7000000@+01	K01= 7.2934817@-02	K11= 4.3590613@-02
S= 2.9000000@+01	K01= 7.9070122@-02	K11= 4.7147598@-02
S= 3.1000000@+01	K01= 8.4663501@-02	K11= 5.0376478@-02
S= 3.3000000@+01	K01= 8.9785627@-02	K11= 5.3321815@-02
S= 3.5000000@+01	K01= 9.4495099@-02	K11= 5.6020269@-02
S= 3.7000000@+01	K01= 9.8840972@-02	K11= 5.8502311@-02
S= 3.9000000@+01	K01= 1.0286466@-01	K11= 6.0793499@-02
S= 4.1000000@+01	K01= 1.0660140@-01	K11= 6.2915445@-02
S= 4.3000000@+01	K01= 1.1008138@-01	K11= 6.4886563@-02
S= 4.5000000@+01	K01= 1.1333061@-01	K11= 6.6722644@-02
S= 4.7000000@+01	K01= 1.1637168@-01	K11= 6.8437320@-02
S= 4.9000000@+01	K01= 1.1922425@-01	K11= 7.0042419@-02
S= 5.1000000@+01	K01= 1.2190556@-01	K11= 7.1548262@-02

Table 13. Contribution of Cut Along Left Real Axis for s < 0 With CDD Pole (Continued)

KAPPA= 1.0000000@+01		TAU= 1.0000000@-03
S= 2.1000000@+01	K01= 5.0308809@-02	K11= 3.0331350@-02
S= 2.3000000@+01	K01= 5.8674080@-02	K11= 3.5259867@-02
S= 2.5000000@+01	K01= 6.6171908@-02	K11= 3.9650927@-02
S= 2.7000000@+01	K01= 7.2935340@-02	K11= 4.3590826@-02
S= 2.9000000@+01	K01= 7.9070689@-02	K11= 4.7147828@-02
S= 3.1000000@+01	K01= 8.4664108@-02	K11= 5.0376721@-02
S= 3.3000000@+01	K01= 8.9786271@-02	K11= 5.3322070@-02
S= 3.5000000@+01	K01= 9.4495777@-02	K11= 5.6020535@-02
S= 3.7000000@+01	K01= 9.8841682@-02	K11= 5.8502588@-02
S= 3.9000000@+01	K01= 1.0286540@-01	K11= 6.0793785@-02
S= 4.1000000@+01	K01= 1.0660217@-01	K11= 6.2915739@-02
S= 4.3000000@+01	K01= 1.1008217@-01	K11= 6.4886864@-02
S= 4.5000000@+01	K01= 1.1333143@-01	K11= 6.6722953@-02
S= 4.7000000@+01	K01= 1.1637251@-01	K11= 6.8437635@-02
S= 4.9000000@+01	K01= 1.1922510@-01	K11= 7.0042740@-02
S= 5.1000000@+01	K01= 1.2190643@-01	K11= 7.1548588@-02
KAPPA= 1.0000000@+01		TAU= 1.0000000@-04
S= 2.1000000@+01	K01= 5.0308840@-02	K11= 3.0331360@-02
S= 2.3000000@+01	K01= 5.8674116@-02	K11= 3.5259877@-02
S= 2.5000000@+01	K01= 6.6171948@-02	K11= 3.9650938@-02
S= 2.7000000@+01	K01= 7.2935384@-02	K11= 4.3590839@-02
S= 2.9000000@+01	K01= 7.9070736@-02	K11= 4.7147841@-02
S= 3.1000000@+01	K01= 8.4664158@-02	K11= 5.0376735@-02
S= 3.3000000@+01	K01= 8.9786324@-02	K11= 5.3322084@-02
S= 3.5000000@+01	K01= 9.4495833@-02	K11= 5.6020550@-02
S= 3.7000000@+01	K01= 9.8841740@-02	K11= 5.8502602@-02
S= 3.9000000@+01	K01= 1.0286546@-01	K11= 6.0793800@-02
S= 4.1000000@+01	K01= 1.0660223@-01	K11= 6.2915755@-02
S= 4.3000000@+01	K01= 1.1008223@-01	K11= 6.4886880@-02
S= 4.5000000@+01	K01= 1.1333149@-01	K11= 6.6722968@-02
S= 4.7000000@+01	K01= 1.1637258@-01	K11= 6.8437650@-02
S= 4.9000000@+01	K01= 1.1922517@-01	K11= 7.0042756@-02
S= 5.1000000@+01	K01= 1.2190650@-01	K11= 7.1548604@-02

P-Wave Phase Shifts With and Without CDD Pole

```
REAL   S,X,KSQ,KS,Q,TAU,KAPPA,DELT,DELP,PI,A,B,M    ;
WRITE (FOUT,F01)    ;
WRITE (FOUT,F02)    ;
PI ← 3.14159    ;
M←(0.495/0.14)    ;
A ← (M+1)*2    ;
B ← (M-1)*2    ;
KAPPA ← 10      ;
TAU ← 0.001    ;
FOR S ← 35 STEP 0.10 UNTIL 48 DO
      BEGIN
KS ← SQRT((S-A)×(S-B))/S    ;
KSQ ← (S-A)×(S-B)/(4×S)    ;
X ← 21.5×(41-S)/(KS×KSQ)    ;
DELT ← PI/2 - ARCTAN(X)    ;
Q ← KAPPA  ×  (S-41)/((TAU*2+(S-41)*2)×KS)    ;
DELP ← PI/2 - ARCTAN(X+Q)    ;
WRITE (FOUT,F03,S,DELT,DELP)    ;
      END    ;
END    .
```

Table 14. P-Wave Phase Shifts

	WITHOUT POLE	WITH POLE
S= 3.600000@+01	DELT= 1.7480925@-02	DELP= 1.8575599@-02
S= 3.610000@+01	DELT= 1.8002613@-02	DELP= 1.9188351@-02
S= 3.620000@+01	DELT= 1.8546401@-02	DELP= 1.9832514@-02
S= 3.630000@+01	DELT= 1.9113685@-02	DELP= 2.0510671@-02
S= 3.640000@+01	DELT= 1.9706024@-02	DELP= 2.1225706@-02
S= 3.650000@+01	DELT= 2.0325052@-02	DELP= 2.1980851@-02
S= 3.660000@+01	DELT= 2.0972596@-02	DELP= 2.2779746@-02
S= 3.670000@+01	DELT= 2.1650640@-02	DELP= 2.3626502@-02
S= 3.680000@+01	DELT= 2.2361357@-02	DELP= 2.4525783@-02
S= 3.690000@+01	DELT= 2.3107133@-02	DELP= 2.5482908@-02
S= 3.700000@+01	DELT= 2.3890591@-02	DELP= 2.6503966@-02
S= 3.710000@+01	DELT= 2.4714623@-02	DELP= 2.7595969@-02
S= 3.720000@+01	DELT= 2.5582425@-02	DELP= 2.8767037@-02
S= 3.730000@+01	DELT= 2.6497538@-02	DELP= 3.0026628@-02
S= 3.740000@+01	DELT= 2.7463897@-02	DELP= 3.1385834@-02
S= 3.750000@+01	DELT= 2.8485884@-02	DELP= 3.2857758@-02
S= 3.760000@+01	DELT= 2.9568397@-02	DELP= 3.4457994@-02
S= 3.770000@+01	DELT= 3.0716925@-02	DELP= 3.6205266@-02
S= 3.780000@+01	DELT= 3.1937642@-02	DELP= 3.8122266@-02
S= 3.790000@+01	DELT= 3.3237518@-02	DELP= 4.0236785@-02
S= 3.800000@+01	DELT= 3.4624450@-02	DELP= 4.2583244@-02
S= 3.810000@+01	DELT= 3.6107420@-02	DELP= 4.5204838@-02
S= 3.820000@+01	DELT= 3.7696689@-02	DELP= 4.8156546@-02
S= 3.830000@+01	DELT= 3.9404036@-02	DELP= 5.1509507@-02
S= 3.840000@+01	DELT= 4.1243044@-02	DELP= 5.5357481@-02
S= 3.850000@+01	DELT= 4.3229460@-02	DELP= 5.9826712@-02
S= 3.860000@+01	DELT= 4.5381649@-02	DELP= 6.5091447@-02
S= 3.870000@+01	DELT= 4.7721152@-02	DELP= 7.1399296@-02
S= 3.880000@+01	DELT= 5.0273409@-02	DELP= 7.9114607@-02
S= 3.890000@+01	DELT= 5.3068682@-02	DELP= 8.8796702@-02
S= 3.900000@+01	DELT= 5.6143247@-02	DELP= 1.0135069@-01
S= 3.910000@+01	DELT= 5.9540970@-02	DELP= 1.1834343@-01
S= 3.920000@+01	DELT= 6.3315396@-02	DELP= 1.4274126@-01
S= 3.930000@+01	DELT= 6.7532565@-02	DELP= 1.8090657@-01
S= 3.940000@+01	DELT= 7.2274878@-02	DELP= 2.4928772@-01
S= 3.950000@+01	DELT= 7.7646485@-02	DELP= 4.0583535@-01
S= 3.960000@+01	DELT= 8.3780943@-02	DELP= 9.9538090@-01
S= 3.970000@+01	DELT= 9.0852347@-02	DELP= 2.4168735@+00
S= 3.980000@+01	DELT= 9.9091905@-02	DELP= 2.8233312@+00
S= 3.990000@+01	DELT= 1.0881333@-01	DELP= 2.9482603@+00
S= 4.000000@+01	DELT= 1.2045303@-01	DELP= 3.0072942@+00
S= 4.010000@+01	DELT= 1.3463608@-01	DELP= 3.0418622@+00
S= 4.020000@+01	DELT= 1.5228957@-01	DELP= 3.0648348@+00
S= 4.030000@+01	DELT= 1.7484756@-01	DELP= 3.0814643@+00
S= 4.040000@+01	DELT= 2.0464609@-01	DELP= 3.0942930@+00
S= 4.050000@+01	DELT= 2.4574516@-01	DELP= 3.1047071@+00
S= 4.060000@+01	DELT= 3.0580859@-01	DELP= 3.1135343@+00

Table 14. P-Wave Phase Shifts
(Continued)

S= 4.070000n@+01	DELT= 4.0092092@-01	DELP= 3.1213087@+00
S= 4.080000n@+01	DELT= 5.6946889@-01	DELP= 3.1284005@+00
S= 4.090000n@+01	DELT= 9.1108449@-01	DELP= 3.1350861@+00
S= 4.100000n@+01	DELT= 1.5707950@+00	DELP= 1.5923452@+00
S= 4.110000n@+01	DELT= 2.2239265@+00	DELP= 6.5224894@-03
S= 4.120000n@+01	DELT= 2.5596925@+00	DELP= 1.3260728@-02
S= 4.130000n@+01	DELT= 2.7257908@+00	DELP= 2.0428263@-02
S= 4.140000n@+01	DELT= 2.8198009@+00	DELP= 2.8278857@-02
S= 4.150000n@+01	DELT= 2.8792970@+00	DELP= 3.7138824@-02
S= 4.160000n@+01	DELT= 2.9200708@+00	DELP= 4.7457127@-02
S= 4.170000n@+01	DELT= 2.9496672@+00	DELP= 5.9891247@-02
S= 4.180000n@+01	DELT= 2.9720915@+00	DELP= 7.5466351@-02
S= 4.190000n@+01	DELT= 2.9896523@+00	DELP= 9.5896259@-02
S= 4.200000n@+01	DELT= 3.0037687@+00	DELP= 1.2429896@-01
S= 4.210000n@+01	DELT= 3.0153589@+00	DELP= 1.6701233@-01
S= 4.220000n@+01	DELT= 3.0250427@+00	DELP= 2.3909910@-01
S= 4.230000n@+01	DELT= 3.0332530@+00	DELP= 3.8592951@-01
S= 4.240000n@+01	DELT= 3.0403014@+00	DELP= 8.0079698@-01
S= 4.250000n@+01	DELT= 3.0464174@+00	DELP= 1.9518733@+00
S= 4.260000n@+01	DELT= 3.0517741@+00	DELP= 2.6023477@+00
S= 4.270000n@+01	DELT= 3.0565042@+00	DELP= 2.8050144@+00
S= 4.280000n@+01	DELT= 3.0607114@+00	DELP= 2.8950839@+00
S= 4.290000n@+01	DELT= 3.0644776@+00	DELP= 2.9453272@+00
S= 4.300000n@+01	DELT= 3.0678684@+00	DELP= 2.9773131@+00
S= 4.310000n@+01	DELT= 3.0709373@+00	DELP= 2.9994762@+00
S= 4.320000n@+01	DELT= 3.0737279@+00	DELP= 3.0157606@+00
S= 4.330000n@+01	DELT= 3.0762762@+00	DELP= 3.0282499@+00
S= 4.340000n@+01	DELT= 3.0786125@+00	DELP= 3.0381472@+00
S= 4.350000n@+01	DELT= 3.0807620@+00	DELP= 3.0461947@+00
S= 4.360000n@+01	DELT= 3.0827463@+00	DELP= 3.0528753@+00
S= 4.370000n@+01	DELT= 3.0845837@+00	DELP= 3.0585167@+00
S= 4.380000n@+01	DELT= 3.0862897@+00	DELP= 3.0633490@+00
S= 4.390000n@+01	DELT= 3.0878781@+00	DELP= 3.0675387@+00
S= 4.400000n@+01	DELT= 3.0893604@+00	DELP= 3.0712092@+00
S= 4.410000n@+01	DELT= 3.0907470@+00	DELP= 3.0744539@+00
S= 4.420000n@+01	DELT= 3.0920468@+00	DELP= 3.0773449@+00
S= 4.430000n@+01	DELT= 3.0932677@+00	DELP= 3.0799387@+00
S= 4.440000n@+01	DELT= 3.0944165@+00	DELP= 3.0822802@+00
S= 4.450000n@+01	DELT= 3.0954996@+00	DELP= 3.0844058@+00
S= 4.460000n@+01	DELT= 3.0965223@+00	DELP= 3.0863448@+00
S= 4.470000n@+01	DELT= 3.0974895@+00	DELP= 3.0881216@+00
S= 4.480000n@+01	DELT= 3.0984057@+00	DELP= 3.0897563@+00
S= 4.490000n@+01	DELT= 3.0992747@+00	DELP= 3.0912659@+00
S= 4.500000n@+01	DELT= 3.1001000@+00	DELP= 3.0926647@+00
S= 4.510000n@+01	DELT= 3.1008849@+00	DELP= 3.0939648@+00
S= 4.520000n@+01	DELT= 3.1016322@+00	DELP= 3.0951767@+00
S= 4.530000n@+01	DELT= 3.1023446@+00	DELP= 3.0963093@+00

Absorptive Part of the Amplitudes, Im $A_0(s)$ and Im $A_1(s)$ in the Unphysical Region of Channel I

(This program was written in Fortran II and run on IBM 1620 at Tennessee State University, Nashville, Tennessee.)

```
E=0.495/0.140
E2=E*E
A=(E-1.0)**2
B=(E+1.0)**2
C=E2+1.0
A1=21.5
SR=41.0
B1=0.25
TAU=0.001
CAPPA=10.00
PRINT 40
DO 30 I=1,21
U=I
S=0.95 - U
N=100+10*I
R=N
PS=SQRTF((S-A)*(S-B))/S
PSQ=S*(PS*PS)/4.0
F=2.0*C - S
DX=(B-F)/R
SUMO=0.0
SUM1=0.0
DO 20 J=1,N
T=J
X=F+(T-0.5)*DX
Q=CAPPA/(TAU*TAU + (X-SR)*(X-SR))
PX = SQRTF((X-A)*(X-B))/X
PX2 = PX*PX
PXSQ = X*PX2/4.0
YMAO = PX/(PX2 + B1*B1)
AR=A1*(SR-X)
TAR=AR+Q*PXSQ*(X-SR)
TPX=PX+Q*TAU
YMA1=PXSQ*TPX/(TAR*TAR+ (PXSQ*TPX)*(PXSQ*TPX))
DUMMY=YMAO+3.*(2.0*PXSQ+2.0*C-X-S)*YMA1/2.0
SUMO=SUMO+DUMMY
SUM1 = SUM1 + (2.0*PSQ+2.0*C-X-S)*DUMMY
YMAOL=SUMO*DX/(4.0*PSQ)
YMAIL=SUM1*DX/(8.0*PSQ*PSQ)
PRINT 10,S,YMAOL,YMAIL
CALL EXIT
END
```

Table 15. Im $A_\ell(s)$ in Unphysical Region of Channel I With and Without CDD Pole (The Pole Has a Strength, $\kappa = 10$, and Position, $\tau = 0.001$)

S	Im $A_0(s)$	Im $A_0(s)$ With Pole	Im $A_1(s)$	Im $A_1(1)$ With Pole
6.4	0.6994	0.6994	-0.05932	-0.05932
5.8	1.9421	1.9421	-0.03688	-0.03688
5.2	1.9426	1.9426	0.02646	0.02646
4.6	1.8351	1.8351	0.06257	0.06257
4.0	1.7139	1.7139	0.08312	0.08313
3.4	1.5959	1.5953	0.09519	0.09582
2.8	1.4099	1.4102	0.13496	0.13637
2.2	1.3350	1.3375	0.09566	0.09660
1.6	1.2527	1.2490	0.08143	0.07991
1.0	1.1609	1.1646	0.07048	0.07319
0.4	1.0547	1.0558	0.05091	0.05192
-0.05	0.0044	0.0044	0.00444	0.00444
-1.0	0.0883	0.0883	0.08405	0.08405
-2.0	0.1632	0.1632	0.14832	0.14832
-4.0	0.2901	0.2901	0.24134	0.24134
-6.0	0.3925	0.3925	0.30028	0.30028
-8.0	0.4761	0.4761	0.33641	0.33642
-10.0	0.5452	0.5452	0.35720	0.35722
-12.0	0.6031	0.6035	0.36779	0.36811
-14.0	0.6746	0.6708	0.39359	0.38884
-16.0	0.7369	0.7352	0.40949	0.40791
-18.0	0.7800	0.7795	0.40778	0.40733
-20.0	0.8176	0.8172	0.40236	0.40211

BIBLIOGRAPHY

Literature Cited

1. R. Kronig. 1926. *Journal of the Optical Society of America,* Vol. 12, p. 547.

2. H. A. Kramers. 1927. *Atti del Congresso Internazionale de Fisica,* Como, Italy, Vol. 2, p. 545.

3. R. Kronig. 1946. *Physica,* Vol. 12, p. 543.

4. M. Gell-Mann, M. L. Goldberger and W. Thirring. 1954. *Physical Review,* Vol. 95, p. 1612.

5. M. L. Goldberger. 1955. *Physical Review,* Vol. 97, p. 508.

6. M. L. Goldberger, H. Miyazawa and R. Oehme. 1955. *Physical Review,* Vol. 99, p. 986.

7. H. L. Anderson, W. C. Davidon and U. F. Kruse. 1955. *Physical Review,* Vol. 100, p. 339.

8. G. F. Chew, M. L. Goldberger, F. E. Low and Y. Nambu. 1957. *Physical Review,* Vol. 106, p. 1337.

9. K. Symanzik. 1957. *Physical Review,* Vol. 105, p. 743.

10. N. N. Bogoliubov and D. V. Shirkov. 1959. *Introduction to the Theory of Quantized Fields.* Interscience, New York, Ch. 9.

11. S. Mandelstam. 1958. *Physical Review,* Vol. 112, p. 1344.

12. G. F. Chew and F. Low. 1956. *Physical Review,* Vol. 101, p. 1570.

13. G. F. Chew and S. Mandelstam. 1960. *Physical Review,* Vol. 119, p. 467.

14. J. W. Moffat. 1961. *Physical Review,* Vol. 121, No. 3, p. 926.

15. R. Omnes. 1958. *Il Nuovo Cimento,* Vol. 8, p. 316.

16. L. Castillejo, R. H. Dalitz and F. J. Dyson. 1956. *Physical Review,* Vol. 101, p. 453.

17. B. H. Bransden and J. W. Moffat, 1961. *Il Nuovo Cimento,* Vol. 31, p. 505.

18. B. H. Bransden, I. R. Gatland, J. W. Moffat. 1962. *Physical Review,* Vol. 128, p. 859.

19. I. R. Gatland, 1966. Annual Report for NSF Grant No. GP4500 at Georgia Institute of Technology. (Unpublished.)

20. M. Alston, L. Alvarez, P. Eberhart, M. Good, W. Graziano, H. Ticho, and S. Wojcicki. 1961. *Physical Review Letters,* Vol. 6, No. 6, p. 300.

21. G. Smith, J. Swartz, D. Miller, G. Kalbflerch, R. Huff, O. Dahl, and G. Alexander. 1963. *Physical Review Letters,* Vol. 10, No. 4, p. 138.

22. J. Sakurai. 1962. *Physical Review Letters,* Vol. 9, p. 472.

23. C. Moller. 1945. *Kgl. Danske Vidensk. Selskab. Mat-fys.* Medd, 23, 1.

24. B. W. Lee. 1960. *Physical Review,* Vol. 120, No. 1, p. 325.

25. B. W. Lee and K. S. Cho. 1961. *Il Nuovo Cimento,* Vol. 20, p. 553.

26. S. W. MacDowell. 1959. *Physical Review,* Vol. 116, No. 3, p. 774.

27. R. Oehme. 1960. *Physical Review Letters,* Vol. 4, p. 246. Errata p. 320.

28. S. Mandelstam. 1960, *Physical Review Letters,* Vol. 4, p. 84.

29. W. Frazer and J. Fulco. 1960. *Physical Review,* Vol. 117, No. 6, p. 1603.

30. I. R. Gatland and J. W. Moffat. 1963. *Physical Review,* Vol. 129, No. 2, p. 937.

Other References

Ferro-Luzzi, M., R. George, Y. Goldschmidt-Clermont, V. Henri, B. Jongejans, D. Leith, G. Lynch, F. Muller and J. Perreau. 1965. *Il Nuovo Cimento.* Vol. 36. No. 4, p. 2381-2399.

Ford, K. 1963. *The World of Elementary Particles,* Blaisdell Publishing Company, New York.

Frazer, W. 1966. *Elementary Particles*, Prentice-Hall, Inc. New Jersey.

Gasiorowicz, S. 1966. *Elementary Particle Physics*, John Wiley and Sons, Inc., New York.

Morse, P. and H. Feshbach. 1953. *Methods of Theoretical Physics*, McGraw-Hill Book Company, New York, Ch. 4.

Screaton, G. R., Ed. 1960. *Dispersion Relations*, Scottish Universities' Summer School, Interscience Publishers Inc., New York.

VITA

Patricia Hull was born Patricia Ann Groves in Lindale, Georgia, in 1938. She was educated in the Georgia public schools and was graduated second in her class from Chamblee High School in 1956. She entered Auburn University in Auburn, Alabama, in June, 1956, and was elected to Alpha Lambda Alpha, a women's scholastic honorary society, in 1957. She received a Bachelor of Science degree in physics from Auburn in 1960. The following fall, she entered Auburn University graduate school as a teaching assistant to pursue a Master of Science degree in physics. While a graduate student at Auburn University, Patricia married a fellow student, Robert Lanier Hull. She received her Master of Science degree with a major in physics and a minor in mathematics from Auburn in March, 1962. She remained at Auburn until June, 1962, as an instructor in physics. From June, 1962, until September, 1964, she was employed as a research engineer at Lockheed Aircraft Corporation in Marietta, Georgia, where she directed the physical optics research laboratory. In September, 1964, she enrolled in the Georgia Institute of Technology graduate school to pursue a doctorate degree in physics. While a graduate student at Georgia Tech, Patricia was employed by Oglethorpe College in Atlanta as an instructor of physics and mathematics. From the fall of 1966 until the spring of 1968, Patricia received financial assistance from the National Science Foundation to carry on the research required for the doctoral

dissertation. In September, 1968, Patricia was employed by Tennessee State University, Nashville, Tennessee, as Associate Professor of Physics.